Epigenetic interplay between histone H3K9me2 and JIL-1 mediated histone H3S10ph

by

Chao Wang

A dissertation submitted to the graduate faculty

in partial fulfillment of the requirements for the degree of

DOCTOR OF PHILOSOPHY

Major: Molecular, Cellular and Developmental Biology

Program of Study Committee:
Kristen M. Johansen, Major Professor
Jørgen Johansen
Jack Girton
Yanhai Yin
Michael Shogren-Knaak

Iowa State University

Ames, Iowa

2014

To my family

Table of Contents

ABSTRACT

In *Drosophila*, JIL-1 Kinase specifically localizes to euchromatic interband regions of polytene chromosomes and is responsible for histone H3S10 phosphorylation at interphase. Previous genetic interaction assays have demonstrated that the JIL-1 protein can counterbalance the effect of the major heterochromatin components Su(var)3-7 on position-effect variegation (PEV). In this study, we show that the haplo-enhancer effect of JIL-1 has the ability to counterbalance the haplo-suppressor effect of two other major heterochromatin components, Su(var)3-9 and Su(var)2-5, on position-effect variegation, providing evidence that a finely tuned balance between the levels of JIL-1 and the major heterochromatin components contributes to the regulation of gene expression. To test whether this was a causative effect of the epigenetic H3S10 phosphorylation mark, or whether the effect of the JIL-1 protein on PEV was in fact caused by other functions or structural features of the protein, we transgenically expressed various truncated versions of JIL-1, with or without kinase activity, and assessed their effect on PEV and heterochromatic spreading. The results indicate that the gross perturbation of polytene chromosome morphology observed in *JIL-1* null mutants is unrelated to gene silencing in PEV and is likely to occur as a result of faulty polytene chromosome alignment and/or organization, separate from epigenetic regulation of chromatin structure.

Interestingly, *JIL-1* loss-of-function alleles can act either as an enhancer or indirectly as a suppressor of w^{m4} PEV depending on the precise levels of JIL-1 kinase activity. To explore the relationship between PEV and the relative levels of the H3S10ph and H3K9me2 marks at the *white* gene locus, we performed ChIP-qPCR analysis. Our results indicate that the H3K9me2 level at the *white* gene locus directly correlates with its level of expression and that H3K9me2 levels in turn are regulated by H3S10ph.

To further study the localization of H3S10 phosphorylation and H3K9 dimethylation as well as their interplay, genome-wide analysis of JIL-1 kinase binding sites and H3S10ph or H3K9me2 distribution by ChIP-seq was conducted. Furthermore, an analysis of whole genome transcription level changes by RNA-seq in the absence of JIL-1 was used to study the role of this interplay in regulation of gene transcription. The results show that down-regulation of genes in the *JIL-1* mutant was correlated with higher levels or acquisition of the H3K9me2 mark whereas up-regulation of a gene was correlated with loss of or diminished H3K9me2. These results are compatible with a model where gene expression levels are modulated by the levels of the H3K9me2 mark independent of the state of the H3S10ph mark, which is not required for either transcription or gene activation to occur. Rather, H3S10ph functions to indirectly maintain active transcription by counteracting H3K9me2 and gene silencing.

CHAPTER 1. GENERAL INTRODUCTION

Introduction

In eukaryotes, chromatin plays important roles in many biological processes such as gene replication, transcription, recombination and heterochromatin formation. Global and local positioning of nucleosomes may restrict the DNA accessibility and prevent transcription factor or other element binding to the genomic DNA (Boyle and Furey, 2009). Chromatin structure and organization change can facilitate gene transcription. There are three mechanisms for this change: ATP dependent chromatin remodeling, histone modification and histone exchange (Baker and Grant, 2007).

ATP dependent remodeling is one of the most important mechanisms in chromatin structure remodeling and regulation. In *Drosophila*, three ATP-dependent remodeling complexes have been identified: nucleosome remodeling factor (NURF), ATP-utilizing chromatin assembly and remodeling factor (ACF) and chromatin accessibility complex (CHRAC). Further studies have found that an ATPase ISWI plays an important role in all of these three complexes (Farkas et al., 2000). A loss of function mutant of ISWI leads to a disordered structure of the X chromosome (Deuring et al., 2000)

Histone exchange is another major chromatin epigenetic regulation mechanism. During this process, the normal histone is replaced by other histone variants that affect nucleosome stability or recruit remodeling factors (Henikoff, 2008).

Covalent modification on histone residues also can change chromatin structure and stability. Histone modifications can be identified by Mass Spectrometry (MS), protein sequencing and antibodies. Different histone modifications interplay with each other to

construct a “network” to regulate chromatin status and transcription activities. The mechanisms underlying histone modifications remodeling include interference between nucleosome interactions, recruitment of remodeling factors, and direct alteration of the chromatin structure (Kouzarides, 2007).

Histone acetylation, methylation and phosphorylation are the three best-studied modifications. Although not as well-characterized, histone phosphorylation has been demonstrated in many important biological processes. There are two major but seemingly contradictory functions of histone H3S10 phosphorylation at different stages of the cell cycle: promoting chromosome condensation and segregation in metaphase and facilitating chromatin remodeling and transcription activation in interphase (Hendzel et al., 1997, Wei et al., 1999, Sassone-Corsi et al., 1999). In interphase cells, MSK1/2 kinase, RSK and yeast SNF1 have been identified as H3S10 phosphorylation kinases (Kouzarides et al., 2007).

Johansen’s lab first identified JIL-1, a homolog of MSK1/2 and RSK in *Drosophila* through expression library screening with the mAb2A (Johansen et al., 1996). The JIL-1 full-length protein contains 1207 amino-acids which are organized into four domains: N-terminal domain (NTD), kinase domain I (KDI), kinase domain II (KD II) and C-terminal domain (CTD). Both kinase domains are predicted to be serine/threonine kinase domains. Kinase domain I (KDI) of JIL-1 shows the highest identity (63%) to human MSK1 and lower identity (47%) to *Drosophila* RSK while kinase domain II (KDII) shares just 32% and 28% homology with the human MSK1 and *Drosophila* RSK. The phylogenetic analysis shows that JIL-1 is grouped with 95% bootstrap support with human MSK1, which suggests it has a very high conservation with the MSK1 kinase domain (Jin et al., 1999). Distinct from human MSK1, JIL-1 has a much longer N-terminal domain (NTD) and C-terminal domain (CTD), which suggests that JIL-1 may have a more complicated regulation mechanism (Jin et al., 1999).

In in-vitro kinase assay JIL-1 has been shown to phosphorylate histone H3S10 and auto-phosphorylate (Jin et al., 1999). Loss of function mutants of *JIL-1*, especially the null mutant *JIL-1*^{Z2}/*JIL-1*^{Z2}, show significant decrease of H3S10 phosphorylation levels revealed by immunostaining of polytene chromosome and immunoblot analysis. However, in mutant mitotic neuroblast cells, H3S10 phosphorylation levels do not change, which suggests JIL-1 is required for H3S10 phosphorylation in interphase but not in metaphase (Wang et al., 2001). JIL-1 is also very critical for *Drosophila* development and maintaining chromosome structure. Null mutant *JIL-1*^{Z2}/*JIL-1*^{Z2} cannot survive to the adult stage and the polytene chromosome structure is disrupted severely. All the autosomes and the female X chromosome become more coiled and folded and lose their banding pattern (Wang et al., 2001). The male X chromosome totally is even more disrupted which gives a typical mutant phenotype of JIL-1 (Deng et al., 2005). Interestingly, decreased JIL-1 levels can result in the enhancement of position effect variegation (PEV), while the gain of function JIL-1 allele Su(var)3-1 shows a strong suppressor phenotype in the same centromeric P-element insertion 118E-10 PEV system. This result suggests JIL-1 may be involved in gene activation or silencing pathways (Bao et al., 2007).

Another interesting epigenetic change in the *JIL-1* null mutant *JIL-1*^{Z2}/*JIL-1*^{Z2} is that H3K9 dimethylation spreads from the chromocenter to chromosome arms, especially on the X chromosome (Zhang et al., 2006). It is well known that H3K9 dimethylation is a heterochromatin mark related to gene inactivation and transcriptional silencing. The *Drosophila* H3K9 histone methytransferase (HMT) *Su(var)3-9* and *JIL-1* show antagonistic effects in PEV. Furthermore, a *Su(var)3-9* loss of function mutant can rescue both the chromosome morphology and viability defects of the *JIL-1* null mutant (Zhang et al., 2006, Deng et al., 2007). Studies show that JIL-1 can phosphorylate Su(var)3-9 (Boeke et al., 2010) and JIL-1 counteracts another important heterochromatin component, the zinc-finger

protein Su(var)3-7 (Deng et al., 2010). These results suggest JIL-1 is involved in regulation of heterochromatin formation and gene transcription.

In *Drosophila*, the dosage compensation mediated by MSL complex is that the male X-linked genes equal their expression levels to those on the two female X chromosomes (Akhtar and Becker, 2000). JIL-1 localizes to interband regions of polytene chromosome and is up-regulated on the male X chromosome (Jin et al., 1999). Evidence shows that JIL-1 co-localizes with the MSL complex and male X chromosome is more sensitive than female X chromosome and autosomes to loss of JIL-1 (Jin et al., 2000). These results suggest that JIL-1 may be involved in the dosage compensation pathway.

As described above, JIL-1 has four domains: N-terminal domain (NTD), kinase domain I (KDI), kinase domain II (KDII) and C-terminal domain (CTD). Although KDI and KDII share 63% and 32% amino-acid sequence identity with human MSK1, we still know very little about the mechanism of these kinase domains' function. In contrast, more is known about the C-terminal domain regarding structure and function. The CTD can be almost equally divided into a highly acidic region and a highly basic region containing a potential globular domain (Bao et al., 2005). The JIL-1 CTD is required not only for JIL-1 correct targeting on the polytene chromosome but it also can interact with lamin Dm0 and the H3 histone tail (Bao et al., 2005, Bao et al., 2008). It is surprising that although over-expression of JIL-1 CTD decreases the H3S10 phophorylation level suggesting the CTD may have a dominant negative effect, the JIL-1 CTD alone can rescue both the chromosome morphology and viability of the $JIL\text{-}1^{Z2}/JIL\text{-}1^{Z2}$ mutant (Bao et al., 2008).

In this thesis, two questions were addressed by a series of experiments:

1 How does JIL-1 mediated H3S10 phosphorylation affect euchomatin and heterochromatin status?

We measured PEV in the eye of *Drosophila* to determine the effect of JIL-1-mediated H3S10 phosphorylation on gene expression and polytene chromosome morphology. The hypothesis is that H3S10 phosphorylation activities of JIL-1 are responsible for antagonizing heterochromatic spreading and silencing independently of JIL-1's effect on chromosome morphology. We transgenically expressed truncated and full-length JIL-1 proteins in both wild-type and JIL-1 null mutant backgrounds and quantified the effect on PEV for different reporters (the chromosomal inversion w^{m4} and the pericentric insertion line *118E-10*) and probed the distribution of heterochromatin marks in these different transgenic flies. To further study the relationship between JIL-1 and heterochromatin factors, we performed the PEV assay on haplo-dosage *JIL-1* with *Su(var)2-5 (HP1)* and *Su(var)3-9*. We show that the haplo-enhancer effect of *JIL-1* has the ability to counterbalance the haplo-suppressor effect of both *Su(var)3-9* and *Su(var)2-5* on position effect variegation

2 How does H3S10 phosphorylation interplay with H3K9 dimethylation regulate gene transcription and chromatin status?

Genetic interaction assays have suggested that the epigenetic histone H3S10ph mark functions to antagonize heterochromatization, thus participating in a dynamic balance between factors promoting repression and those promoting activation of gene expression. In this study, we have explored the relationship between PEV and the relative levels of the H3S10ph and H3K9me2 marks at the *white* gene in both wild-type and w^{m4} background by ChIP-qPCR analysis. To further address the function of JIL-1-mediated H3S10 phosphorylation on chromosome remodeling and transcription regulation at the genome-wide level, we performed chromatin immunoprecipitation combined with next generation sequencing (ChIP-seq) using antibodies specific to JIL-1, H3S10ph or H3K9me2, and we

performed RNA sequencing (RNA-seq) upon depletion of JIL-1. The results show that down-regulation of genes in the *JIL*-1 mutant was correlated with higher levels or acquisition of the H3K9me2 marks whereas up-regulation of a gene was correlated with loss of or diminished H3K9me2.

Thesis Organization

The first chapter of this thesis is a general introduction including background of chromatin status, chromatin remodeling, histone modification "cross talk" and JIL-1 kinase functions. A literature review about chromatin structure, histone modifications, and next generation sequencing is given after the background introduction.

Chapter 2 to Chapter 5 includes four published papers. The first paper was published in *Journal of Cell Science* in 2011. This paper focuses on the position effect variegation (PEV) of the JIL-1 C-terminal domain and the relationship between histone H3S10 phosphorylation and heterochromatin status regulation. Chao Wang made the JIL-1 full-length and truncated transgenic flies, performed the PEV assay, ChIP-qPCR, Immunohistochemistry, immunoblotting, and applied the statistical analysis (Figure 1 to Figure 8). Dr. Huai Deng contributed the Immunohistochemistry of Figure 9.

The second paper was published in *Genetics* in 2011. The paper discussed the haplo-enhancer effect of *JIL-1* counterbalancing the haplo-suppressor effect of both *Su(var)3-9* and *Su(var)2-5* on PEV. Chao Wang did the genetic crosses of *Su(var)2-5*, *Su(var)3-9* and *JIL-1*^{Z2}/*JIL-1*^{Z60}, performed the PEV assays and statistical analysis. Dr. Jack Girton contributed to the genetic cross of JIL-1 mutant and modifiers.

The third paper was published in *Fly (Austin)* in 2012. This paper connected the genetic interaction between H3S10ph and H3K9me2 with the distribution of these epigenetic marks at the *white* gene locus. Chao Wang did the genetic crosses, PEV assays and ChIP-qPCR analysis. Dr. Weili Cai and Yeran Li contributed to the ChIP sample preparation.

The fourth paper was published in *Nucleic Acid Research* in 2014. The paper focuses on JIL-1, H3S10ph and H3K9me2 genome-wide localization and function in the regulation of gene expression. Dr. Weili Cai, Chao Wang and Yeran Li prepared ChIP and RNA samples and the qPCR assay. Dr. Sanzhen Liu contributed to the next generation sequencing (NGS) data trimming. Dr. Weili Cai, Chao Wang, Yeran Li and Lu Shen contributed to the statistical and bioinformatics analysis of NGS data.

Chapter 6 is a general conclusion of JIL-1 functions and discussion about future research directions.

Literature Review

Chromatin structure and organization

In eukaryotic cells, chromatin is the state in which genomic DNA is packaged (Kornberg, 1974). As the fundamental unit of chromatin, the nucleosome contains 4 pairs of core histones (H2A, H2B, H3 and H4) in a wedge-shaped disc, which is wrapped by 146 base pairs of double-stranded genomic DNA (Luger et al, 1997). The “histone fold” motif, which contains 3 alpha helixes with loops, mediates histone interactions within the same nucleosome. The H4 in an H3/H4 tetramer interacts with two H2As in the H2A/H2B

heterodimers to establish the core histone octamer (Luger et al, 1997). The unstructured basic N-terminal domains of histones extending from the core octamer are called “Histone tails”. Several residues in the core histone region and a number of residues within histone tails can be covalently modified. These modifications interact with each other and other histones, DNA, or proteins to regulate chromatin structure and a series of biological processes. (Strahl and Allis, 2000)

The nucleosomes are packed into higher order chromatin structure termed the “30 nm fiber” with the help of linker histone H1 (Finch and Klug, 1976). The 30 nm fibers are further compacted into chromosomes. The specific mechanism of the higher order chromosome packaging in mitosis is still controversial (Hirano, 2002). Three accepted models have been proposed: the radial loop model, the hierarchical folding/axial glue model, and the chromatin network model. The classic radial loop model hypothesizes condensin I/II, ScII and Topoisomerase 2 form an axial scaffold that anchors the 30 nm fibers (Saitoh, et al., 1994). Kireeva et al. (2004) examined early chromosome condensation and propose a hierarchical folding/axial glue model of chromosome structure: in early mitosis, hierarchical folding drives chromatin compaction, whereas axial distribution of topoisomerase II and the condensin stabilizes chromosome shape and compaction later in mitosis (Kireeva et al., 2004). Poirier and Marko’s study supported a network model: there is no mechanically contiguous “scaffold” organized by condensin proteins, instead a “cross-linked” network is a better description of the mitotic chromosome (Poirier and Marko, 2002).

Specialized chromosomes called polytene chromosome are found in some insect, plant and mammalian cells. These specialized chromosomes undergo repeated rounds of DNA replication without cell division, leading to increasing cell volume (Zhimulev, 1996). In the salivary glands of some insects, especially *Drosophila melanogaster*, the polytene chromosomes are widely used as a research model to elucidate in chromosome structure,

protein localization, and transcription factor interaction. There are 1024 copies of sister chromatids aligned precisely in parallel in a *Drosophila* salivary gland nucleus. Under microscopy the “banding patterns” are clearly identified as “band region” and “interband region”. The “band regions” are highly condensed chromatin which represent less active chromatin regions while “interband regions” correspond to less condensed and more active chromatin regions (Zhimulev et al., 2004). Since the polytene chromosome in *Drosophila melanogaster* salivary glands is much bigger than chromosomes form other cell types, the study of polytene chromosome morphology has a great advantage to address the chromosome remodeling process, and to identify mutants of chromatin-related genes due to the alteration of the interphase polytene chromosomes (Wang et al., 2001, Deng et al., 2005, Rath et al., 2006. Eggert et al., 2004, Spierer et al., 2005).

Further study of interphase chromatin identified two distinct types of chromatin: euchromatin and heterochromatin. Euchromatin is usually gene-rich, less compacted and transcriptionally active while heterochromatin is gene-poor, tightly compacted and transcriptionally inactive (Weiler and Wakimoto, 1995). Two subtypes of heterochromatin are further classified as constitutive heterochromatin, which is usually located at the chromosome centromere and telomere regions, and facultative heterochromatin which is regulated and varies between cell types in different species (Oberdoerffer and Sinclair, 2007). Heterochromatin usually contains few genes with highly repetitive satellite DNA and transposable elements (Grewal and Jia, 2007). Heterochromatin also functions in nuclear organization, post-transcriptional gene silencing, higher order structured chromatin interactions, and gene elimination in some somatic cells (Crydermanet al., 1998; Zhimulev and Belyaeva, 2003).

When a gene that normally is present in a euchromatic region is placed in or adjacent to a heterochromatic region, it may be silenced by the inactivating heterochromatic

packaging, giving rise to a mosaic phenotype called position- effect variegation (PEV) (Wallrath and Elgin, 1995). There are two main mechanisms to mediate PEV in the *Drosophila* chromosome. One is mediated by chromosome rearrangements that place euchromatic genes adjacent to a region of centromeric heterochromatin that induces a variegated phenotype by heterochromatic spreading from the breakpoint. The other is mediated by positioning euchromatic chromosomal regions into heterochromatic nuclear compartments by P element insertions that place euchromatic genes into heterochromatic regions (Girton and Johansen, 2008). PEV is strongly affected by trans-acting modifiers that decrease the degree of the mutant phenotype (suppress variegation) or increase the degree of the mutant phenotype (enhance variegation). More than 150 heterochromatin associated proteins including HP1, SuUR, proteins in Su(var) families, and modified histones such as methylated H3K9 have been identified as PEV modifiers that mediate heterochromatin formation and enhance/suppress gene silencing (Weiler and Wakimoto, 1995, Makunin et al., 2002, Kellum, 2003, Cowell et al., 2002). For example, Su(var)3-9 is a histone methyltransferase (HMT) that catalyzes histone H3 lysine 9 residue dimethylation. In Su(var)3-9 null mutants, H3K9 methylation at chromocenter heterochromatin is significantly reduced, which suggests that Su(var)3-9 is the major heterochromatin-specific HMT in *Drosophila* and critical for heterochromatin formation as a PEV suppressor (Schotta et al., 2002).

Histone modifications

Over 60 residues on N-terminal histone tails and a few on core regions of histones can be covalently modified. Till now, nine major classes of modifications have been identified: phosphorylation (ph), methylation (me), acetylation (ac), ubiquitylation (ub),

sumoylation (su), ADPribosylation (ar), biotinylation, deimination, and proline isomerization (Turner, 2005, Kouzarides, 2007, Sterner and Berger, 2000). Evidence has shown that these modifications function in gene transcription and expression regulation, DNA replication, and repair, chromosome structure regulation and chromosome recombination (Shogren-Knaak et al., 2006, Wolffe and Hayes, 1999, Cheung et al., 2000). Most of the modifications are dynamic and reversible, and are controlled by different enzymes. At least two characterized consequences underlying histone modification functions have been identified thus far: remodeling the nucleosomes by disrupting the contacts between them and recruiting other proteins that contain enzymatic activities that remodel nucleosome structure (Kouzarides, 2007). Recently, increasing numbers of proteins have been found to be recruited by different histone modifications. For example, the NURF complex can be recruited to H3K4 trimethylation via a PHD domain (Wysocka et al., 2006) and 14-3-3 can be recruited by H3S10 phosphorylation (Macdonald et al., 2005).

Different histone modifications crosstalk with each other to form different "combinatorial codes" and they recruit different enzymes or chaperones to regulate gene expression (Strahl and Allis, 2000; Turner, 2002). This model proposes that a specific combination of histone modification "codes" will trigger a specific biological process. And different modifications create active or repressive marks to regulate gene transcription. For example H3K9ac, H3K4me and H3K36me are active marks while H3K9me, H3K27me or H4K20me mark inactive gene regions. However, some studies suggest that histone modifications have context-dependent effects, which means the same histone modification combination may direct the biological process to different outcomes in timing and mechanism (Zippo et al., 2009).

Phosphorylation

Till now very little is known about histone phosphorylation. Different kinases are responsible for the phosphorylation on different histone residues. Different histone phosphorylation sites correspond to different events including gene transcription, DNA double strand break repair and apoptosis (Rogakou et al., 1998, Cheung et al., 2003, Yang et al., 2012).

Serine and threonine are two major residues that can be phosphorylated. H3S10 phosphorylation and H3S28 phosphorylation, which are mediated by Aurora B kinase, provide two mitotic markers on the mitotic chromosomes (Giet and Glover, 2001; Adams et al., 2001).

Early studies indicate H3S10 phosphorylation can function in mitotic and meiotic chromosome condensation and segregation (Wei et al., 1999). Increasing evidence suggests that histone phosphorylation, especially H3S10 phosphorylation, is also very important to function in chromatin structure and gene transcription regulation. Some evidence shows that H3S10 phosphorylation plays an important role in transcriptional activation and elongation (Deng et al., 2008, Zippo et al., 2009). But evidence suggests RNA polymerase II-mediated transcription does not require histone H3S10 phosphorylation but instead its effect on transcription is at the chromatin structure level (Cai et al., 2008). Different kinases such as mitogen- and stress-activated kinase 1/2 (MSK1/2) and ribosomal S6 serine-threonine kinase 2 (RSK2) in mammals, have been found to be responsible for phosphorylating H3S10 (Kouzarides, 2007). This phosphorylation is involved in the MAPK (mitogen-activated protein kinase) pathway, and activates ‘‘immediate early’’ (IE) genes such as c-fos and c-jun (Clayton et al., 2000).

JIL-1, a homolog of MSK1/2 and RSK in *Drosophila* is a chromosomal tandem kinase that was first identified through an expression library screen with mAb2A (Johansen

et al., 1996). JIL-1 has been demonstrated to phosphorylate histone H3S10 specifically in interphase cells (Jin et al., 1999; Wang et al., 2001). JIL-1 is also critical for *Drosophila* development and maintaining chromosome structure. Null mutant $JIL\text{-}1^{Z2}/ JIL\text{-}1^{Z2}$ cannot survive to the adult stage and the polytene chromosome structure is disrupted severely (Wang et al., 2001, Zhang et al., 2006, Deng et al., 2005; Deng et al., 2007).

Other histone phosphorylations are associated with chromatin remodeling, DNA repair, and heat shock response. For instance, H2Av S137 phosphorylation is postulated to be critical for poly(ADP-ribose) polymerase 1 (PARP1) activation to further remodel the chromatin for gene transcription activation (Thomas et al., 2014, Kotova et al., 2011).

Methylation

Some lysine and arginine residues on histones can be methylated by a histone methyltransferase (HMT) to regulate transcription activation and repression. Methylations on different residues are characterized as either a transcriptional activation mark or a repression mark. Even on the same residue, different levels of methylation (mono-, di-, or tri-methylation) may lead to different outcomes on the biological process. Methylation on H3K4 (histone H3 lysine 4), H3K79 and H3K36 are associated with gene transcription activation while H3K9, H3K27 and H4K20 methylation are linked to gene transcription repression (Shlatifard, 2006, Kouzarides, 2007).

There are two major types of HMTs in *Drosophila*: SET (Su(var)3-9, Enhancer of Zeste, Trithorax) domain proteins and non-SET domain proteins. In Su(var)3-9, the conserved ~ 140 amino acid SET domain is critical for the activity of histone H3 lysine 9 methylation (Rea et al., 2000). H3K9 methylation is mostly localized in the pericentric region of the chromosomes. It recruits heterochromatin protein 1 (HP1) through its chromo (chromosome organization and modification) domain to stabilize the heterochromatin

(Lachner et al., 2001, Elgin and Grewal, 2007, Schotta et al., 2002). Later studies showed that euchromatic H3K9 can also be methylated by HMT G9a to regulate gene expression (Tachibana et al., 2002). Other histone methylations such as H3K4 methylation by Trx, H3K27 methylation by Polycomb group protein, EZH2, H4K20 methylation by Su(var)4-20 and H3K36 methylation by Set2 play important roles in different biological processes (Yan and Boyd, 2006, Jha and Strahl, 2014, Kouzarides, 2007, Swaminathan et al., 2005).

Arginine methylation is less understood. H3R2, H3R8, H3R17, H3R26 and H4R3 are five well studied arginine methylations (Wysocka et al., 2006, Guccione et al., 2007). They are involved in RNA processing, DNA repair and transcription activation (Shilatifard, 2006).

Acetylation

Unlike methylation involved in both transcription activation and repression, histone acetylation happens only on lysine and is generally associated with gene activation. The balance between histone acetylation by HATs (histone acetyltransferase) and deacetylation by HDACs (Histone deacetylase) is important to regulate gene expression and chromosome structure. Till now, three families of HATs have been identified: GNAT (Gcn5-related N-acetyltansferase), MYST(MOZ/YBF2/SAS2/TIP60), and CBP/p300 (Sterner and Berger, 2000). SAGA, a GCN5 acetyltransferase complex is responsible for the acetylation of H3K14, which results gene expression activation (Grant et al., 1997; Wang et al., 1998). Another widespread histone acetylation is H4K16, which is acetylated by MOF (MYST1). H4K16 is associated with dosage compensation and DNA damage repair (Hilfker et al., 1997, Akhtar et al., 2000, Li et al., 2010). The bromodomain, which contains a conserved sequence with about 100 amino acids, is a motif that binds acetylated residues in many

different proteins. This recognition usually promotes chromatin remodeling and gene activation (Dhalluin et al., 1999).

HDACs are classified into 4 families: HDAC I (HDAC1, 2, 3 and 8), HDAC II (HDAC 4, 5, 6, 7, 9 and 10), HDAC IIII (sirtuins 1-7) and HDAC IV (HDAC 11) (Kouzarides, 2007). HDACs work with HATs to maintain the histone acetylation at the proper level. The HDACs inhibitors are well studied in recent years, as these inhibitors hold potential to be prospective therapeutic drugs for cancer treatment (Dokmanovic et al., 2007, Bolden et al., 2006, Gryder et al., 2013).

Although most of the histone acetylations are active marks, recent studies on H4K12 acetylation suggested that H3K9 methylation and HP1-mediated heterochromatin formation require high level of H4K12 acetylation. (Swaminathan et al., 2005, Zhou et al., 2011).

Histone modifications "cross talk"

Not only do single histone modifications affect biological processes, the interplay between different histone modifications may play an even more important role in gene expression regulation. HAT activity of Gcn5 on H3K14 acetylation is increased more than 10 fold upon H3S10 phosphorylation (Cheung et al., 2000). Also H3S10 phosphorylation can synergize with H4K16 acetylation to facilitate transcription elongation (Zippo et al., 2009). Kusch et al. (2014) found H3K4 methylation can increase H2Av acetylation to mediate H2A/H2Av histone exchange. Other studies on H2Av phosphorylation, H3S10 phosphorylation and poly-ADPribosylation suggest these modifications may interact with each other to regulate transcription (Kotova et al., 2011; Thomas et al., 2014). More and more evidence points towards that histone modifications may establish a complicated multi-

level “network”. A “language” may be more appropriate to describe this network rather than a simple “histone code” (Lee et al., 2010).

Next generation sequencing in epigenetics

In 1975 Sanger and Coulson developed a “Plus and Minus” sequencing method using DNA polymerase with radiolabelled nucleotides (Sanger and Coulson, 1975). Two years later, Sanger and colleagues introduced the "dideoxy" chain-termination method for sequencing DNA molecules, which is called the “Sanger sequencing method” (Sanger et al, 1977). For more than 30 years, the standard “Sanger method” was widely used and become one of the most significant techniques in science history. The “Sanger method” has many advantages such as long reads (up to 1000 bp), easy set up, and sequencing of individual clones. The “Sanger method” tremendously facilitated development of molecular cloning technology, gene manipulation and molecular genetics. However, when biology research moved on to the “genome-wide” and “transcriptome-wide” stage, the “Sanger method” proved too inefficient to satisfy the “high throughput” requirement.

In 2005 a revolution in genomic research started by development of the first practical “next generation” sequencing platform. High throughput, high accuracy and low cost are three major principles in the development of NGS technology (Meaburn and Schulz, 2011). Till today there are three mature and widely used NGS platforms: Roche 454 (GS FLX), Illumina Solexa (GA, Hiseq), and Life Technologies SOLIiD (5500GA, SOLiD 4) (Boley et al., 2014). Roche 454 uses pyrosequencing that produces long read lengths (1000 bp) but requires longer preparation time (Ronaghi et al., 1998). Illumina Solexa has many advantages like relatively lower cost, easy preparation and massive parallel sequencing with high throughput. But short read length production is a limitation of this

platform. Life Technologies SOLiD platform is better than Solexa in accuracy but it requires more complex sample preparation (Metzker, 2009). There are more newly developed NGS techniques which potentially will have better performance in the future such as nanoball sequencing, single molecule real time (SMRT) sequencing, nanopore DNA sequencing, RNA polymerase (RNAP) sequencing, and ion semiconductor sequencing (Rusk, 2011, Porreca, 2010, Stoddart et al., 2009, Pareek et al., 2011).

Waddington defined the term “epigenetics” when he studied cell fate modelling in 1942 (Waddington, 1942). Typically, epigenetics refers to mechanisms that regulate overall or tissue specific transcription/ gene expression levels and cell fate by reversible biochemical modifications of DNA and histones without altering the DNA sequence (Meaburn and Schulz, 2011). There are several major research aspects of epigenetics: DNA methylation, histone modification, chromosome remodeling, antisense RNA, micro-RNA and riboswitch (Ziller et al., 2013, Martinowich et al., 2003, Cruickshanks et al., 2013, Andolfo et al., 2012, Bastet et al., 2011).

Before 2005, genome-wide epigenetics research was largely dependent on DNA microarray technology. For example, ChIP-on-chip (Chromatin immunoprecipitation based on DNA microarray hybridization) was used to study histone modifications and DNA methylation and MeDIP-chip (Methylated DNA immunoprecipitation based on DNA microarray) was applied to the study of DNA methylation. The arrival of NGS technology significantly promoted the development of epigenetics with higher throughput, higher efficiency, higher accuracy, and lower cost.

In recent years a number of sequencing-based methodologies associated with epigenetics have been developed such as WGBS (Whole Genome Bisulfite Sequencing), RRBS (Reduced Representation Bisulfite Sequencing), MeDIP-seq (Methylated DNA Immunoprecipitation Sequencing), ChIP-seq (Chromatin Immunoprecipitation Sequencing),

DNase-seq (DNase I hypersensitive sites Sequencing), RNA-seq (RNA Sequencing) and 3C (Chromosome conformation capture) (Ku et al., 2011). Based on these new technologies, numerous DNA methylation and histone modifications profiles were published, which led epigenetics studies to a “genome-wide age”.

References

Adams RR, Carmena M and Earnshaw WC. (2001) Chromosomal passengers and the (aurora) ABCs of mitosis. *Trends Cell Biol*. 11:49-54.

Akhtar A and Becker PB. (2000) Activation of transcription through histone H4 acetylation by MOF, an acetyltransferase essential for dosage compensation in *Drosophila*. *Mol Cell*. 5(2):367-375.

Andolfo I, Liguori L, De Antonellis P, Cusanelli E, Marinaro F, Pistollato F, Garzia L, De Vita G, Petrosino G, Accordi B, Migliorati R, Basso G, Iolascon A, Cinalli G, Zollo M. (2012) The micro-RNA 199b-5p regulatory circuit involves Hes1, CD15, and epigenetic modifications in medulloblastoma. *Neuro Oncol.* 14(5):596-612.

Baker SP, Grant PA. (2007) The SAGA continues: expanding the cellular role of a transcriptional co-activator complex. *Oncogene*. 26(37):5329-40.

Bao X, Zhang W, Krencik R, Deng H, Wang Y, Girton J, Johansen J and Johansen KM. (2005) The JIL-1 kinase interacts with lamin Dm0 and regulates nuclear lamina morphology of *Drosophila* nurse cells. *J Cell Sci.* 118:5079-5087.

Bao X, Deng H, Johansen J, Girton J, Johansen KM. (2007) Loss-of-function alleles of the JIL-1 histone H3S10 kinase enhance position-effect variegation at pericentric sites in *Drosophila* heterochromatin. *Genetics*. 176(2):1355-8.

Bao X, Cai W, Deng H, Zhang W, Krencik R, Girton J, Johansen J and Johansen KM. (2008) The COOH-terminal domain of the JIL-1 histone H3S10 kinase interacts with histone H3 and is required for correct targeting to chromatin. *J Biol Chem*. 283:32741-32750.

Bastet L, Dubé A, Massé E,Lafontaine DA (2011). New insights into riboswitch regulation mechanisms. *Mol Microbiol.* 80(5):1148-54.

Boeke J, Regnard C, Cai W, Johansen J, Johansen KM, Becker PB, Imhof A.(2010) Phosphorylation of SU(VAR)3-9 by the chromosomal kinase JIL-1. *PLoS One.*5(4):e10042.

Bolden JE, Peart MJ and Johnstone RW. (2006) Anticancer activities of histone deacetylase inhibitors. *Nat Rev Drug Discov.* 5:769-784.

Boyle AP, Furey TS. (2009) High-resolution mapping studies of chromatin and gene regulatory elements. *Epigenomics.* 1;1(2):319-329.

Boley N, Wan KH, Bickel PJ, Celniker SE. (2014) Navigating and mining modENCODE data. *Methods.*15;68(1):38-47.

Cai W, Bao X, Deng H, Jin Y, Girton J, Johansen J and Johansen KM. (2008) RNA polymerase II-mediated transcription at active loci does not require histone H3S10 phosphorylation in *Drosophila*. *Development.* 135:2917-2925.

Cheung P, Allis CD and Sassone-Corsi P. (2000) Signaling to chromatin through histone modifications. *Cell.* 103:263-271.

Cheung WL, Ajiro K, Samejima K, Kloc M, Cheung P, Mizzen CA, Beeser A, Etkin LD, Chernoff J, Earnshaw WJ, and Allis CD. (2003). Apoptotic phosphorylation of histone H2B is mediated by mammalian sterile twenty kinase. *Cell*. 113:507-517.

Clayton AL, Rose S, Barratt MJ and Mahadevan LC. (2000) Phosphoacetylation of histone H3 on *c-fos*- and *c-jun*-associated nucleosomes upon gene activation. *EMBO J.* 19:3714-3726.

Cowell, I.G., Aucott, R., Mahadevaiah, S.K., Burgoyne, P.S., Huskisson, N., Bongiorni, S., Prantera, G., Fanti, L., Pimpinelli, S., Wu, R., Gilbert, D.M., Shi, W., Fundele, R., Morrison, H., Jeppesen, P., and Singh, P.B. (2002) Heterochromatin, HP1 and methylation at lysine 9 of histone H3 in animals. *Chromosoma* 111: 22-36.

Cryderman DE, Cuaycong MH, Elgin SCR and Wallrath LL. (1998) Characterization of sequences associated with position-effect-variegation at pericentric sites in *Drosophila* heterochromatin. *Chromosoma.* 107:277-285.

Cruickshank MN, Oshlack A, Theda C, Davis PG, Martino D, Sheehan P, Dai Y, Saffery R, Doyle LW, Craig JM. (2013) Analysis of epigenetics changes in survivors of

preterm birth reveals the effect of gestational age and evidence for a long term legacy. *Genome Med.*5(10):96

Deng H, Zhang W, Bao X, Martin JN, Girton J, Johansen J and Johansen KM. (2005) The JIL-1 kinase regulates the structure of *Drosophila* polytene chromosomes. *Chromosoma.* 114:173-182.

Deng H, Bao X, Zhang W, Girton J, Johansen J and Johansen KM. (2007) Reduced levels of SU(VAR)3-9 but not SU(VAR)2-5 (HP1) counteract the effects on chromatin structure and viability in loss-of-function mutants of the JIL-1 histone H3S10 kinase. *Genetics.* 177:79-87.

Deng H, Bao X, Cai W, Blacketer MJ, Belmont AS, Girton J, Johansen J and Johansen KM (2008) Ectopic histone H3S10 phosphorylation causes chromatin structure remodeling in *Drosophila*. *Development* 135: 699-705.

Deng, H, Cai W, Wang C, Lerach S, Delattre M, Girton, J, Johansen J and Johansen KM. (2010) JIL-1 and SU(VAR)3-7 interact genetically and counterbalance each others' effect on position effect variegation in *Drosophila*. *Genetics.* 185:1183-1192.

Deuring R, Fanti L, Armstrong JA, Sarte M, Papoulas O, Prestel M, Daubresse G, Verardo M, Moseley SL, Berloco M, Tsukiyama T, Wu C, Pimpinelli S, Tamkun JW. (2000) The ISWI chromatin-remodeling protein is required for gene expression and the maintenance of higher order chromatin structure in vivo. *Mol Cell.* 5(2):355-65.

Dhalluin C, Carlson JE, Zeng L, He C, Aggarwal AK and Zhou MM. (1999) Structure and ligand of a histone acetyltransferase bromodomain. *Nature*. 399(6735):491-496.

Dokmanovic M, Perez G, Xu W, Ngo L, Clarke C, Parmigiani RB and Marks PA. (2007) Histone deacetylase inhibitors selectively suppress expression of HDAC7. *Mol Cancer Ther*. 6(9):2525-2534.

Eggert H, Gortchakov A and Saumweber H. (2004) Identification of the *Drosophila* interband- specific protein Z4 as a DNA-binding zinc-finger protein determining chromosomal structure*. J Cell Sci.* 117:4253-4264.

Elgin SC, and Grewal SI (2003) Heterochromatin: silence is golden. Curr. Biol. 13: R895-898.

Finch JT and Klug A. (1976) Solenoidal model for superstructure in chromatin. *Proc NatlAcad Sci U S A*. 73(6):1897-1901.

Farkas G, Leibovitch BA, Elgin SC. (2000) Chromatin organization and transcriptional control of gene expression in *Drosophila*. *Gene.* 253(2):117-36.

Giet R and Glover DM. (2001) *Drosophila* aurora B kinase is required for histone H3 phosphorylation and condensin recruitment during chromosome condensation and to organize the central spindle during cytokinesis. *J Cell Biol*. 152(4):669-682.

Girton JR and Johansen KM (2008) Chapter 1: Chromatin Structure and the Regulation of Gene Expression: The Lessons of PEV in *Drosophila*. *Adv Genet* 61: 1-43.

Henikoff S. (2008) Nucleosome destabilization in the epigenetic regulation of gene expression. *Nat Rev Genet.* 9:15-26.

Grewal SI and Jia S (2007) Heterochromatin revisited. *Nat Rev Genet* 8: 35-46.

Gryder BE, Rood MK, Johnson KA, Patil V, Raftery ED, Yao LP, Rice M, Azizi B, Doyle DF, Oyelere AK. (2013) Histone deacetylase inhibitors equipped with estrogen receptor modulation activity. *J Med Chem.* 25;56(14):5782-96.

Guccione E, Bassi C, Casadio F, Martinato F, Cesaroni M, Schuchlautz H, Lüscher B and Amati B. (2007) Methylation of histone H3R2 by PRMT6 and H3K4 by an MLL complex are mutually exclusive. *Nature*. 449(7164):933-937.

Hendzel MJ, Wei Y, Mancini MA, Van Hooser A, Ranalli T, Brinkley BR, Bazett-Jones DP and Allis CD. (1997) Mitosis-specific phosphorylation of histone H3 initiates primarily within pericentromeric heterochromatin during G2 and spreads in an ordered fashion coincident with mitotic chromosome condensation. *Chromosoma*.106(6):348-360.

Hilfiker A, Hilfiker-Kleiner D, Pannuti A and Lucchesi JC. (1997) *mof*, a putative acetyl transferase gene related to the *Tip60* and *MOZ* human genes and to the *SAS* genes of yeast, is required for dosage compensation in *Drosophila*. *EMBO J.* 16:2054-2060.

Hirano T. (2000) Chromosome cohesion, condensation, and separation. *Annu Rev Biochem.* 69:115-144.

Jha DK, Strahl BD (2014) An RNA polymerase II-coupled function for histone H3K36 methylation in checkpoint activation and DSB repair. Nat Commun. 9;5:3965.

Jin Y, Wang Y, Walker DL, Dong H, Conley C, Johansen J and Johansen KM. (1999) JIL-1: a novel chromosomal tandem kinase implicated in transcriptional regulation in *Drosophila*. *Mol Cell.* 4:129-135.

Jin Y, Wang Y, Johansen J and Johansen KM. (2000) JIL-1, a chromosomal kinase implicated in regulation of chromatin structure, associates with the MSL dosage compensation complex. *J Cell Biol.* 149:1005-1010.

Johansen KM. (1996) Dynamic remodeling of nuclear architecture during the cell cycle. *J Cell Biochem.* 60:289-296.

Kellum, R. (2003) Is HP1 an RNA detector that functions both in repression and activation? *J. Cell Biol.* 161: 671-672.

Kireeva N, Lakonishok M, Kireev I, Hirano T and Belmont AS. (2004) Visualization of early chromosome condensation: a hierarchical folding, axial glue model of chromosome structure. *J Cell Biol.* 166:775-785.

Kornberg, R.D. (1974). Chromatin structure: a repeating unit of histones and DNA. Science184: 868-871.

Kotova E, Lodhi N, Jarnik M, Pinnola AD, Ji Y and Tulin AV. (2011) *Drosophila* histone H2A variant (H2Av) controls poly(ADP-ribose) polymerase 1 (PARP1) activation in chromatin*. Proc Natl Acad Sci U S A*. 108(15):6205-6210.

Kouzarides T. (2007) Chromatin modifications and their function. *Cell.* 128:693-705.

Ku CS, Naidoo N, Wu M,Soong R. (2011)Studying the epigenome using next generation sequencing.*J Med Genet.* 48(11):721-30.

Lachner M, O'Carroll D, Rea S, Mechtler K and Jenuwein T. (2001) Methylation of histone H3 lysine 9 creates a binding site for HP1 proteins. *Nature.* 410:116-120.

Kusch T, Mei A, Nguyen C. (2014) Histone H3 lysine 4 trimethylation regulates cotranscriptional H2A variant exchange by Tip60 complexes to maximize gene expression. *Proc Natl Acad Sci* 1;111(13):4850-5.

Lee JS, Smith E, Shilatifard A.(2010) The language of histone crosstalk. *Cell.* 142(5):682-5.

Li X, Corsa CA, Pan PW, Wu L, Ferguson D, Yu X, Min J, Dou Y (2010) MOF and H4 K16 acetylation play important roles in DNA damage repair by modulating recruitment of DNA damage repair protein Mdc1. *Mol Cell Biol.* 30(22):5335-47.

Luger K, Mader AW, Richmond RK, Sargent DF and Richmond TJ. (1997) Crystal structure of the nucleosome core particle at 2.8 Å resolution. *Nature.* 389:251-260.

Macdonald N. (2005) Molecular basis for the recognition of phosphorylated and phosphoacetylated histone h3 by 14-3-3. *Mol Cell*. 20(2):199-211.

Makunin, I.V., Volkova, E.I., Belyaeva, E.S., Nabirochkina, E.N., Pirrotta, V., and Zhimulev, I.F. (2002) The *Drosophila* suppressor of underreplication protein binds to late-replicating regions of polytene chromosomes. *Genetics* 160: 1023-1034.

Martinowich K, Hattori D, Wu H, Fouse S, He F, Hu Y, Fan G, Sun Y. (2003) DNA methylation-related chromatin remodeling in activity-dependent BDNF gene regulation. *Science.* 302(5646):890-3.

Meanburn E, Schulz R (2011) Next generation sequencing in epigenetics: insights and challenges. *Semin Cell Dev Biol.* 23(2):192-9

Metzker M (2009) Sequencing technologies — the next generation. *Nature Reviews Genetics* 11, 31-46

Oberdoerffer P and Sinclair DA. (2007) The role of nuclear architecture in genomic instability and ageing. *Nat Rev Mol Cell Biol*. 8(9):692-702.

Pareek CS, Smoczynski R, Tretyn A.(2011) Sequencing technologies and genome sequencing. *J Appl Genet,* 52(4):413-35.

Poirier MG and Marko JF. (2002) Micromechanical studies of mitotic chromosomes. *J Muscle Res Cell Motil*, 23(5-6):409-31.

Porreca GJ (2010) Genome sequencing on nanoballs. *Nat Biotechnol* 28(1):43-4

Rath U, Ding Y, Deng H, Qi H, Bao X, Zhang W, Girton J, Johansen J and Johansen KM. (2006) The chromodomain protein, Chromator, interacts with JIL-1 kinase and regulates the structure of *Drosophila* polytene chromosomes. *J Cell Sci.* 119:2332-2341.

Rea S, Eisenhaber F, O'Carroll D, Strahl BD, Sun ZW, Schmid M, Opravil S, Mechtler K, Ponting CP, Allis CD and Jenuwein T. (2000) Regulation of chromatin structure by site-specific histone H3 methyltransferases. *Nature*. 406(6796):593-599.

Rogakou EP, Pilch DR, Orr AH, Ivanova VS, and Bonner WM. (1998). DNA double-stranded breaks induce histone H2A.X phosphorylation on serine 139. *J Biol Chem*. 273:5858-5868.

Ronaghi M, Uhlén M, Nyrén P (1998) A Sequencing Method Based on Real-Time Pyrophosphate. *Science*. 281 (5375), 363-365.

Rusk, N. (2011). Torrents of sequence. *Nat Meth* 8(1): 44-44.

Saitoh N, Goldberg IG, Wood ER and Earnshaw WC. (1994) ScII: an abundant chromosome scaffold protein is a member of a family of putative ATPases with an unusual predicted tertiary structure. *J Cell Biol.* 127:303–318

Sanger F, Coulson AR (1975) A rapid method for determining sequences in DNA by primed synthesis with DNA polymerase. *J Mol Biol.* 25;94(3):441-8

Sanger F, Nicklen S, Coulson AR. (1977) DNA sequencing with chain-terminating inhibitors. *Proc Natl Acad Sci* 74(12):5463-7.

Sassone-Corsi P, Mizzen CA, Cheung P, Crosio C, Monaco L, Jacquot S, Hanauer A and Allis CD. (1999) Requirement of Rsk-2 for epidermal growth factor-activated phosphorylation of histone H3. *Science.* 285:886-891.

Schotta, G., Ebert, A., Krauss, V., Fischer, A., Hoffmann, J., Rea, S., Jenuwein, T., Dorn, R., Reuter, G. (2002). Central role of *Drosophila* SU(VAR)3-9 in histone H3-K9 methylation and heterochromatic gene silencing. *EMBO J.* 21**,** 1121-1131.

Shilatifard A. (2006) Chromatin Modifications by Methylation and Ubiquitination: Implications in the Regulation of Gene Expression. *Annu Rev Biochem.* 75:243–269.

Shogren-Knaak M, Ishii H, Sun JM, Pazin MJ, Davie JR and Peterson CL. (2006) Histone H4- K16 acetylation controls chromatin structure and protein interactions. *Science.* 311:844-847.

Spierer A, Seum C, Delattre M and Spierer P. (2005) Loss of the modifiers of variegation SU(VAR)3-7 or HP1 impacts male X polytene chromosome morphology and dosage compensation. *J Cell Sci.* 118:5047-5057.

Sterner DE and Berger SL. (2000) Acetylation of histones and transcription-related factors. *Microbiol Mol Biol Rev*. 64(2):435-459.

Stoddart D, Heron AJ, Mikhailova E, Maglia G, Bayley H. (2009) Single-nucleotide discrimination in immobilized DNA oligonucleotides with a biological nanopore. *Proc Natl Acad Sci* 12;106(19):7702-7.

Strahl BD and Allis CD. (2000) The language of covalent histone modifications. *Nature.*403:41-45.

Swaminathan J, Baxter EM and Corces VG. (2005) The role of histone H2Av variant replacement and histone H4 acetylation in the establishment of *Drosophila* heterochromatin. *Genes Dev.* 19:65–76.

Tachibana M, Sugimoto K, Nozaki M, Ueda J, Ohta T, Ohki M, Fukuda M, Takeda N, Niida H, Kato H, and Shinkai Y (2002) G9a histone methyltransferase plays a dominant role in euchromatic histone H3 lysine 9 methylation and is essential for early embryogenesis. *Genes Dev.* 16:1779-1791.

Thomas C, Kotova E, Andrake M, Adolf-Bryfogle, J, Glaser R, Regnard C, Tulin AV (2014) Kinase-Mediated Changes in Nucleosome Conformation Trigger Chromatin Decondensation via Poly(ADP-Ribosyl)ation *Mol Cell*.6;53(5):831-42

Turner BM. (2002) Cellular memory and the histone code. *Cell.* 111(3):285-91.

Turner BM. (2005) Reading signals on the nucleosome with a new nomenclature for modified histones. *Nat Struct Mol Biol.* 12:110-112.

Waddington C. (1942) The epigenotype. *Endeavour* 1942;1:18–20.

Wallrath L, and Elgin S. (1995) *Genes Dev*. 9, 1263-1277.

Wang Y, Zhang W, Jin Y, Johansen J and Johansen KM. (2001) The JIL-1 tandem kinase mediates histone H3 phosphorylation and is required for maintenance of chromatin structure in *Drosophila*. *Cell* 105:433-443.

Wei Y, Yu L, Bowen J, Gorovsky MA and Allis CD. (1999) Phosphorylation of histone H3 is required for proper chromosome condensation and segregation. *Cell*. 97(1):99-109.

Weiler KS and Wakimoto BT. (1995) Heterochromatin and gene expression in *Drosophila*. *Annu Rev Genet.* 29:577-605.

Wolffe AP and Hayes JJ. (1999) Chromatin disruption and modification. *Nucl Acids Res*. 27:711-720.

Wysocka J, Swigut T, Xiao H, Milne TA, Kwon SY, Landry J, Kauer M, Tackett AJ, Chait BT, Badenhorst P, Wu C and Allis CD. (2006) A PHD finger of NURF couples histone H3 lysine 4 trimethylation with chromatin remodelling. *Nature.* 442:86-90.

Yan C and Boyd DD (2006) Regulation of matrix metalloproteinase gene expression. J Cell Physiol. 211(1):19-26.

Yang W, Xia Y, Hawke D, Li X, Liang J, Xing D, Aldape K, Hunter T, Yung WK, Lu Z (2012) PKM2 Phosphorylates Histone H3 and Promotes Gene Transcription and Tumorigenesis, *Cell* 150(4):685-96

Zhang W, Deng H, Bao X, Lerach S, Girton J, Johansen J and Johansen KM. (2006) The JIL-1 histone H3S10 kinase regulates dimethyl H3K9 modifications and heterochromatic spreading in *Drosophila*. *Development.* 133:229-235.

Zhimulev IF. (1996) Morphology and structure of polytene chromosomes. *Adv Genet.* 34:1-497.

Zhimulev IF and Belyaeva ES. (2003) Intercalary heterochromatin and genetic silencing. *Bioassays.* 25:1040-1051.

Zhimulev IF, Belyaeva ES, Semeshin VF, Koryakov DE, Demakov SA, Demakova OV, Pokholkova GV and Andreyeva EN. (2004) Polytene chromosomes: 70 years of geneticresearch. *Int Rev Cytol.* 241:203–275.

Zhou B, Wang S, Zhang Y, Fu X, Dang W, Lenzmeier BA and Zhou J. (2011) Histone H4 lysine 12 acetylation regulates telomeric heterochromatin plasticity in Saccharomyces cerevisiae. *PLoS Genet.* 7(1) e1001272.

Ziller MJ, Gu H, Müller F, Donaghey J, Tsai LT, Kohlbacher O, De Jager PL, Rosen ED, Bennett DA, Bernstein BE, Gnirke A, Meissner A.(2013) Charting a dynamic DNA methylation landscape of the human genome. *Nature*. 500(7463):477-81.

Zippo A, Serafini R, Rocchigiani M, Pennacchini S, Krepelova A and Oliviero S. (2009) Histone crosstalk between H3S10ph and H4K16ac generates a histone code that mediates transcription elongation. *Cell*. 138(6):1122-1136.

CHAPTER 2. THE EPIGENETIC H3S10ph MARK IS REQUIRED FOR COUNTERACTING HETEROCHROMATIC SPREADING AND GENE SILENCING IN *DROSOPHILA*

A paper published in the *Journal of Cell Science*

Chao Wang, Weili Cai, Yeran Li, Huai Deng, Xiaomin Bao, Jack Girton,
Jørgen Johansen and Kristen M. Johansen

Summary

The JIL-1 kinase localizes specifically to euchromatin interband regions of polytene chromosomes and is the kinase responsible for histone H3S10 phosphorylation at interphase. Genetic interaction assays with strong *JIL-1* hypomorphic loss-of-function alleles have demonstrated that JIL-1 can counterbalance the effect of the major heterochromatin components on position-effect variegation (PEV) and gene silencing. However, it has not been clear whether this was a causative effect of the epigenetic H3S10ph mark or whether JIL-1's effect on PEV instead was caused by other functions or structural features of the JIL-1 protein. Here we show by transgenically expressing various truncated versions of JIL-1, with or without kinase activity, and assessing their effect on PEV and heterochromatic spreading that the gross perturbation of polytene chromosome morphology observed in *JIL-1* null mutants is unrelated to gene silencing in PEV and is likely a result of faulty polytene chromosome alignment and/or organization separate from epigenetic regulation of chromatin structure. Furthermore, the findings provide evidence that the epigenetic H3S10 phosphorylation mark itself is necessary for causing the

prevention of the observed heterochromatic spreading independently of any structural contributions from the JIL-1 protein.

Introduction

The JIL-1 kinase is a multidomain protein that localizes specifically to euchromatin interband regions of polytene chromosomes and is the kinase responsible for histone H3S10 phosphorylation at interphase (Jin et al., 1999; Wang et al., 2001). Mutational analyses have shown that *JIL-1* is essential for viability (Wang et al., 2001; Zhang et al., 2003) and that a reduction in JIL-1 kinase activity leads to a global disruption of polytene chromosome morphology (Wang et al., 2001; Deng et al., 2005). Furthermore genetic interaction assays with *JIL-1* hypomorphic and null allelic combinations demonstrated that JIL-1 can counterbalance the effect of the three major heterochromatin components Su(var)3-9, Su(var)3-7, and Su(var)2-5 (HP1a) on position-effect variegation (PEV) (Deng et al., 2010; Wang et al., 2011). Based on these observations it has been proposed that the epigenetic H3S10ph mark functions to counteract heterochromatic spreading and gene silencing in *Drosophila* (Ebert et al., 2004; Zhang et al., 2006; Deng et al., 2007; 2010). However, the previous experiments were not able to rule out that JIL-1's effect on PEV instead was caused by the gross alterations of polytene chromosome morphology observed in the absence of JIL-1 or due to structural contributions of the JIL-1 protein independent of its H3S10 phosphorylation activity. In order to distinguish between these scenarios we have cloned various full-length and truncated versions of JIL-1 into the pYES vector that contains a *yellow* selection marker (Patton et al., 1992), generated transgenic animals, and assessed the effect of these lines on PEV of two different reporters, the chromosomal

inversion w^{m4} and the pericentric insertion line *118E-10*. Especially, we have taken advantage of the finding that the CTD-domain alone, that is completely without kinase activity, can restore partial viability and fully rescue the gross alteration in polytene chromosome morphology of *JIL-1* null mutants (Bao et al., 2008). We show that expression of the CTD-domain in a wild-type background displaces native JIL-1, reduces H3S10 phosphorylation dramatically, and phenocopies the effect of strong *JIL-1* hypomorphic mutations on PEV. In addition, we provide evidence that expression of the CTD domain in a *JIL-1* null mutant background enhanced PEV of the *118E-10* allele even when overall polytene chromosome morphology was restored to normal. In contrast, expression of a CTD construct that is without the CTD domain, but that retains its ability to phosphorylate H3S10 strongly suppressed PEV of the *118E-10* allele. Taken together these findings strongly support the hypothesis that the epigenetic H3S10ph mark is necessary to counteract heterochromatic spreading and gene silencing.

Results

JIL-1 transgene expression.

JIL-1 can be divided into four main domains including a NH_2-terminal domain (NTD), the first kinase domain (KDI), the second kinase domain (KDII), and a COOH-terminal domain (CTD) (Jin et al., 1999) (Fig. 1A). In order to further explore the relative contributions of the different JIL-1 domains and the H3S10 phosphorylation mark to regulation of PEV we expressed three CFP-tagged JIL-1 UAS P-element insertion constructs transgenically in wild-type and *JIL-1* null mutant animals using the pYES vector

(Patton et al., 1992). This vector contains a *yellow* selection marker to avoid any influence on eye pigmentation levels. A full-length construct (FL), a construct without the COOH-terminal domain (CTD), and a construct containing only the COOH-terminal domain (CTD) were made (Fig. 1A). All three constructs had properties identical to those previously reported for similar GFP- or CFP-tagged JIL-1 constructs (Wang et al., 2001; Bao et al., 2008). In addition, a transgenic line was selected for each construct that expressed at levels comparable to those of endogenous JIL-1 using a *da-GAL4* driver line as illustrated in Fig. 1B. FL rescued all aspects of the *JIL-1* null mutant phenotype including polytene chromosome morphology, viability, and like endogenous JIL-1, FL was upregulated on the male X chromosome (data not shown). The CTD lacks the COOH-terminal sequences required for proper chromatin localization leading to mislocalization of the protein (Bao et al., 2008). However, it does retain its kinase activity resulting in ectopic histone H3S10 phosphorylation (Bao et al., 2008). Interestingly, the *JIL-1*$^{Su(var)3-1}$ series of alleles generates truncated proteins with COOH-terminal deletions (Fig. 1A) that also mislocalize to ectopic chromatin sites (Zhang et al., 2006) and give rise to some of the strongest suppressor-of-variegation phenotypes yet described (Ebert et al., 2004; Lerach et al., 2006). The CTD rescues autosome polytene chromosome morphology but only partially rescues that of the male X chromosome in *JIL-1* null mutants (Bao et al., 2008). In contrast, the CTD fully restores *JIL-1* null mutant chromosome morphology including that of the male X chromosome (Bao et al., 2008). Furthermore, when the CTD is expressed in a wild-type background it has a dominant-negative effect and displaces endogenous JIL-1 (Bao et al., 2008) leading to a striking decrease in histone H3S10ph levels as shown in Fig. 1C.

The effect of CTD expression on regulation of PEV in a wild-type JIL-1 background

PEV in *Drosophila* occurs when euchromatic genes are transcriptionally silenced as

a result of their placement in or near heterochromatin (reviewed in Girton and Johansen, 2008). Silencing typically occurs in only a subset of cells and can be heritable leading to mosaic patterns of gene expression (Schotta et al., 2003; Delattre et al., 2004). PEV in *Drosophila* has served as a major paradigm for the identification and genetic analysis of evolutionarily conserved determinants of epigenetic regulation of chromatin structure (Schotta et al., 2003; reviewed in Girton and Johansen, 2008). In previous experiments we have shown that combinations of strong *JIL-1* hypomorphic loss-of-function mutations act as enhancers of PEV of transgenes inserted directly into pericentric heterochromatin (Bao et al., 2007). Furthermore, in the absence of the JIL-1 kinase the major heterochromatin marker H3K9me2 spreads to ectopic locations on the chromosome arms with the most pronounced increase on the X chromosome (Zhang et al., 2006; Deng et al., 2007). These findings suggested a model for a dynamic balance between euchromatin and heterochromatin, where the boundary between these two types of chromatin is regulated by the state of histone H3S10 phosphorylation (Ebert et al., 2004; Zhang et al., 2006; Deng et al., 2007; 2010). In order to determine whether the H3S10ph mark itself was required to control this balance we explored the effect of expression of the CTD on the regulation of PEV caused by both a P-element insertion of a reporter gene (*118E-10*) as well as of a chromosome rearrangement (w^{m4}).

118E-10. Insertion of the P element (*P[hsp26-pt, hsp70-w]*) into euchromatic sites results in a uniform red eye phenotype whereas insertion into a known heterochromatic region of the fourth chromosome (line *118E-10*) results in a variegating eye phenotype (Figure 2A) (Wallrath and Elgin, 1995; Wallrath et al., 1996; Cryderman et al., 1998; Bao et al., 2007). In the experiments we compared the eye pigment levels of flies homozygous for the transgenic reporter line *118E-10* and expressing the CTD or the CTD, respectively. Pigment assays were performed essentially as in Kavi and Birchler (2009) using 3 sets of

10 pooled fly heads from each genotype. Although both male and female flies were scored, due to sex differences only results from male flies are shown. However, the trend observed in female flies was identical to that in male flies. As illustrated in Figs. 2A and 2B, expression of the CTD enhances PEV as indicated by the increased proportion of white ommatidia and a 55% decrease in the optical density (OD) of the eye pigment levels (0.0168±0.0031, n=3) as compared to control flies (0.0370±0.0035, n=3). This reduction was statistically significant ($p<0.002$). In contrast, expression of the CTD suppresses PEV as indicated by an increase of the proportion of red ommatidia and a statistically significant ($p<0.0001$) 305% increase in the OD of the eye pigment levels (0.1130±0.0074, n=3). These opposite effects on PEV of the CTD and CTD correlates well with the finding that expression of the CTD depressed histone H3S10 phosphorylation whereas H3S10ph levels remained robust when CTD was expressed (Fig. 1C). Furthermore, as illustrated in Fig. 3 of polytene squash preparations from larvae expressing the CTD, the heterochromatic H3K9me2 mark spread to the chromosome arms with especially pronounced spreading on the X chromosome in both male and females as would be predicted by the model in the absence of H3S10 phosphorylation (Deng et al., 2007; 2010).

w^{m4}. The *In(1)*w^{m4} X chromosome contains an inversion that juxtaposes the euchromatic *white* gene and centric heterochromatic sequences distal to the nucleolus organizer (Muller 1930; Pirrotta et al., 1983). The resulting somatic variegation of w^{m4} expression occurs in clonal patches in the eye reflecting heterochromatic spreading from the inversion breakpoint that silences w^{m4} expression in the white patches and euchromatic packaging of the *w* gene in those patches that appear red (reviewed in Grewal and Elgin 2002). Studies of this effect suggest that the degree of spreading may depend on the amount of heterochromatic factors at the breakpoint (reviewed in Weiler and Wakimoto 1995; Girton and Johansen 2008). Interestingly, strong hypomorphic combinations of *JIL-1*

alleles, in which heterochromatic factors spread to ectopic locations (Zhang et al., 2006; Deng et al., 2007), act as suppressors not enhancers of PEV of the w^{m4} allele (Lerach et al., 2006). Based on these findings Lerach et al. (2006) proposed a model where the suppression of PEV of w^{m4} in strong *JIL-1* hypomorphic backgrounds is due to a reduction in the level of heterochromatic factors at the pericentromeric heterochromatin near the inversion breakpoint site that reduces its potential for heterochromatic spreading and silencing. Thus a prediction of this model is that expression of the CTD and the CTD both should lead to suppression of PEV of w^{m4}. To test this hypothesis we expressed the CTD and the CTD in w^{m4}/Y flies. As illustrated in Figures 4A and 4B, expression of the CTD suppressed PEV as indicated by the increased proportion of red ommatidia and a 343% increase in the optical density (OD) of the eye pigment levels (0.1223±0.0120, n=3) as compared to control flies (0.0357±0.0038, n=3). This increase was statistically significant ($p<0.0005$). Expression of the CTD also suppressed PEV as indicated by an increase of the proportion of red ommatidia and a statistically significant ($p<0.005$) 348% (0.1243±0.0214, n=3) increase in the OD of the eye pigment levels providing strong support for the hypothesis of Lerach et al. (2006).

The effect of CTD expression on regulation of PEV in a JIL-1 null background

The finding that CTD or CTD expression can partially rescue the viability of *JIL-1* null mutants allowed us to further examine the effect of expression of these constructs on PEV of *118E-10* in the absence of endogenous JIL-1. For these experiment we first recombined the *da-GAL4* driver onto the $JIL\text{-}1^{z2}$ chromosome in order to generate "*JIL-1* transgene"/+; $JIL\text{-}1^{z2}$/ $JIL\text{-}1^{z2}$ *da-GAL4*; *118E-10*/+ flies. The $JIL\text{-}1^{z2}$ allele is a true null allele generated by P-element mobilization (Wang et al., 2001; Zhang et al., 2003). As illustrated in Fig. 5 when the FL was expressed in such a genetic background it led to a variegated eye phenotype with an OD of the eye pigment levels of 0.0163±0.0007 (n=3). However,

when the CTD was expressed PEV was enhanced as indicated by a decrease in the proportion of red ommatidia and a statistically significant ($p<0.0001$) 54% decrease in the OD (0.0075±0.0002, n=3) of eye pigment levels (Fig. 5A and 5B). In contrast, expression of the CTD led to suppression of PEV as indicated by an increase in the proportion of red ommatidia and a statistically significant ($p<0.0001$) 151% increase in the OD (0.0246±0.0018, n=3) of eye pigment levels as compared to when the FL was expressed (Fig. 5A and 5B). Immunoblot analysis demonstrated that the expression levels of the FL, CTD, and CTD were comparable (Fig. 6A). Furthermore, while the FL phosphorylated histone H3S10 close to wild-type levels, the CTD phosphorylated H3S10 at enhanced levels, whereas there was no detectable levels of H3S10ph when the CTD was expressed (Fig. 6B). Thus, the observed effects of expression of these constructs on PEV correlated well with the degree to which they phosphorylated histone H3S10.

In order to directly demonstrate that H3S10ph and H3K9me2 levels at the *hsp70-white* gene reporter in the P-element insertion line *118E-10* were affected in the experiments, we performed ChIP assays as in Legube et al. (2006). Chromatin was immunoprecipitated (ip) from salivary glands from "*JIL-1* transgene"/+; *JIL-1*^{z2}/ *JIL-1*^{z2} *da-GAL4*; *118E-10*/+ larvae using rabbit anti-H3S10ph antibody or with purified rabbit IgG antibody (negative control) or with mAbs to H3K9me2 or GST (negative control). Primers corresponding to the *hsp70-white* gene were used to amplify the precipitated material (Hines et al., 2009). Experiments were done in duplicate and relative enrichment of *hsp70-white* DNA from the H3S10ph and H3K9me2 ips were normalized to the corresponding control antibody ips performed in tandem for each experimental sample. As illustrated in Fig. 7A in FL expressing salivary glands there was an approximately 5 fold relative enrichment of H3S10ph immunoprecipitated *hsp70-white* DNA compared to the control ip. This enrichment increased to about 100 fold when CTD was expressed. In contrast, in

CTD expressing salivary glands the relative enrichment was close to control levels (Fig. 7A). Figure 7B shows that when FL or CTD was expressed the relative enrichment of H3K9me2 immunoprecipitated *hsp70-white* DNA was very low. However, when the CTD was expressed there was an approximately 3-4 fold increase in the relative enrichment level as compared to when FL or CTD was expressed. These experiments indicate that H3S10ph and H3K9me2 levels at the *hsp70-white* reporter gene in *118E-10* were directly correlated with the different H3S10 phosphorylation capabilities of FL, CTD, and CTD. Furthermore, the results show that in the absence of H3S10 phosphorylation as in CTD expressing salivary glands there were a concomitant increase in H3K9me2 levels at the *hsp70-white* reporter gene.

In order to determine how this effect on PEV correlated with polytene chromosome morphology and H3K9me2 localization we performed immunolabeling of polytene squash preparations. As illustrated in Fig. 8 in a *JIL-1*^{z2} null background without transgene expression polytene morphology is greatly perturbed with ectopic spreading of the H3K9me2 mark especially prominent on the X chromosome. Expression of the FL or the CTD construct restored the chromosome morphology and prevented the H3K9me2 spreading (Fig. 8). Interestingly, however; expression of the CTD restored chromosome morphology without counteracting the heterochromatic spreading of the H3K9me2 mark in both males and females. Taken together these findings suggest that the H3S10ph mark is required to counteract heterochromatic spreading and that this effect is independent from any potential structural contributions from the JIL-1 protein. However, these experiments could not rule out that the presence of the NTD and/or the kinase domains present in the full-length JIL-1 protein in the absence of kinase activity would be able to prevent the spreading of the H3K9me2 mark. Thus, in order to further address this issue we expressed a "kinase dead" version of full-length JIL-1 in which the crucial lysine for catalytic activity in

each of the two kinase domains (K^{293} and K^{652}) was changed to alanine and which previously has been shown to be without kinase activity (Deng et al., 2008) in a *JIL-1* null mutant background. As illustrated in Fig. 9 expression of this construct, which only differs from wild-type JIL-1 at two amino acid positions, did not prevent the spreading of the heterochromatic mark H3K9me2. This is in contrast to preparations expressing the CTD that retains its H3S10ph kinase activity (Bao et al., 2008) and where no heterochromatic spreading could be detected (Fig. 8), strongly suggesting that the H3S10ph mark is required for counteracting this activity.

Discussion

In this study we have explored the hypothesis that the epigenetic H3S10ph mark is required to counteract heterochromatic spreading and gene silencing in *Drosophila*. We show that when the CTD-domain, which displaces endogenous JIL-1, was expressed in a wild-type background it had a dominant-negative effect and essentially phenocopied the effect of hypomorphic *JIL-1* alleles on PEV. These effects on PEV were correlated with the spreading of the heterochromatic mark H3K9me2 to the chromosome arms and a decrease in H3S10ph levels. Furthermore, we demonstrate that expression of the CTD-domain in a *JIL-1* null mutant background enhanced PEV of the *118E-10* allele compared to when a wild-type JIL-1 construct was expressed. Interestingly, although spreading of the heterochromatic H3K9me2 mark was not counteracted by expression of the CTD in the absence of H3S10 phosphorylation, the grossly perturbed polytene chromosomes of the *JIL-1* null mutant salivary glands were restored to essentially wild-type morphology. Moreover, a "kinase dead" version of JIL-1 that only differed from wild-type JIL-1 at two amino acid positions did not prevent the heterochromatic spreading. Taken together these

findings suggest that: 1) the gross perturbation of polytene chromosome morphology observed in *JIL-1* null mutants is unrelated to gene silencing in PEV and is likely a result of faulty polytene chromosome alignment and/or organization separate from epigenetic regulation of chromatin structure; 2) structural contributions from the JIL-1 protein are unlikely to play a role in counteracting heterochromatic spreading and gene silencing in PEV; 3) the epigenetic H3S10 phosphorylation mark is required for preventing the observed heterochromatic spreading as well as gene silencing in PEV assays.

It should be noted that it recently has been demonstrated that JIL-1 can directly interact with Su(var)3-9 and potentially regulate its function by phosphorylating it at residue S191 (Boeke et al., 2010). However, phosphorylation of Su(var)3-9 by JIL-1 did not affect its enzymatic activity or its ability to repress transcription (Boeke et al., 2010). Furthermore, the direct protein-protein interaction is mediated by the COOH-terminus of JIL-1 (Boeke et al., 2010). Since expression of the CTD, which lacks this interaction domain, prevented heterochromatic spreading in a *JIL-1* mutant background, it is not likely that phosphorylation of Su(var)3-9 by JIL-1 is involved in regulating its role in PEV. However, an interesting possibility is that direct interactions between JIL-1 and Su(var)3-9 may contribute to other aspects of the *JIL-1* null phenotype. For example, in genetic interaction assays monitoring the lethality as well as the polytene chromosome morphology defects associated with the null *JIL-1* phenotype, among the three major heterochromatin components only a reduction in the dose of the *Su(var)3-9* gene rescued both phenotypes (Zhang et al., 2006; Deng et al., 2007; 2010). A reduction of *Su(var)3-7* rescued the lethality, but not the chromosome defects (Deng et al., 2010), and no genetic interactions were detectable between *JIL-1* and *Su(var)2-5* in these assays (Deng et al., 2007). Thus, these findings indicate that while Su(var)3-9 activity may be a contributing factor in the lethality and polytene chromatin structure perturbations associated with loss of the JIL-1 histone H3S10 kinase, these

effects are likely to be uncoupled from HP1a and to a lesser degree from Su(var)3-7. Thus, these findings provide additional evidence that these parameters are likely to be independent of and separate from the mechanisms of classical heterochromatin assembly and gene silencing. This hypothesis is supported by experiments probing for dynamic interactions between loss-of-function alleles of *JIL-1* and *Su(var)3-9*, *Su(var)3-7*, or *Su(var)2-5* using PEV assays (Deng et al., 2010; Wang et al., 2011). In these assays a direct antagonistic and counterbalancing effect on gene expression between JIL-1 and all three heterochromatic factors have been demonstrated.

Almost all known histone modifications correlate with activating or repressive functions dependent on which histone variant or amino acid residue is modified (Allis et al., 2007). However, these histone modifications do not occur in isolation but rather in a combinatorial manner leading to both synergistic and antagonistic pathways (Allis et al., 2007) in which the same mark may participate (Berger 2007). This has made it difficult to establish a defined causative biological effect of the addition or removal of a single mark in vivo. Here we have provided evidence that the histone H3S10ph mark at euchromatic regions is required for counteracting the spreading of heterochromatic factors and gene silencing. This repression of gene activity is likely to be independent of a direct effect on the transcriptional machinery since it has been demonstrated that RNA polymerase II-mediated transcription occurs at robust levels in the absence of H3S10 phosphorylation in *Drosophila* (Cai et al., 2008). Furthermore, using a LacI-tethering system Deng et al. (2008) provided direct evidence that phosphorylation of the histone H3S10 residue by JIL-1 can play a causative role in establishing euchromatic chromatin regions. Thus, these findings together with those of the present study strongly support the hypothesis that a function of the epigenetic histone H3S10ph mark is to antagonize heterochromatization by participating in a dynamic balance between factors promoting repression and activation of gene expression.

Materials and Methods

JIL-1 CFP-tagged fusion constructs

A full length JIL-1 (1-1207) construct (FL), a CTD construct containing residue 1-926, and a CTD construct containing sequences from aa 927-1207 with an in-frame CFP-tag were cloned into the pYES vector (Patton et al., 1992) using standard methods (Sambrook and Russell, 2001). For the CTD construct that did not contain the endogenous JIL-1 nuclear localization sequence (NLS) that is situated in the NH_2-terminal domain (Jin et al., 1999) the NLS from Clontech's NLS-pECFP vector was added to the NH_2-terminus. The fidelity of all constructs was verified by sequencing at the Iowa State University Sequencing facility.

Drosophila melanogaster stocks

Fly stocks were maintained at 25°C according to standard protocols (Roberts, 1998). The *JIL-1*^{z2} null allele is described in Wang et al. (2001) as well as in Zhang et al. (2003). JIL-1 construct pYES lines were generated by standard P-element transformation (BestGene, Inc.) and expression of the transgenes were driven using a *da-GAL4* driver introduced by standard genetic crosses. Recombinant *JIL-1*^{z2} *da-GAL4* chromosomes were generated as described in Ji et al. (2005) and the presence of *JIL-1*^{z2} confirmed by PCR as in Zhang et al. (2003). Expression levels of each of the JIL-1 constructs were monitored by immunoblot analysis as described below. The "kinase dead" lacI-JIL-1 construct was previously described in Deng et al. (2008) and driven using the *Sgs3-GAL4* driver. All driver lines and the *In(1)w*^{m4} allele was obtained from the Bloomington Stock Center. The P-

element insertion line *118E-10* was the generous gift of Dr. L. Wallrath. Balancer chromosomes and markers are described in Lindsley and Zimm (1992).

PEV assays were performed as previously described (Lerach et al., 2006; Bao et al., 2007; Deng et al., 2010; Wang et al., 2011). In short, we generated flies expressing the various JIL-1 constructs in a background of the two PEV arrangements, *118E-10* or w^{m4}, by standard crossing. To quantify the variegated phenotype adult flies were collected from the respective crosses at eclosion, aged 6 days at 25°C, frozen in liquid nitrogen, and stored at -80˚C until assayed. The pigment assays were performed essentially as in Kavi and Birchler (2009) using three sets of 10 fly heads of each genotype collected from males and females, respectively. For each sample the heads from the 10 flies were homogenized in 200 µl of methanol with 0.1% hydrochloric acid, centrifuged, and the optical density (OD) of the supernatant spectrophotometrically measured at a wavelength of 480 nm. Statistical comparisons were performed using a two-tailed Student's t-test. Eyes from representative individuals from these crosses were photographed using an Olympus Stereo Microscope and a Spot digital camera (Diagnostic Instruments).

Immunohistochemistry

Standard polytene chromosome squash preparations were performed as in Cai et al. (2010) using either 1 or 5 minute fixation protocols and labeled with antibody as described in Jin et al. (1999) and in Wang et al. (2001). In some preparations the male X chromosome was identified by double labeling with MSL antibody as previously described (Jin et al., 2000). Primary antibodies used in this study include rabbit anti-H3S10ph (Cell Signaling), rabbit anti-histone H3 (Cell Signaling), rabbit anti-MSL-2 (generous gift of Dr. M. Kuroda, Harvard University, Boston), Rabbit anti-H3K9me2 (Upstate Biotechnology), mouse anti-tubulin (Sigma), rabbit anti-JIL-1 (Jin et al., 1999), chicken anti-JIL-1 (Jin et al.,

2000), and anti-JIL-1 mAb 5C9 (Jin et al., 2000). DNA was visualized by staining with Hoechst 33258 (Molecular Probes) in PBS. The appropriate species- and isotype- specific Texas Red-, TRITC-, and FITC-conjugated secondary antibodies (Cappel/ICN, Southern Biotech) were used (1:200 dilution) to visualize primary antibody labeling. The final preparations were mounted in 90% glycerol containing 0.5% *n*-propyl gallate. The preparations were examined using epifluorescence optics on a Zeiss Axioskop microscope and images were captured and digitized using a cooled Spot CCD camera. Images were imported into Photoshop where they were pseudocolored, image processed, and merged. In some images non-linear adjustments were made to the channel with Hoechst labeling for optimal visualization of chromosomes.

Immunoblot analysis

Protein extracts were prepared from adult flies or from dissected third instar larval salivary glands homogenized in a buffer containing: 20 mM Tris-HCl pH8.0, 150 mM NaCl, 10 mM EDTA, 1 mM EGTA, 0.2% Triton X-100, 0.2% NP-40, 2 mM Na_3VO_4, 1 mM PMSF, 1.5 µg/ml aprotinin. Proteins were separated by SDS-PAGE according to standard procedures (Sambrook and Russell, 2001). Electroblot transfer was performed as in Towbin et al. (1979) with transfer buffer containing 20% methanol and in most cases including 0.04% SDS. For these experiments we used the Bio-Rad Mini PROTEAN III system, electroblotting to 0.2 µm nitrocellulose, and using anti-mouse or anti-rabbit HRP-conjugated secondary antibody (Bio-Rad) (1:3000) for visualization of primary antibody. Antibody labeling was visualized using chemiluminescent detection methods (SuperSignal West Pico Chemiluminescent Substrate, Pierce). The immunoblots were digitized using a flatbed scanner (Epson Expression 1680).

Chromatin immunoprecipitation

For ChIP experiments 50 pairs of salivary glands per sample were dissected from third instar larvae and fixed for 15 min at room temperature in 1 ml of fixative (50 mM HEPES at pH 7.6, 100 mM NaCl, 0.1 mM EDTA at pH 8, 0.5 mM EGTA at pH 8, 2% formaldehyde). Preparation of chromatin for immunoprecipitation was performed as previously described in Legube et al. (2006). Rabbit anti-H3S10ph antibody (Cell Signaling), purified rabbit IgG antibody (Sigma), anti-H3K9me2 mAb (Abcam), or anti-GST mAb 8C7 (Rath et al. 2004) was used for immunoprecipitation. For each sample the chromatin lysate was divided into equal amounts and immunoprecipitated with experimental and control antibody, respectively. DNA from the immunoprecipitated chromatin fragments (500 bp average) was purified by a Wizard SV DNA purification kit (Promega). The isolated DNA was used as template for quantitative real-time (qRT) PCR performed with the Stratagene Mx4000 real-time cycler. The PCR mixture contained Brilliant II SYBR Green QPCR Master Mix (Stratagene) as well as the corresponding primers: *hsp70-white*-forward 5'-GCAACCAAGTAAATCAACTGC-3', *hsp70-white*-reverse 5'-GTTTTGGCACAGCACTTTGTG-3' which amplify region +149 to +250 (Hines et al., 2009). Cycling parameters were 10 min at 95°C, followed by 40 cycles of 30 sec at 95°C, 30 sec at 55°C, and 30 sec at 72°C. Fluorescence intensities were plotted against the number of cycles using an algorithm provided by Stratagene. DNA levels were quantified using a calibration curve based on dilution of concentrated DNA. For each experimental condition the relative enrichment was normalized to the corresponding control immunoprecipitation from the same chromatin lysate.

Acknowledgements

We thank members of the laboratory for discussion, advice, and critical reading of the manuscript. We also wish to acknowledge Mr. Kevin Bieniek for technical assistance. We especially thank Drs. L. Wallrath, P. Geyer, and M. Kuroda for providing fly stocks and reagents. This work was supported by NIH Grant GM062916 (KMJ/JJ).

Figures

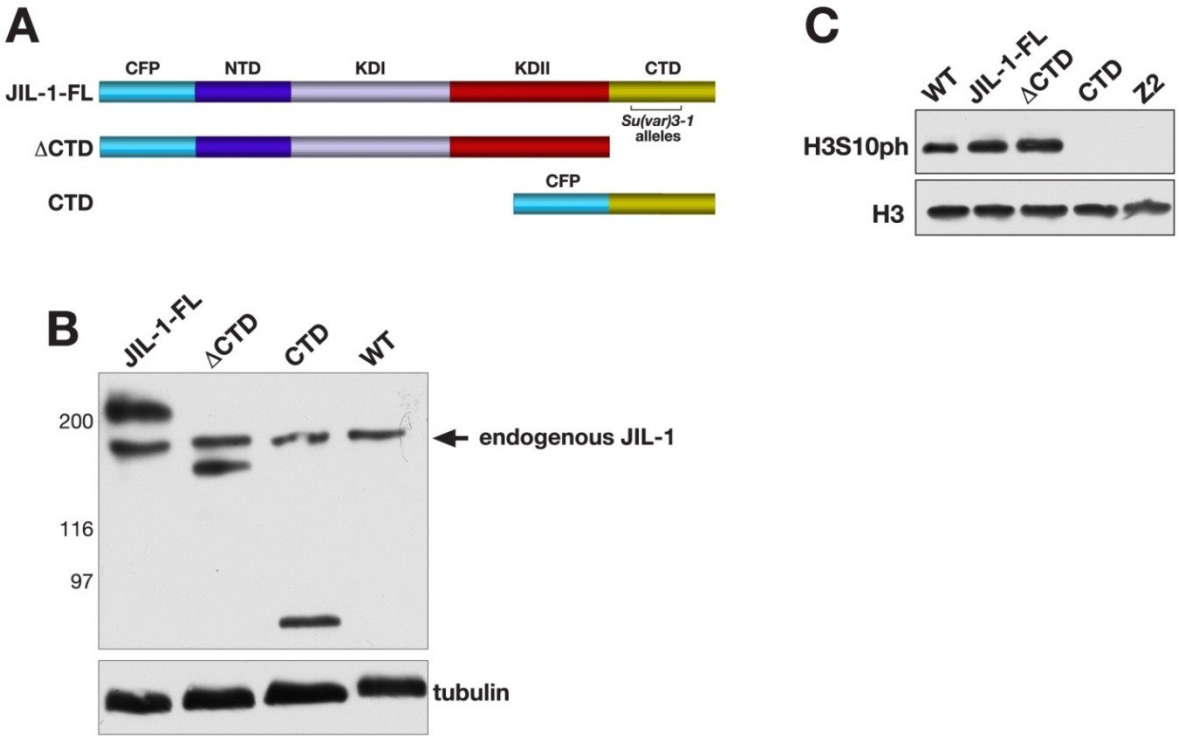

Fig. 1. Expression of JIL-1 constructs transgenically in a wild-type background. (A) Diagrams of the JIL-1 CFP-tagged constructs analyzed. The region in the CTD where *JIL-1*$^{Su(var)3-1}$ alleles resulting in COOH-terminally truncated proteins have been mapped (Ebert et al., 2004) is indicated by a bracket. (B) Immunoblot labeled with JIL-1 antibody of protein

extracts from wild type (wt) and from flies expressing the FL, the CTD, and the CTD, respectively. Labeling with tubulin antibody was used as a loading control. The relative migration of molecular size markers is indicated to the left of the immunoblot in kDa. (C) Immunoblot labeled with H3S10ph antibody of protein extracts from salivary glands from wild type third instar larvae (wt), from larvae expressing the FL, the CTD, and the CTD, respectively, and from *JIL-1* null larvae (z2). Labeling with histone H3 antibody was used as a loading control.

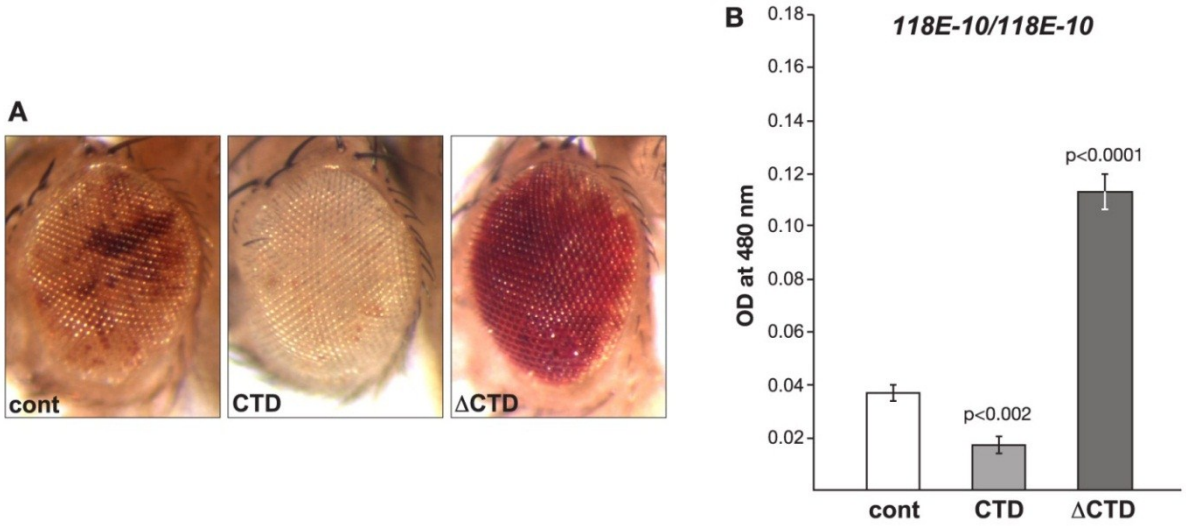

Fig. 2. The effect on PEV of the *118E-10* allele by expression of the CTD or the CTD. (A) Examples of the degree of PEV in the eyes of wild-type *JIL-1* flies (cont), wild-type *JIL-1* flies expressing the CTD, and wild-type *JIL-1* flies expressing the CTD in a *118E-10/118E10* background. All images are from male flies. (B) Histograms of the levels of eye pigment of wild-type *JIL-1* flies (cont), wild-type *JIL-1* flies expressing the CTD, and wild-type *JIL-1* flies expressing the CTD in a male *118E-10/118E10* background. The average pigment level when the CTD or the CTD was expressed was compared to the control level using a two-tailed Student's t-test.

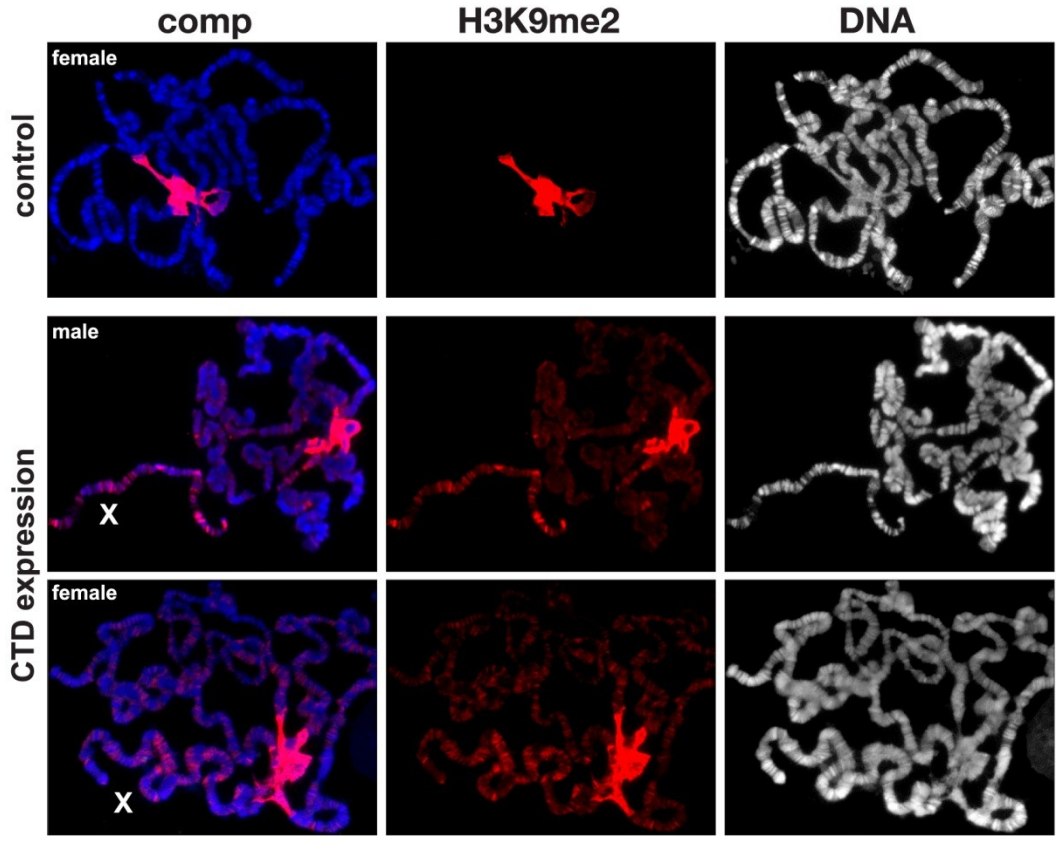

Fig. 3. The effect on H3K9me2 localization in polytene chromosomes expressing the CTD. The polytene squash preparations were labeled with antibody to H3K9me2 (in red) and with Hoechst (DNA, in blue/gray). The X chromosome is indicated by an X. Preparations from wild-type (control) and male and female larvae expressing the CTD are shown. In wild-type preparations H3K9me2 labeling was mainly localized to and abundant at the chromocenter; however, when the CTD was expressed the H3K9me2 labeling spread to the autosomes and particularly to the X chromosome in both males and females.

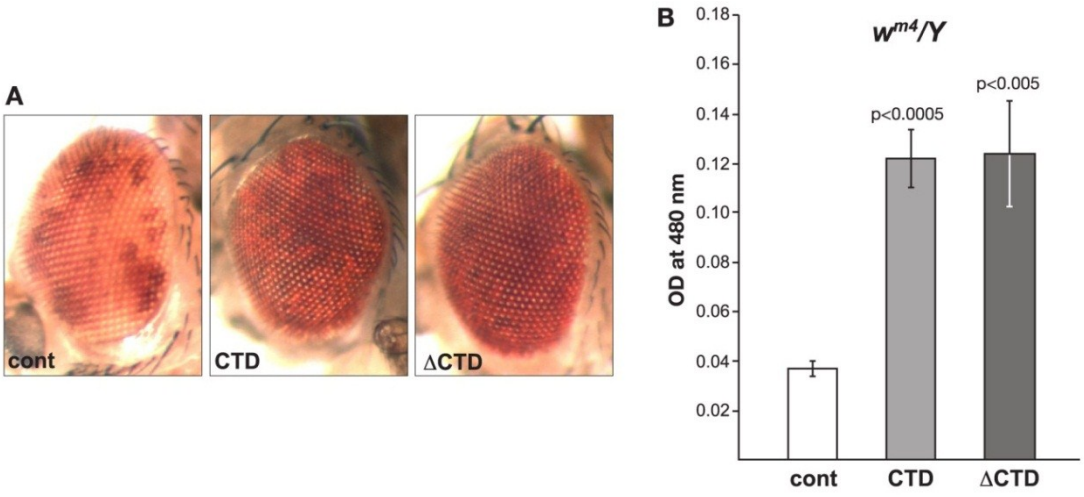

Fig. 4. The effect on PEV of the w^{m4} allele by expression of the CTD or the CTD. (A) Examples of the degree of PEV in the eyes of wild-type *JIL-1* flies (cont), wild-type *JIL-1* flies expressing the CTD, and wild-type *JIL-1* flies expressing the CTD in a w^{m4}/Y background. (B) Histograms of the levels of eye pigment of wild-type *JIL-1* flies (cont), wild-type *JIL-1* flies expressing the CTD, and wild-type *JIL-1* flies expressing the CTD in a w^{m4}/Y background. The average pigment level when the CTD or the CTD was expressed was compared to the control level using a two-tailed Student's t-test.

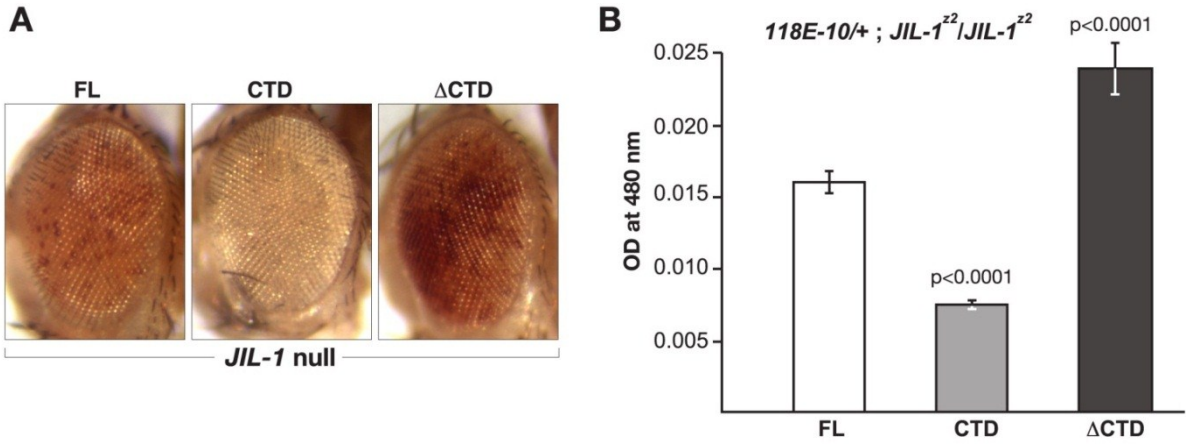

Fig. 5. The effect on PEV of the *118E-10* allele in *JIL-1* null flies expressing the FL, the CTD, or the CTD. (A) Examples of the degree of PEV in the eyes of $JIL\text{-}1^{z2}/JIL\text{-}1^{z2}$

null flies expressing the FL, the CTD, or the CTD in a *118E-10/+* background. All images are from male flies. (B) Histograms of the levels of eye pigment of male *JIL-1^{z2}/JIL-1^{z2}* null flies expressing the FL, the CTD, or the CTD in a *118E-10/+* background. The average pigment level when the CTD or the CTD was expressed was compared to the level when the FL was expressed using a two-tailed Student's t-test.

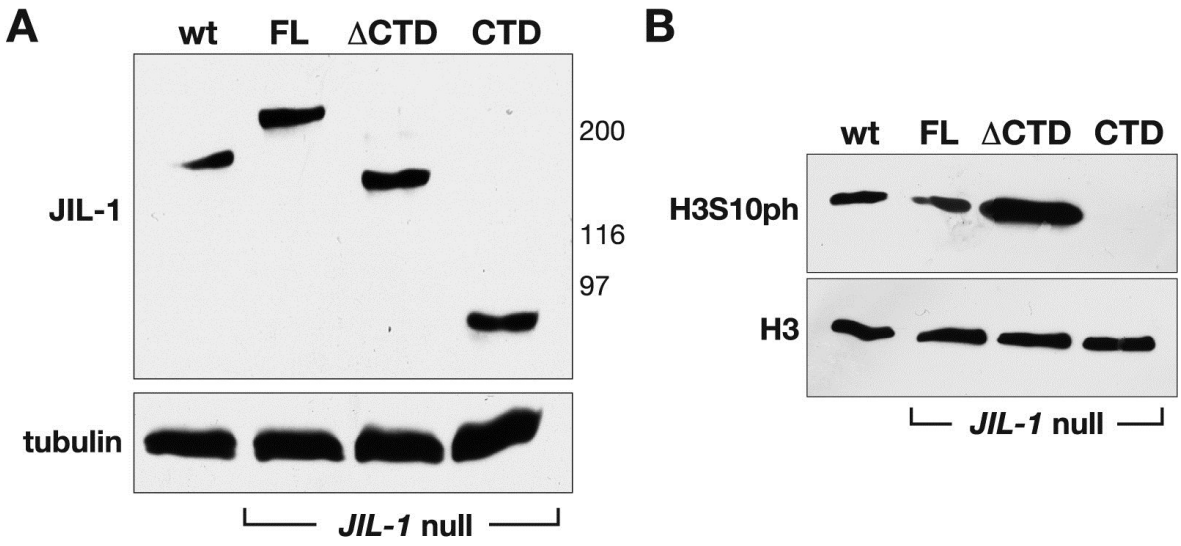

Fig. 6. Expression of transgenic JIL-1 constructs in *JIL-1* null flies. (A) Immunoblot labeled with JIL-1 antibody of protein extracts from wild type (wt) and from *JIL-1^{z2}/JIL-1^{z2}* null flies expressing the FL, the CTD, and the CTD, respectively. Labeling with tubulin antibody was used as a loading control. The relative migration of molecular size markers is indicated to the right of the immunoblot in kDa. (B) Immunoblot labeled with H3S10ph antibody of protein extracts from salivary glands from wild type third instar larvae (wt) and from *JIL-1^{z2}/JIL-1^{z2}* null larvae expressing the FL, the CTD, and the CTD, respectively. Labeling with histone H3 antibody was used as a loading control.

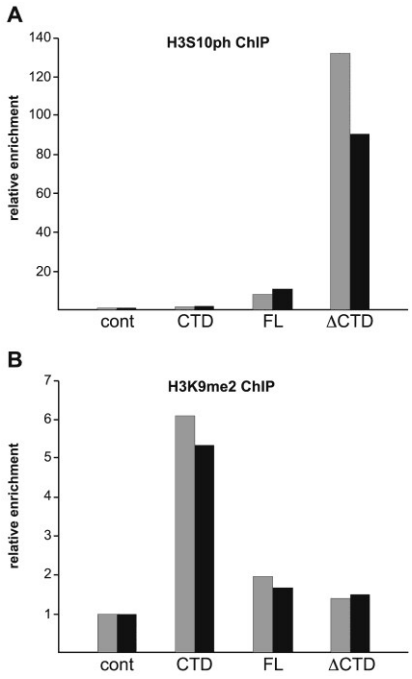

Fig. 7. Chip analysis of the reporter gene *hsp70-white* in the *118E-10* P-element insertion. (A) Histograms of the relative enrichment of chromatin immunoprecipitated by anti-H3S10ph antibody from salivary glands from *JIL-1*^{z2}*/JIL-1*^{z2} null third instar larvae expressing the FL, the CTD, or the CTD in a *118E-10/+* background. For each experimental condition the relative enrichment was normalized to the corresponding control immunoprecipitation with purified rabbit IgG antibody (cont). The graph shows the results from two independent experiments. (B) Histograms of the relative enrichment of chromatin immunoprecipitated by anti-H3K9me2 mAb from salivary glands from *JIL-1*^{z2}*/JIL-1*^{z2} null third instar larvae expressing the FL, the CTD, or the CTD in a *118E-10/+* background. For each experimental condition the relative enrichment was normalized to the corresponding control immunoprecipitation with GST mAb 8C7 (cont). The graph shows the results from two independent experiments.

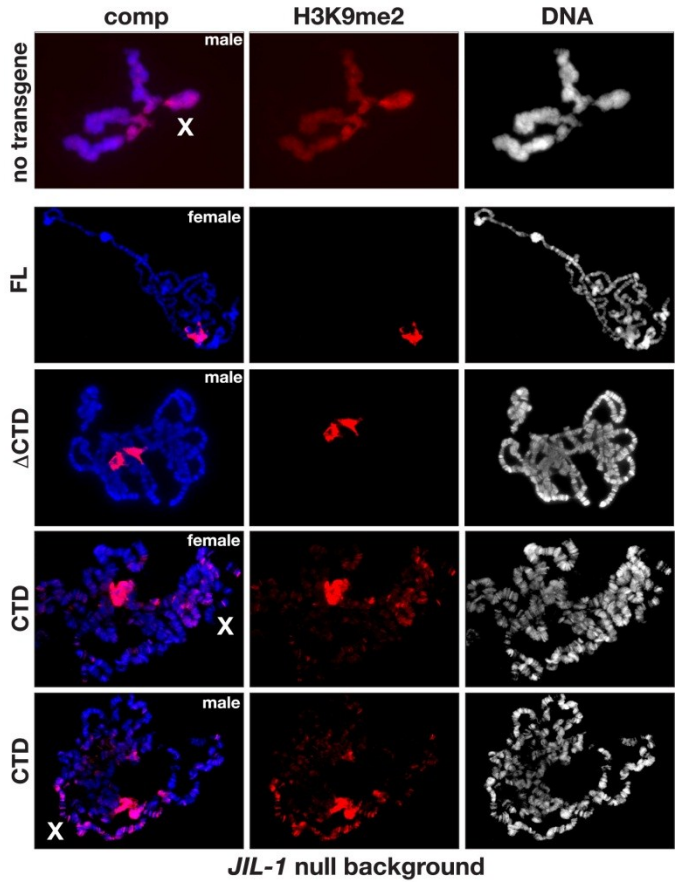

Fig. 8. The effect on H3K9me2 localization in polytene chromosomes from *JIL-1* null larvae expressing the FL, the CTD, or the CTD. The polytene squash preparations were labeled with antibody to H3K9me2 (in red) and with Hoechst (DNA, in blue/gray). The X chromosome is indicated by an X. Preparations from *JIL-1*^{z2}/*JIL-1*^{z2} null larvae expressing either the FL, the CTD, or the CTD are shown. The top panel shows a preparation from a *JIL-1*^{z2}/*JIL-1*^{z2} null larvae without transgene expression for comparison.

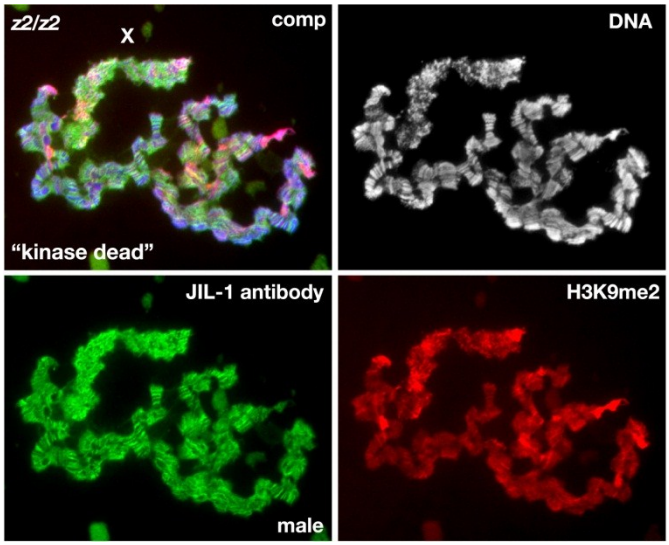

Fig. 9. The effect on H3K9me2 localization in polytene chromosomes from *JIL-1* null larvae expressing a "kinase dead" JIL-1 construct. The polytene squash preparation is from a male *JIL-1* null (*JIL-1*^{z2}/*JIL-1*^{z2}) third instar larvae triple labeled with Hoechst (DNA, in blue/gray), H3K9me2 antibody (in red), and JIL-1 antibody (in green). Note that although expression of the "kinase dead" construct is near wild-type levels, localized on the chromosome arms, and upregulated on the male X chromosome (X), the chromosome morphology as well as the spreading and upregulation of histone H3K9 dimethylation on the X chromosome is indistinguishable from that observed in *JIL-1* null third instar larvae (Fig. 7).

References

Allis, C.D., Jenuwein, T., Reinberg, D. (2007). *Epigenetics* (Cold Sping Harbor Laboratory PressCold Spring Harbor, NY).

Bao, X., Deng, H., Johansen, J., Girton, J. and Johansen, K.M. (2007). Loss-of-function alleles of the JIL-1 histone H3S10 kinase enhance position-effect-variegation at pericentric sites in Drosophila heterochromatin. *Genetics* **176,** 1355-1358.

Bao, X., Cai, W., Deng, H., Zhang, W., Krencik, R., Girton, J. and Johansen, K.M. (2008). The COOH-terminal domain of the JIL-1 histone H3S10 kinase interacts with histone H3 and is required for correct targeting to chromatin. *J. Biol. Chem.* **283**, 32741-32750.

Berger, S.L. (2007). The complex language of chromatin regulation during transcription. *Nature* **447,** 407-412.

Boeke, J., Regnard, C., Cai, W., Johansen, J., Johansen, K.M., Becker, P.B., and Imhof, A. (2010). Phosphorylation of SU(VAR)3-9 by the chromosomal kinase JIL-1. *PLoS ONE* : e10042.

Cai, W., Bao, X., Deng, H., Jin, Y., Girton, J., Johansen, J., and Johansen, K.M. (2008). RNA polymerase II-mediated transcription at active loci does not require histone H3S10 phosphorylation in *Drosophila*. *Development* **135**, 2917-2925.

Cai, W., Jin, Y., Girton, J., Johansen, J., and Johansen, K.M. (2010). Preparation of polytene chromosome squashes for antibody labeling. *J. Vis. Exp.* http://www.jove.com/index/Details.stp?ID=1748.

Cryderman, D.E., Cuaycong, M.H., Elgin, S.C.R., and Wallrath, L.L. (1998). Characterization of sequences associated with position-effect-variegation at pericentric sites in *Drosophila* heterochromatin. *Chromosoma* **107,** 277-285.

Delattre, M., Spierer, A., Jaquet, Y., and Spierer, P. (2004). Increased expression of *Drosophila* Su(var)3-7 triggers Su(var)3-9-dependent heterochromatin formation. *J. Cell. Sci.* **117,** 6239-6247.

Deng, H., Zhang, W., Bao, X., Martin, J.N., Girton, J., Johansen, J., and Johansen, K.M. (2005). The JIL-1 kinase regulates the structure of *Drosophila* polytene chromosomes. *Chromosoma* **114,** 173-182.

Deng, H., Bao, X., Zhang, W., Girton, J., Johansen, J., and Johansen, K.M. (2007). Reduced levels of Su(var)3-9 but not Su(var)2-5 (HP1) counteract the effects on chromatin structure and viability in loss-of-function mutants of the JIL-1 histone H3S10 kinase. *Genetics* **177,** 79-87.

Deng, H., Bao, X., Cai, W., Blacketer, M.J., Belmont, A.S., Girton, J., Johansen, J., and Johansen, K.M. (2008). Ectopic histone H3S10 phosphorylation causes chromatin structure remodeling in *Drosophila. Development* **135,** 699-705.

Deng, H., Cai, W., Wang C., Lerach, S., Delattre M., Girton, J., Johansen, J., and Johansen, K.M. (2010). *JIL-1* and *Su(var)3-7* interact genetically and counterbalance

each others' effect on position effect variegation in *Drosophila*. *Genetics* **185**, 1183-1192.

Ebert, A., Schotta, G., Lein, S., Kubicek, S., Krauss, V., Jenuwein, T., and Reuter, G. (2004). Su(var) genes regulate the balance between euchromatin and heterochromatin in *Drosophila*. *Genes Dev.* **18,** 2973-2983.

Girton, J., and Johansen, K.M. (2008). Chromatin structure and regulation of gene expression: the lessons of PEV in *Drosophila*. *Adv. Genet.* **61**, 1-43.

Greval, S.I., and Elgin, S.C. (2002). Heterochromatin: new possibilities for the inheritance of structure. *Curr. Opin. Genet. Dev.* **12,** 178-187.

Hines, K.A., Cryderman, D.E., Flannery, K.M., Yang, H., Vitalini, M.W., Hazelrigg, T., Mizzen, C.A., and Wallrath, L.L. (2009). Domains of Heterochromatin Protein 1 required for *Drosophila melanogaster* heterochromatin spreading *Genetics* **182,** 967-977.

Ji, Y., Rath, U., Girton, J., Johansen, K.M., and Johansen, J. (2005). D-Hillarin, a novel W180-domain protein, affects cytokinesis through interaction with the septin family member Pnut. *J. Neurobiol.* **64,** 157-169.

Jin, Y., Wang, Y., Walker, D.L, Dong, H., Conley, C., Johansen, J., and Johansen, K.M. (1999). JIL-1: a novel chromosomal tandem kinase implicated in transcriptional regulation in *Drosophila*. *Mol. Cell* **4,** 129-135.

Jin, Y., Wang, Y., Johansen, J., and Johansen, K.M. (2000). JIL-1, a chromosomal kinase implicated in regulation of chromatin structure, associates with the MSL dosage compensation complex. *J. Cell Biol.* **149,** 1005-1010.

Kavi, H.H., and Birchler, J.A. (2009). Interaction of RNA polymerase II and the small RNA machinery affects heterochromatic silencing in *Drosophila*. *Epigenetics Chromatin* **2, 15-30.**

Legube, G., McWeeney, S.K., Lercher, M.J., and Akhtar, A. (2006). X-chromosome-wide profiling of MSL-1 distribution and dosage compensation in *Drosophila*. *Genes Dev.* **20,** 871-883.

Lerach, S., Zhang, W., Bao, X., Deng, H., Girton, J., Johansen, J., and Johansen, K.M. (2006). Loss-of-function alleles of the JIL-1 kinase are strong suppressors of position effect variegation of the w^{m4} allele in Drosophila. *Genetics* **173,** 2403-2406.

Lindsley, D.L. and Zimm, G.G. (1992). *The genome of Drosophila melanogaster*. Academic Press, New York, NY.

Muller, H.J. (1930). Types of visible variegations induced by X-rays in *Drosophila*. *J. Genetics* **22,** 299-335.

Patton, J.S., Gomes, X.V., and Geyer, P.K. (1992) Position-independent germline transformation in *Drosophila* using a cuticle pigmentation gene as a selectable marker. *Nucleic Acids Res.* **20,** 5859-5860.

Pirrotta, V., Hadfield, C., and Pretorius, G.H.J. (1983). Microdissection and cloning of the white locus and the 3B1 – 3C2 region of the *Drosophila* X chromosome. *EMBO* **2,** 927 – 934.

Rath, U., Wang, D., Ding, Y., Xu. Y.-Z., Qi, H., Blacketer, M.J., Girton, J., Johansen, J., and Johansen, K.M. (2004). Chromator, a novel and essential chromodomain protein interacts directly with the putative spindle matrix protein Skeletor. *J. Cell. Biochem.* **93,** 1033-1047.

Roberts, D.B. (1998). In *Drosophila: A Practical Approach* IRL Press, Oxford, UK.

Sambrook, J. and Russell, D. W. (2001). Molecular Cloning: A Laboratory Manual. (Cold Spring Harbor Laboratory Press, NY).

Schotta, G., Ebert, A., Dorn, R., and Reuter, G. (2003). Position-effect variegation and the genetic dissection of chromatin regulation in *Drosophila*. *Semin. Cell Dev. Biol.* **14,** 67-75.

Towbin, H., Staehelin, T., Gordon, J. (1979). Electrophoretic transfer of proteins from polyacrylamide gels to nitrocellulose sheets: Procedure and some applications. *Proc. Natl. Acad. Sci. USA* **76,** 4350-4354.

Wallrath, L.L., and Elgin, S.C.R. (1995). Position effect variegation in *Drosophila* is associated with altered chromatin structure. *Genes Dev.* **9,** 1263-1277.

Wallrath, L.L., Guntur, V.P., Rosman, L.E., and Elgin, S.C.R. (1996). DNA representation of variegating heterochromatic P-element inserts in diploid and polytene tissues of *Drosophila melanogaster*. *Chromosoma* **104,** 519-527.

Wang, C., Girton, J., Johansen, J. and Johansen, K.M. (2011). A balance between euchromatic (JIL-1) and heterochromatic (SU(VAR)2-5 and SU(VAR)3-9) factors regulates position-effect variegation in Drosophila. *Genetics* **188,** 745-748.

Wang, Y., Zhang, W., Jin, Y., Johansen, J., and Johansen, K.M. (2001). The JIL-1 tandem kinase mediates histone H3 phosphorylation and is required for maintenance of chromatin structure in *Drosophila*. *Cell* **105,** 433-443.

Weiler, K.S. and Wakimoto, B.T. (1995). Heterochromatin and gene expression in *Drosophila*. *Annu. Rev. Genet.* **29,** 577-605.

Zhang, W., Jin, Y., Ji, Y., Girton, J., Johansen, J., and Johansen, K.M. (2003). Genetic and phenotypic analysis of alleles of the *Drosophila* chromosomal JIL-1 kinase reveals a functional requirement at multiple developmental stages. *Genetics* **165,** 1341-1354.

Zhang, W., Deng, H., Bao, X., Lerach, S., Girton, J., Johansen, J. and Johansen, K.M. (2006). The JIL-1 histone H3S10 kinase regulates dimethyl H3K9 modifications and heterochromatic spreading in *Drosophila*. *Development* **133,** 229-235.

CHAPTER 3. A GENETIC BALANCE BETWEEN THE EUCHROMATIC FACTOR *JIL-1* AND THE HETEROCHROMATIC FACTORS *SU(VAR)2-5* AND *SU(VAR)3-9* REGULATES PEV

A paper published in the *Journal of Cell Science*

Chao Wang, Jack Girton, Jørgen Johansen and Kristen M. Johansen

Summary

In this study we show that the haplo-enhancer effect of *JIL-1* can counterbalance the haplo-suppressor effect of both *Su(var)3-9* and *Su(var)2-5* on position-effect variegation, providing strong evidence that a finely tuned balance between the levels of JIL-1 and the major heterochromatin components contribute to the regulation of gene expression.

Results and Discussions

The essential JIL-1 histone H3S10 kinase (JIN *et al.* 1999; WANG *et al.* 2001) is a major regulator of chromatin structure (DENG *et al.* 2005; 2008) that functions to maintain euchromatic domains while counteracting heterochromatization and gene silencing (EBERT *et al.* 2004; ZHANG *et al.* 2006; LERACH *et al.* 2006; BAO *et al.* 2007). In the absence of the JIL-1 kinase the major heterochromatin markers H3K9me2, HP1a (Su(var)2-5), and Su(var)3-7 spread to ectopic locations on the chromosome arms (ZHANG *et al.* 2006; DENG *et al.* 2007; 2010). These observations suggested a model for a dynamic balance

between euchromatin and heterochromatin (EBERT *et al.* 2004; ZHANG *et al.* 2006; DENG *et al.* 2010), where as can be monitored in position-effect variegation (PEV) arrangements, the boundary between these two states is determined by antagonistic functions of a euchromatic regulator (JIL-1) and the major determinants of heterochromatin assembly, e.g. Su(var)3-9, HP1a, and Su(var)3-7 (for review see WEILER and WAKIMOTO 1995; GIRTON and JOHANSEN 2008). In support of this model, DENG *et al.* (2010) recently showed that *Su(var)3-7* and *JIL-1* loss-of-function mutations have an antagonistic and counterbalancing effect on gene expression using PEV assays; however, potential dynamic interactions between *JIL-1* and the other two heterochromatin genes, *Su(var)3-9* and *Su(var)2-5* were not addressed in this study. Interestingly, in other genetic interaction assays monitoring the lethality as well as the chromosome morphology defects associated with the null *JIL-1* phenotype, only a reduction in the dose of the *Su(var)3-9* gene (ZHANG *et al.* 2006; DENG *et al.* 2007) rescued both phenotypes. In contrast, in the same assays a reduction of *Su(var)3-7* rescued the lethality, but not the chromosome defects (DENG *et al.* 2010), and no genetic interactions were detectable between *JIL-1* and *Su(var)2-5* (DENG *et al.* 2007). Thus, these findings indicate that while Su(var)3-9 activity may be a major factor in the lethality and chromatin structure perturbations associated with loss of the JIL-1 histone H3S10 kinase, these effects are likely to be uncoupled from HP1a and to a lesser degree from Su(var)3-7. This raises the question whether *JIL-1* dynamically interacts with the two other heterochromatin genes, *Su(var)2-5* and *Su(var)3-9* in regulating gene expression, as it does with *Su(var)3-7*.

To answer this question we explored the effect of various combinations of loss-of-function alleles of *JIL-1* and *Su(var)3-9* or *Su(var)2-5* on PEV caused by the P-element insertion line *118E-10* (WALLRATH and ELGIN 1995; WALLRATH *et al.* 1996). Insertion of this P element (*P[hsp26-pt, hsp70-w]*) into euchromatic sites results in a uniform red eye

phenotype whereas insertion into a known heterochromatin region of the fourth chromosome results in a variegating eye phenotype (CRYDERMAN *et al.* 1998; BAO *et al.* 2007) (Figures 1 and 2). It has been demonstrated that loss-of-function *JIL-1* alleles can act as strong haplo-enhancers of PEV resulting in increased silencing of gene expression (DENG *et al.* 2010) whereas loci for structural components of heterochromatin such as *Su(var)3-9*, *Su(var)2-5*, and *Su(var)3-7* act as strong haplo-suppressors (REUTER *et al.* 1990; EISSENBERG *et al.* 1990; TSCHIERSCH *et al.* 1994). In the experiments the transgenic reporter line *118E-10* was crossed into $JIL\text{-}1^{z2}$/+, $Su(var)3\text{-}9^{06}$/+, and $Su(var)2\text{-}5^{05}$/+ mutant backgrounds as well as into $JIL\text{-}1^{z2}$/ $Su(var)3\text{-}9^{06}$ and $JIL\text{-}1^{z2}$/ $Su(var)2\text{-}5^{05}$ double mutant backgrounds. The $JIL\text{-}1^{z2}$ allele is a true null allele (WANG *et al.* 2001; ZHANG *et al.* 2003), the loss-of-function $Su(var)3\text{-}9^{06}$ allele is due to a DNA insertion (SCHOTTA *et al.* 2002), and the $Su(var)2\text{-}5^{05}$ loss-of-function allele is associated with a frame shift resulting in a nonsense peptide containing only the first 10 amino acids of HP1a (EISSENBERG *et al.* 1992). Thus, in order to test whether the heterozygous $JIL\text{-}1^{z2}$ allele could counterbalance the suppression of the $Su(var)3\text{-}9^{06}$ or $Su(var)2\text{-}5^{05}$ loss-of-function alleles of PEV of *118E-10*, we compared the eye pigment levels of the various genotypes (Figures 1 and 2 and Table 1). Pigment assays were performed essentially as in KAVI and BIRCHLER (2009) using 3 sets of 10 pooled fly heads from each genotype. Although both male and female flies were scored, due to sex differences only results from male flies are shown. However, the trend observed in female flies was identical to that in male flies. As illustrated in Figures 1 and 2, the heterozygous $JIL\text{-}1^{z2}$/+ allele leads to enhancement of PEV as indicated by the increased proportion of white ommatidia and a 59% decrease in the optical density (OD) of the eye pigment levels (0.0083±0.0015, n=3) as compared to +/+ flies (0.0203±0.0021, n=3). This reduction was statistically significant (Table 1). In contrast, the heterozygous $Su(var)3\text{-}9^{06}$/+ and $Su(var)2\text{-}5^{05}$/+ alleles lead to suppression of PEV as

indicated by an increase of the proportion of red ommatidia and a statistically significant (Table 1) 384% (0.078±0.001, n=3) and 330% (0.067±0.004, n=3) increase, respectively, in the OD of the eye pigment levels. However, in the *JIL-1^{z2}/ Su(var)3-9^{06}* and *JIL-1^{z2}/ Su(var)2-5^{05}* double mutant backgrounds, variegation of the proportion of red ommatidia was intermediate and the eye pigment levels (0.0207±0.0031 and 0.0263±0.0035, n=3, respectively) were statistically indistinguishable from when +/+ levels of the JIL-1, Su(var)3-9, and Su(var)2-5 proteins were present (Figures 1 and 2 and Table 1).

These results suggest that the haplo-enhancer effect of *JIL-1* can counterbalance the haplo-suppressor effect of both *Su(var)3-9* and *Su(var)2-5* on PEV of the *118E-10* allele. In previous experiments a genetic interaction between *JIL-1* and *Su(var)2-5* was not detected (DENG *et al.* 2007). However, the assays used to probe for interactions were viability and rescue of polytene chromosome morphology. As indicated by the experiments presented here, these parameters are likely to be independent of and separate from the mechanisms contributing to epigenetic regulation of PEV and gene silencing. Consequently, the present experiments taken together with those of DENG *et al.* (2010) provide strong evidence that a finely tuned balance between the levels of JIL-1 and all of the major heterochromatin components Su(var)3-9, HP1a, and Su(var)3-7 contribute to the regulation of PEV and gene expression.

We thank members of the laboratory for discussion, advice, and critical reading of the manuscript. We also wish to acknowledge Ms. V. Lephart for maintenance of fly stocks and Mr. Kevin Bienik for technical assistance. We especially thank Dr. L. Wallrath for providing fly stocks. This work was supported by NIH Grant GM062916 (KMJ/JJ).

References

BAO, X., H. DENG, J. JOHANSEN, J. GIRTON and K.M. JOHANSEN, 2007 Loss-of-function alleles of the JIL-1 histone H3S10 kinase enhance position-effect-variegation at pericentric sites in Drosophila heterochromatin. Genetics **176:** 1355-1358.

CRYDERMAN, D.E., M.H. CUAYCONG, S.C.R. ELGIN and L.L. WALLRATH, 1998 Characterization of sequences associated with position-effect-variegation at pericentric sites in *Drosophila* heterochromatin. Chromosoma **107:** 277-285.

DENG, H., W. ZHANG, X. BAO, J.N. MARTIN, J. GIRTON, J. JOHANSEN and K.M. JOHANSEN, 2005 The JIL-1 kinase regulates the structure of *Drosophila* polytene chromosomes. Chromosoma **114:** 173-182.

DENG, H., X. BAO, W. ZHANG, J. GIRTON, J. JOHANSEN and K.M. JOHANSEN, 2007 Reduced levels of Su(var)3-9 but not Su(var)2-5 (HP1) counteract the effects on chromatin structure and viability in loss-of-function mutants of the JIL-1 histone H3S10 kinase. Genetics **177:** 79-87.

DENG, H., X. BAO, W. CAI, M.J. BLACKETER, A.S. BELMONT, J. GIRTON, J. JOHANSEN and K.M. JOHANSEN, 2008 Ectopic histone H3S10 phosphorylation causes chromatin structure remodeling in *Drosophila*. Development **135:** 699-705.

DENG, H., W. CAI, C. WANG, S. LERACH, M. DELATTRE, J. GIRTON, J. JOHANSEN and K.M. JOHANSEN, 2010 *JIL-1* and *Su(var)3-7* interact genetically and counteract each other's effect on position-effect variegation in Drosophila. Genetics **185:** 1183-1192.

EBERT, A., G. SCHOTTA, S. LEIN, S. KUBICEK, V. KRAUSS, T. JENUWEIN and G. REUTER, 2004 Su(var) genes regulate the balance between euchromatin and heterochromatin in *Drosophila*. Genes Dev. **18:** 2973-2983.

EISSENBERG, J.C., T. JAMES, D. FOSTER-HARTNETT, D. HARTNETT, V. NGAN and S.C.R. ELGIN, 1990 Mutation in a heterochromatin-specific chromosomal protein is associated with suppression of position-effect variegation in *Drosophila melanogaster*. Proc. Natl. Acad. Sci. USA **87:** 9923-9927.

EISSENBERG, J.C., G.D. MORRIS, G. REUTER and T. HARTNETT, 1992 The heterochromatin-associated protein HP-1 is an essential protein in Drosophila with dosage-dependent effects on position-effect variegation. Genetics **131:** 345-352.

GIRTON, J., and K.M. JOHANSEN, 2008 Chromatin structure and regulation of gene expression: the lessons of PEV in *Drosophila*. Adv. Genet. **61**: 1-43.

JIN, Y., Y. WANG, D. L. WALKER, H. DONG, C. CONLEY, J. JOHANSEN and K.M. JOHANSEN, 1999 JIL-1: A novel chromosomal tandem kinase implicated in transcriptional regulation in *Drosophila*. Mol. Cell **4:** 129-135.

KAVI, H.H., and J.A. BIRCHLER, 2009 Interaction of RNA polymerase II and the smal RNA machinery affects heterochromatic silencing in Drosophila. Epigenetics Chromatin **2:** 15-30.

LERACH, S., W. ZHANG, X. BAO, H. DENG, J. GIRTON, J. JOHANSEN and K.M. JOHANSEN, 2006 Loss-of-function alleles of the JIL-1 kinase are strong suppressors of position effect variegation of the w^{m4} allele in Drosophila. Genetics **173:** 2403-2406.

LINDSLEY, D.L., and G.G. ZIMM, 1992 The Genome of *Drosophila melanogaster*. Academic Press, New York.

REUTER, G., M. GIARRE, J. FARAH, J. GAUSZ, A. SPIERER and P. SPIERER, 1990 Dependence of position-effect varigation in Drosophila on dose of a gene encoding an unusual zinc-finger protein. Nature **344:** 219-223.

ROBERTS, D.B., 1998 *Drosophila*: A Practical Approach. IRL Press, Oxford.

SCHOTTA, G., A. EBERT, V. KRAUSS, A. FISCHER, J. HOFFMANN, S. REA, T. JENUWEIN, R. DORN and G. REUTER, 2002 Central role of *Drosophila* SU(VAR)3-9 in histone H3-K9 methylation and heterochromatic gene silencing. EMBO J. **21:** 1121-1131.

TSCHIERSCH, B., A. HOFMANN, V. KRAUSS, R. DORN, G. KORGE and G. REUTER, 1994 The protein encoded by the *Drosophila* position-effect variegation suppressor gene *Su(var)3-9* combines domains of antagonistic regulators of homeotic gene complexes. EMBO J**. 13:** 3822-3831.

WALLRATH, L.L., and S.C.R. ELGIN, 1995 Position effect variegation in *Drosophila* is associated with altered chromatin structure. Genes Dev. **9:** 1263-1277.

WALLRATH, L.L., V.P. GUNTUR, L.E. ROSMAN and S.C.R. ELGIN, 1996 DNA representation of variegating heterochromatic P-element inserts in diploid and polytene tissues of *Drosophila melanogaster*. Chromosoma **104:** 519-527.

WANG, Y., W. ZHANG, Y. JIN, J. JOHANSEN and K. M. JOHANSEN, 2001 The JIL-1 tandem kinase mediates histone H3 phosphorylation and is required for maintenance of chromatin structure in *Drosophila*. Cell **105:** 433-443.

WEILER, K.S., and B.T. WAKIMOTO, 1995 Heterochromatin and gene expression in *Drosophila*. Annu. Rev. Genet. **29:** 577-605.

ZHANG, W., Y. JIN, Y. JI, J. GIRTON, J. JOHANSEN and K.M. JOHANSEN, 2003 Genetic and phenotypic analysis of alleles of the Drosophila chromosomal JIL-1

kinase reveals a functional requirement at multiple developmental stages. Genetics **165:** 1341-1354.

ZHANG, W., H. DENG, X. BAO, S. LERACH, J. GIRTON, J. JOHANSEN and K.M. JOHANSEN, 2006 The JIL-1 histone H3S10 kinase regulates dimethyl H3K9 modifications and heterochromatic spreading in *Drosophila*. Development **133:** 229-235.

Figures

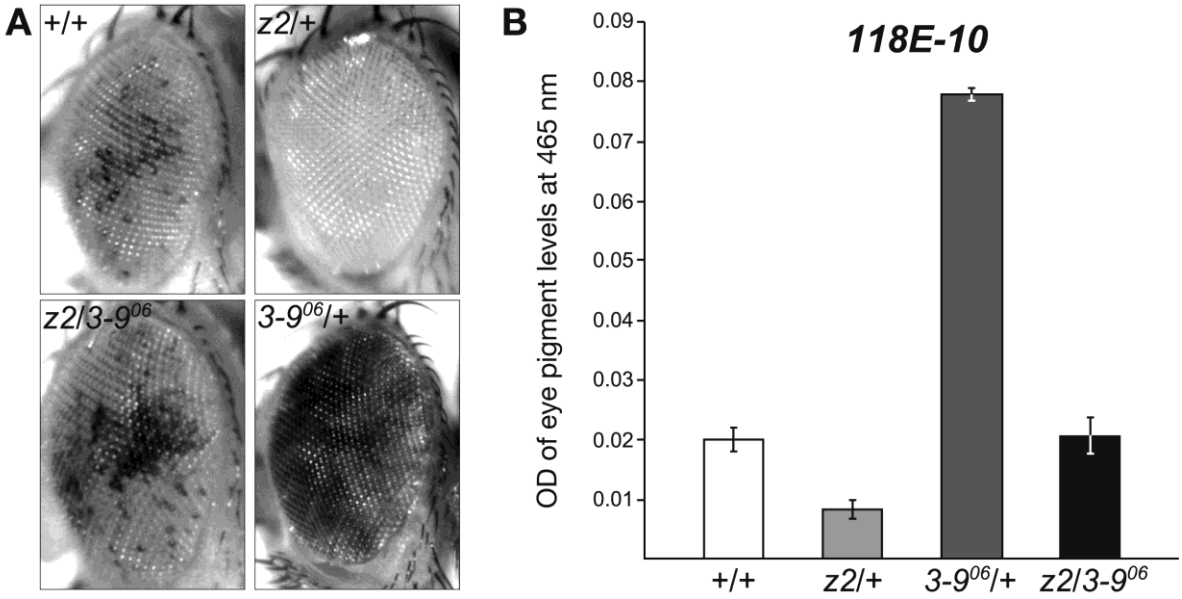

FIGURE 1. Counterbalancing effect of *JIL-1* and *Su(var)3-9* loss-of-function alleles on PEV of the P element insertion line *118E-10*. (A) Examples of the degree of PEV in the eyes of wild-type *JIL-1* and *Su(var)3-9* (+/+), *JIL-1^{z2}*/+ (*z2*/+), *Su(var)3-9^{06}*/+ (*3-9^{06}*/+), and *JIL-1^{z2}/Su(var)3-9^{06}* (*z2/3-9^{06}*) flies in a *118E-10/+* background. All images are from male flies. (B) Histograms of the distribution of the percentage of red ommatidia in +/+, *JIL-1^{z2}*/+ (*z2*/+), *Su(var)3-9^{06}*/+ (*3-9^{06}*/+), and *JIL-1^{z2}/Su(var)3-9^{06}* (*z2/3-9^{06}*) male flies heterozygous for *118E-10*. Fly stocks were maintained according to standard protocols (ROBERTS 1998).

Canton-S was used for wild-type preparations. The *JIL-1*^{z2} allele is described in WANG *et al.* (2001) and in ZHANG *et al.* (2003). The *Su(var)3-9*^{06} and *Su(var)2-5*^{05} alleles are described in SCHOTTA *et al.* (2002) and in EISSENBERG *et al.* (1992). The P-element *P[hsp26-pt, hsp70-w]* insertion line *118E-10* was the generous gift of Dr. L. Wallrath. The *hsp70* promoter is leaky and promotes sufficient expression to generate a variegated eye phenotype under non-heat shock conditions (WALLRATH and ELGIN 1995; BAO *et al.* 2007). Balancer chromosomes and markers are described in LINDSLEY and ZIMM (1992). PEV assays were performed as previously described in LERACH *et al.* (2006) and in BAO *et al.* (2007). In short, various combinations of *JIL-1*, *Su(var)3-9*, or *Su(var)2-5* alleles were introduced into the *118E-10* PEV arrangements by standard crossing. To quantify the variegated phenotype adult flies were collected from the respective crosses at eclosion, aged 6 days at 25°C, frozen in liquid nitrogen, and stored at -80˚C until assayed. The pigment assays were performed essentially as in KAVI and BIRCHLER (2009) using three sets of 10 fly heads of each genotype collected from males and females, respectively. For each sample the heads from the 10 flies were homogenized in 200 µl of methanol with 0.1% hydrochloric acid, centrifuged, and the optical density (OD) of the supernatant spectrophotometrically measured at a wavelength of 480 nm.

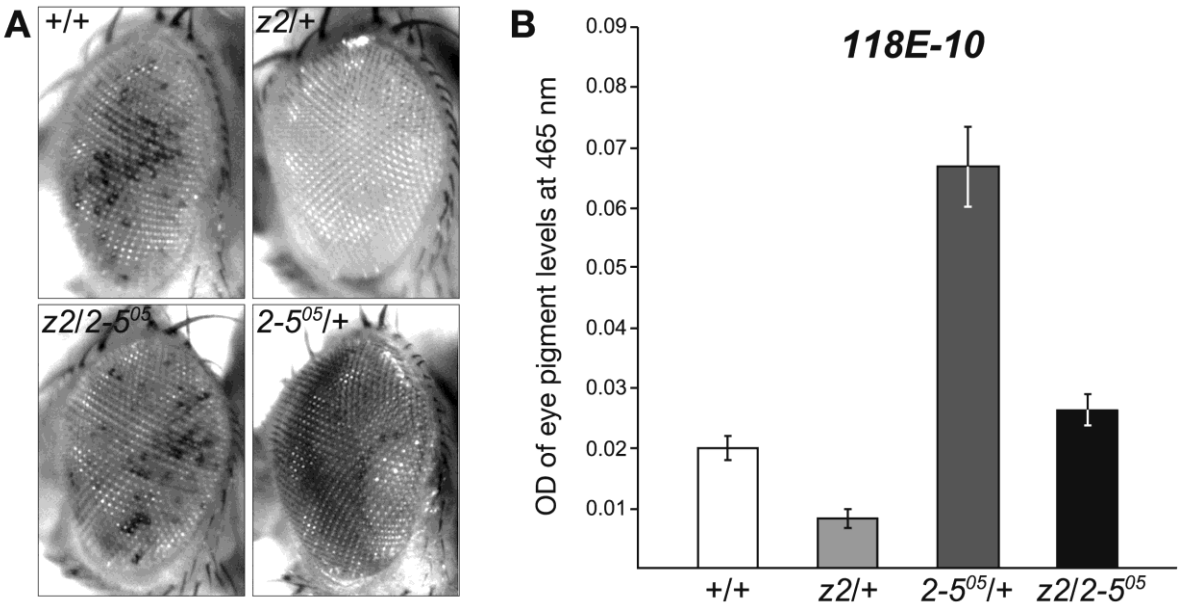

FIGURE 2. Counterbalancing effect of *JIL-1* and *Su(var)2-5* loss-of-function alleles on PEV of the P element insertion line *118E-10*. (A) Examples of the degree of PEV in the eyes of wild-type *JIL-1* and *Su(var)2-5* (+/+), *JIL-1^{z2}*/+ (*z2*/+), *Su(var)2-5^{05}*/+ (*2-5^{05}*/+), and *JIL-1^{z2}/Su(var) 2-5^{05}* (*z2/2-5^{05}*) flies in a *118E-10/*+ background. All images are from male flies. (B) Histograms of the distribution of the percentage of red ommatidia in +/+, *JIL-1^{z2}*/+ (*z2*/+), *Su(var2-5^{05}*/+ (*2-5^{05}*/+), and *JIL-1^{z2}/Su(var) 2-5^{05}* (*z2/2-5^{05}*) male flies heterozygous for *118E-10*.

Tables

Table 1. *Statistical comparison of eye pigment assays*

genotype[a]	*JIL-1^{z2}*/+	*3-9^{06}*/+	*JIL-1^{z2}/3-9^{06}*
118E-10/+			
+/+	$P < 0.005$	$P < 0.0001$	$P > 0.8$
JIL-1^{z2}/+	-	$P < 0.0001$	$P < 0.005$
3-9^{06}/+	-	-	$P < 0.0001$

genotype[a]	*JIL-1^{z2}*/+	*2-5^{05}*/+	*JIL-1^{z2}/2-5^{05}*
118E-10/+			
+/+	$P < 0.005$	$P < 0.0001$	$P > 0.06$
JIL-1^{z2}/+	-	$P < 0.0001$	$P < 0.005$
2-5^{05}/+	-	-	$P < 0.0005$

For each genotype the average pigment level from three sets of measurements from 10 pooled fly heads were compared using a two-tailed Student's t-test.

[a] Only male flies were scored.

CHAPTER 4. H3S10 PHOSPHORYLATION BY THE JIL-1 KINASE REGULATES H3K9 DIMETHYLATION AND GENE EXPRESSION AT THE *WHITE* LOCUS IN *DROSOPHILA*

A paper published in the *Fly (Austin)*

Chao Wang, Weili Cai, Yeran Li, Jack Girton, Jørgen Johansen and Kristen M. Johansen

Summary

The JIL-1 kinase is a multidomain protein that localizes specifically to euchromatin interband regions of polytene chromosomes and is the kinase responsible for histone H3S10 phosphorylation at interphase. Genetic interaction assays have suggested that the function of the epigenetic histone H3S10ph mark is to antagonize heterochromatization by participating in a dynamic balance between factors promoting repression and activation of gene expression as measured by position-effect variegation (PEV) assays. Interestingly, *JIL-1* loss-of-function alleles can act either as an enhancer or indirectly as a suppressor of w^{m4} PEV depending on the precise levels of JIL-1 kinase activity. In this study we have explored the relationship between PEV and the relative levels of the H3S10ph and H3K9me2 marks at the *white* gene in both wild-type and w^{m4} backgrounds by ChIP analysis. Our results indicate that H3K9me2 levels at the *white* gene directly correlate with its level of expression and that H3K9me2 levels in turn are regulated by H3S10 phosphorylation.

Introduction

In the absence of H3S10 phosphorylation by the JIL-1 kinase the major heterochromatin markers H3K9me2, HP1a, and Su(var)3-7 spread to ectopic locations on the chromosome arms of *Drosophila* polytene chromosomes (Zhang et al*.,* 2006; Deng et al., 2007; 2010). These observations suggested a model for a dynamic balance between euchromatin and heterochromatin (Ebert et al., 2004;Zhang et al., 2006; Deng et al., 2010; Wang et al., 2011a), where as can be monitored in position-effect variegation (PEV) arrangements, the level of gene expression is determined by antagonistic functions of the euchromatic H3S10ph mark and the heterochromatic H3K9me2 mark (Lerach et al., 2006; Bao et al., 2007; Deng et al., 2010; Wang et al., 2011a; 2011b). Wang et al. (2011a) tested this model by transgenically expressing various truncated versions of JIL-1, with or without kinase activity, and correlating their effect on PEV with the levels of the H3S10ph and H3K9me2 marks at a *hsp70-white* reporter gene as determined by ChIP assays in the pericentric insertion line *118E-10.* At pericentric sites loss-of-function alleles of JIL-1 act as enhancers of PEV whereas gain-of-function alleles act as suppressors (Bao et al., 2007). As predicted by the model, the results of Wang et al. (2011a) showed that the level of the H3K9me2 mark at the reporter was inversely proportional to the H3S10ph level. PEV was enhanced with increased levels of H3K9me2 in the absence of H3S10 phosphorylation and PEV was suppressed with increased levels of the H3S10ph mark and a concomitant decrease in the level of the H3K9me2 mark (Wang et al., 2011a). However, it has been demonstrated that *JIL-1* can act both as an enhancer as well as a suppressor of w^{m4} PEV depending on the precise levels of JIL-1 (Lerach et al., 2006; Deng et al., 2010), and that the genetic interactions between *JIL-1* and the *Su(var)3-9* and *Su(var)2-5* alleles in

regulating PEV of w^{m4} are more complex than in the case of *118E-10* where reduced levels of JIL-1 always act as an enhancer (Bao et al., 2007; Wang et al., 2011b). Therefore, in the present study we explored the relationship between PEV and the relative levels of the H3S10ph and H3K9me2 marks at the *white* gene in both wild-type and w^{m4} backgrounds by ChIP analysis.

Results and Discussion

The *In(1)*w^{m4} X chromosome contains an inversion that juxtaposes the euchromatic *white* gene and centric heterochromatic sequences distal to the nucleolus organizer (Muller 1930; Pirrotta et al., 1983) (Fig. 1). The resulting somatic variegation of w^{m4} expression occurs in clonal patches in the eye reflecting heterochromatic spreading from the inversion breakpoint that silences w^{m4} expression in the white patches and euchromatic packaging of the *w* gene in those patches that appear red (reviewed in Grewal and Elgin 2002) (Fig. 2B). Studies of this effect suggest that the degree of spreading may depend on the amount of heterochromatic factors at the breakpoint (reviewed in Weiler and Wakimoto 1995; Girton and Johansen 2008). Interestingly, strong hypomorphic combinations of *JIL-1* alleles, in which heterochromatic factors spread to ectopic locations (Zhang et al., 2006; Deng et al., 2007), act as suppressors not enhancers of PEV of the w^{m4} allele (Lerach et al., 2006) (Fig. 2E). Based on these findings, Lerach et al. (2006) proposed a model where the suppression of PEV of w^{m4} in strong *JIL-1* hypomorphic backgrounds is due to a reduction in the level of heterochromatic factors at the pericentromeric heterochromatin near the inversion breakpoint site that reduces the potential for heterochromatic spreading and silencing (Fig. 1).

In order to measure how the relative H3S10ph and H3K9me2 levels at the *white* gene were affected in the experiments, we performed ChIP assays as in Legube et al. (2006) and in Wang et al. (2011a). Chromatin was immunoprecipitated (ip) from larval salivary glands from wild-type, the inversion line w^{m4}, the inversion line in either a heterozygous *JIL-1* mutant background w^{m4}; *JIL-1*^{z2}/+, or a homozygous *JIL-1* mutant background w^{m4}; *JIL-1*^{z2}/*JIL-1*^{z2}, or the inversion line with either a transgenic JIL-1 CTD or DCTD construct w^{m4}; "*JIL-1* transgene"/+; *da-GAL4*/+ using rabbit anti-H3S10ph antibody or purified rabbit IgG antibody (negative control) or mAbs to H3K9me2 or GST (negative control). Primers corresponding to region -110 to +65 of the *white* gene were used to amplify the precipitated material. Experiments were done in triplicate and relative enrichment of *white* DNA from the H3S10ph and H3K9me2 ips were normalized to the corresponding control antibody ips performed in tandem for each experimental sample. Statistical comparisons using a Student's two-tailed t-test of the relative enrichment levels of H3S10ph and H3K9me2 between the various genotypes are provided in Table 1 and 2. As illustrated in Fig. 3 there is a relatively higher enrichment of H3S10ph (4.3±0.8) than of H3K9me2 (2.0±0.5) at the *white* gene in wild-type. However, compared to wild-type (Fig. 2A) the variegated eye phenotype in w^{m4} (Fig. 2B) is correlated with an almost 4-fold decrease in relative H3S10ph enrichment levels (1.4±0.4) and a more than 3-fold increase in the relative H3K9me2 enrichment levels (6.7±1.6). Interestingly, this distribution can be reversed by expression of a JIL-1 DCTD construct which lacks the COOH-terminal sequences required for proper chromatin localization leading to mislocalization of the protein (Bao et al., 2008). However, it does retain its kinase activity resulting in ectopic histone H3S10 phosphorylation (Bao et al., 2008) and suppression of PEV (Wang et al., 2011a) (Fig. 2C). As shown in Fig. 3 expression of JIL-1 DCTD in a w^{m4} background leads to a dramatic increase of almost 10-fold in the relative enrichment of H3S10ph (9.9±0.9) at

the *white* gene accompanied with a decrease in the relative enrichment of H3K9me2 (1.7±0.1) to levels comparable to wild-type (Table 1 and 2).

Because strong hypomorphic combinations of *JIL-1* alleles act as suppressors of PEV (Fig. 2E), the prediction of the model of Lerach et al. (2006) (Fig. 1) is that the relative enrichment of H3K9me2 at the *white* gene in a w^{m4}; $JIL\text{-}1^{z2}/JIL\text{-}1^{z2}$ background should be at or below wild-type levels. $JIL\text{-}1^{z2}$ is a true null allele (Wang et al., 2001) without any detectable H3S10 phosphorylation in interphase cells such as third instar salivary gland cells (Bao et al., 2008). As illustrated in Fig. 4 we found almost no relative enrichment compared to the antibody control ips of both H3K9me2 (1.1±0.1) and H3S10ph (1.1±0.1) in agreement with the above hypothesis. Interestingly, it has been demonstrated that $JIL\text{-}1^{z2}$ can act as an haplo-enhancer (Deng et al., 2010; Wang et al., 2011b) (Fig. 2D) and as shown in Fig. 4 when only one copy of $JIL\text{-}1^{z2}$ is present in a w^{m4} background the relative enrichment of H3K9me2 (6.7±0.8) increases 6-fold compared to the homozygous $JIL\text{-}1^{z2}$ condition whereas the relative enrichment of H3S10ph (1.3±0.4) is indistinguishable from that in the w^{m4} and w^{m4}; $JIL\text{-}1^{z2}/JIL\text{-}1^{z2}$ backgrounds (Table 1 and 2). Furthermore, when a construct containing only the COOH-terminal domain (CTD) of JIL-1 is expressed in a wild-type background it has a dominant-negative effect and displaces endogenous JIL-1 leading to a striking decrease in histone H3S10ph levels (Bao et al., 2008) and spreading of H3K9me2 to the chromosome arms as in $JIL\text{-}1^{z2}/JIL\text{-}1^{z2}$ null mutants (Wang et al., 2011a). As illustrated in Fig. 4 expression of the CTD in a w^{m4} background leads to a relative enrichment of the H3K9me2 (1.4±0.3) and H3S10ph (0.9±0.1) marks indistinguishable from that in the w^{m4}; $JIL\text{-}1^{z2}/JIL\text{-}1^{z2}$ background (Table 1 and 2). Furthermore, this low level of H3K9me2 mark at the *white* gene is correlated with suppression of PEV (Wang et al., 2011a) (Fig. 2F).

Taken together the present experiments indicate that H3K9me2 levels at the *white* gene directly correlate with its level of expression and that H3K9me2 levels in turn are regulated by H3S10 phosphorylation providing strong support for the model depicted in Fig. 1. In wild-type there are low levels of the epigenetic H3K9me2 mark at the *white* gene resulting in its normal expression. However, in the w^{m4} allele heterochromatic factors can spread across the inversion breakpoint leading to high levels of H3K9me2 at the *white* gene and silencing of gene expression. Interestingly, we show that this increase in H3K9me2 level can be counteracted by ectopic H3S10 phosphorylation at the *white* gene restoring gene expression. In contrast, in the absence of H3S10 phosphorylation as it occurs in strong *JIL-1* hypomorphic mutant backgrounds there is a redistribution of heterochromatic factors to ectopic chromosome sites resulting in reduced levels of these factors at the pericentric heterochromatin. This leads to less heterochromatic spreading and low levels of H3K9me2 at the *white* gene in the w^{m4} inversion, thus allowing for *white* gene expression. This expression occurs without H3S10 phosphorylation providing additional evidence that the H3S10 mark is not required for RNA polymerase II-mediated transcription (Cai et al., 2008) but rather regulates transcription indirectly by counteracting H3K9 dimethylation and gene silencing.

Methods

Drosophila melanogaster stocks

Fly stocks were maintained at 25°C according to standard protocols (Roberts, 1998). The $JIL\text{-}1^{z2}$ and the $JIL\text{-}1^{z60}$ alleles are described in Wang et al. (2001) as well as in Zhang et al. (2003). The CTD construct containing residue 1-926 and the CTD construct containing sequences from aa 927-1207 in the pYES vector are described in Wang et al.

(2011a). Expression of the transgenes were driven using a *da-GAL4* driver introduced by standard genetic crosses. The driver line and the *In(1)w*^{m4} allele was obtained from the Bloomington Stock Center. Balancer chromosomes and markers are described in Lindsley and Zimm (1992). w^{m4} flies or larvae (w^{m4}/Y or w^{m4}/w^{m4}) in combination with *JIL-1* mutant alleles or expressing the CTD or CTD constructs were generated by standard crossing. Eyes from representative individuals from these crosses were photographed using an Olympus Stereo Microscope and a Spot digital camera (Diagnostic Instruments).

Chromatin immunoprecipitation

For ChIP experiments 50 pairs of salivary glands per sample were dissected from third instar larvae and fixed for 15 min at room temperature in 1 ml of fixative (50 mM HEPES at pH 7.6, 100 mM NaCl, 0.1 mM EDTA at pH 8, 0.5 mM EGTA at pH 8, 2% formaldehyde). Preparation of chromatin for immunoprecipitation was performed as previously described in Legube et al. (2006). Rabbit anti-H3S10ph antibody (Active Motif), purified rabbit IgG antibody (Sigma), anti-H3K9me2 mAb (Abcam), or anti-GST mAb 8C7 (Rath et al. 2004) was used for immunoprecipitation. For each sample the chromatin lysate was divided into equal amounts and immunoprecipitated with experimental and control antibody, respectively. DNA from the immunoprecipitated chromatin fragments (500 bp average) was purified by a Wizard SV DNA purification kit (Promega). The isolated DNA was used as template for quantitative real-time (qRT) PCR performed with the Stratagene Mx4000 real-time cycler. The PCR mixture contained Brilliant II SYBR Green QPCR Master Mix (Stratagene) as well as the corresponding primers: *white*-forward 5'-GTGCTGTGCCAAAACTCCTC-3', *white*-reverse 5'-GATGCTCGGCAGATGGGTTGT-3' which amplify region -110 to +65. Cycling parameters were 10 min at 95°C, followed by 40 cycles of 30 sec at 95°C, 30 sec at 55°C, and 30 sec at 72°C. Fluorescence intensities were

plotted against the number of cycles using an algorithm provided by Stratagene. DNA levels were quantified using a calibration curve based on dilution of concentrated DNA. For each experimental condition the relative enrichment was normalized to the corresponding control immunoprecipitation from the same chromatin lysate.

Acknowledgements

We thank members of the laboratory for discussion, advice, and critical reading of the manuscript. We also wish to acknowledge Mr. Atrez Norwood for technical assistance. This work was supported by NIH Grant GM062916 (KMJ/JJ).

References

Bao X, Deng H, Johansen J, Girton J, Johansen KM (2007). Loss-of-function alleles of the JIL-1 histone H3S10 kinase enhance position-effect-variegation at pericentric sites in Drosophila heterochromatin. Genetics 176:1355-1358.

Bao X, Cai W, Deng H, Zhang W, Krencik R, Girton J, Johansen J, Johansen KM (2008). The COOH-terminal domain of the JIL-1 histone H3S10 kinase interacts with histone H3 and is required for correct targeting to chromatin. J Biol Chem 283:32741-32750.

Cai W, Bao X, Deng H, Jin Y, Girton J, Johansen J, Johansen KM (2008). RNA polymerase II-mediated transcription at active loci does not require histone H3S10 phosphorylation in *Drosophila*. Development 135:2917-2925.

Deng H, Bao X, Zhang W, Girton J, Johansen J, Johansen KM (2007). Reduced levels of Su(var)3-9 but not Su(var)2-5 (HP1) counteract the effects on chromatin structure and viability in loss-of-function mutants of the JIL-1 histone H3S10 kinase. Genetics 177:79-87.

Deng H, Cai W, Wang C, Lerach S, Delattre M, Girton J, Johansen J, Johansen KM (2010). *JIL-1* and *Su(var)3-7* interact genetically and counterbalance each others' effect on position effect variegation in Drosophila. Genetics 185:1183-1192.

Ebert A, Schotta G, Lein S, Kubicek S, Krauss V, Jenuwein T, Reuter G (2004). *Su(var)* genes regulate the balance between euchromatin and heterochromatin in *Drosophila*. Genes Dev 18:2973-2983.

Girton J, Johansen KM (2008). Chromatin structure and regulation of gene expression: the lessons of PEV in *Drosophila*. Adv Genet 61:1-43.

Greval SI, Elgin SC (2002). Heterochromatin: new possibilities for the inheritance of structure. Curr Opin Genet Dev 12:178-187.

Legube G, McWeeney SK, Lercher MJ, Akhtar A (2006). X-chromosome-wide profiling of MSL-1 distribution and dosage compensation in *Drosophila*. Genes Dev 20:871-883.

Lerach S, Zhang W, Bao X, Deng H, Girton J, Johansen J, Johansen KM (2006). Loss-of-function alleles of the JIL-1 kinase are strong suppressors of position effect variegation of the w^{m4} allele in *Drosophila*. Genetics 173:2403-2406.

Lindsley DL, Zimm GG (1992). The genome of *Drosophila melanogaster*. Academic Press, New York, NY.

Muller HJ (1930). Types of visible variegations induced by X-rays in *Drosophila*. J Genetics 22:299-335.

Pirrotta V, Hadfield C, Pretorius GHJ (1983). Microdissection and cloning of the white locus and the 3B1 – 3C2 region of the Drosophila X chromosome. EMBO J 2:927 – 934.

Rath U, Wang D, Ding Y, Xu Y-Z, Qi H, Blacketer MJ, Girton J, Johansen J, Johansen KM (2004). Chromator, a novel and essential chromodomain protein interacts directly with the putative spindle matrix protein Skeletor. J Cell Biochem 93:1033-1047.

Roberts DB (1998). In *Drosophila*: A Practical Approach IRL Press, Oxford, UK.

Wang C, Cai W, Li Y, Deng H, Bao X, Girton J, Johansen J, Johansen KM (2011a). The epigenetic H3S10 phosphorylation mark is required for counteracting heterochromatic spreading and gene silencing in *Drosophila melanogaster*. J Cell Sci 124:4309-4317.

Wang C, Girton J, Johansen J, Johansen KM (2011b). A balance between euchromatic (JIL-1) and heterochromatic (SU(VAR)2-5 and SU(VAR)3-9) factors regulates position-effect variegation in Drosophila. Genetics 188:745-748.

Wang Y, Zhang W, Jin Y, Johansen J, Johansen KM (2001). The JIL-1 tandem kinase mediates histone H3 phosphorylation and is required for maintenance of chromatin structure in *Drosophila*. Cell 105:433-443.

Weiler KS, Wakimoto BT (1995). Heterochromatin and gene expression in *Drosophila*. Annu Rev Genet 29:577-605.

Zhang W, Jin Y, Ji Y, Girton J, Johansen J, Johansen KM (2003). Genetic and phenotypic analysis of alleles of the Drosophila chromosomal JIL-1 kinase reveals a functional requirement at multiple developmental stages. Genetics 165:1341-1354.

Zhang W, Deng H, Bao X, Lerach S, Girton J, Johansen J, Johansen KM (2006). The JIL-1 histone H3S10 kinase regulates dimethyl H3K9 modifications and heterochromatic spreading in *Drosophila*. Development 133:229-235.

Figures

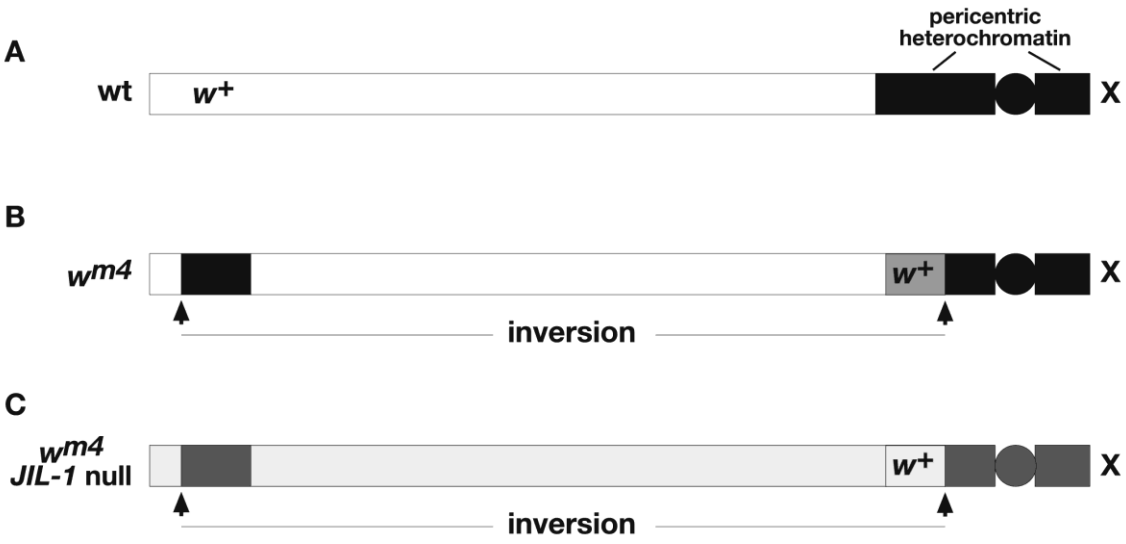

Figure 1 Diagrams of the distribution of heterochromatic factors relative to the *white* gene in wild-type and w^{m4} X chromosomes. (A) In wild-type high levels of heterochromatic factors are confined to pericentric heterochromatin (in black) and the distally located *white* gene is expressed at normal levels. (B) In w^{m4} an inversion juxtaposes the *white* gene to the pericentric heterochromatin where spreading of heterochromatic factors across the inversion breakpoint (in dark grey) represses *white* expression as reflected in PEV. (C) In a *JIL-1* null w^{m4} background in the absence of H3S10 phosphorylation there is a redistribution of heterochromatic factors from the pericentric heterochomatin to ectopic

locations on the chromosome arms (light grey). The resulting decrease in the level of heterochromatic factors at the pericentric heterochromatin (in dark grey) reduces its potential for heterochromatic spreading and gene silencing and under these conditions the *white* gene is expressed.

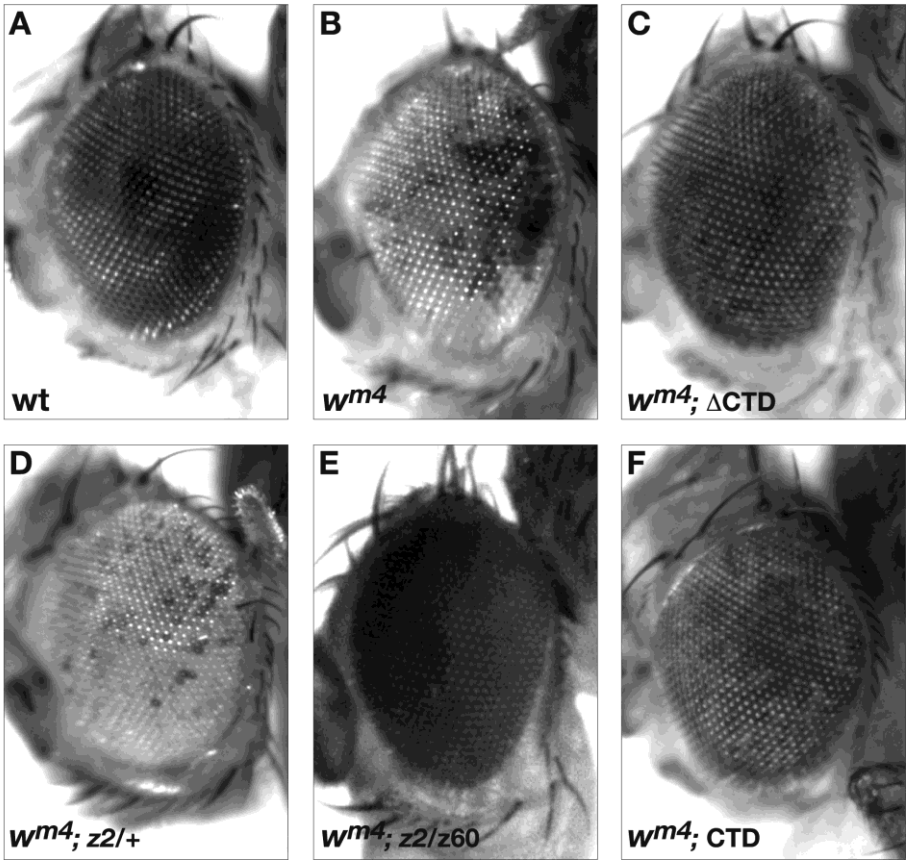

Figure 2 The effect on PEV of the w^{m4} allele by *JIL-1* hypomorphic alleles or by expression of the CTD or the DCTD. Examples of the degree of PEV in the eyes of (A) wild-type flies, (B) w^{m4} flies, (C) w^{m4} flies expressing the DCTD, (D) w^{m4}; *JIL-1*^{z2}/+ flies, (E) w^{m4}; *JIL-1*^{z2}/ *JIL-1*^{z60} flies, and (F) w^{m4} flies expressing the CTD. All pictures are from male flies.

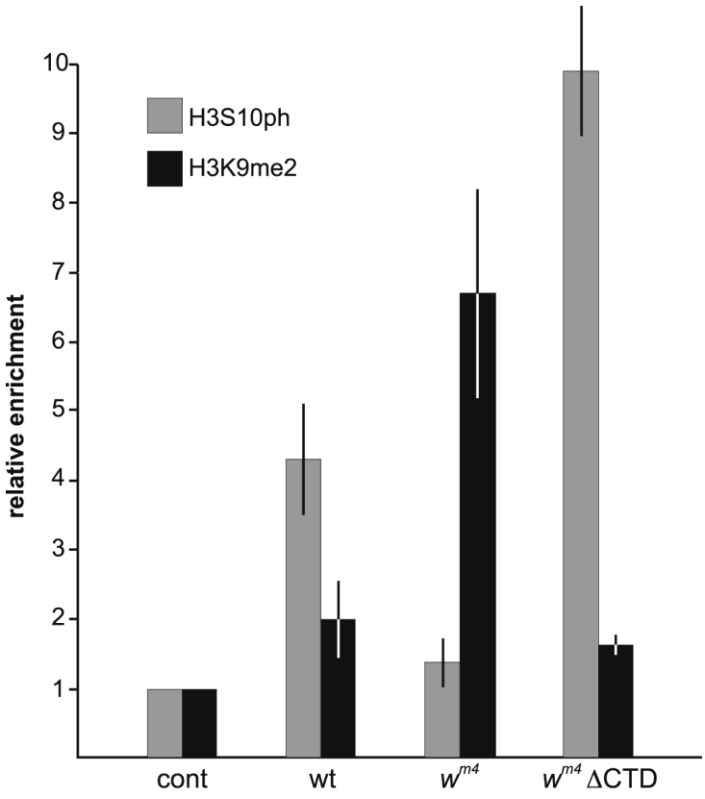

Figure 3 ChIP analysis of the *white* gene in wild-type and w^{m4} backgrounds. Histograms of the relative enrichment of chromatin immunoprecipitated by anti-H3S10ph or anti-H3K9me2 antibody from third instar larval salivary glands from wild-type, w^{m4}, or w^{m4} expressing the DCTD. For each experimental condition the average relative enrichment normalized to the corresponding control immunoprecipitation from three independent experiments with S.D. is shown.

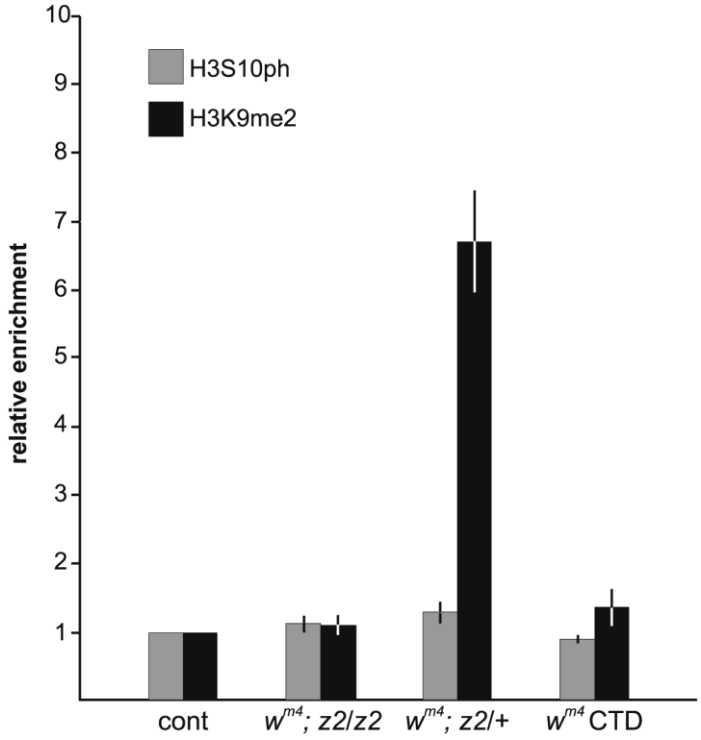

Figure 4 ChIP analysis of the *white* gene in w^{m4}, *JIL-1* hypomorphic allelic backgrounds. Histograms of the relative enrichment of chromatin immunoprecipitated by anti-H3S10ph or anti-H3K9me2 antibody from third instar larval salivary glands from w^{m4}; $JIL\text{-}1^{z2}$/ $JIL\text{-}1^{z2}$, w^{m4}; $JIL\text{-}1^{z2}$/+, or w^{m4} expressing the CTD. For each experimental condition the average relative enrichment normalized to the corresponding control immunoprecipitation from three independent experiments with S.D. is shown.

Tables

Table 1 Statistical comparison of H3K9me2 levels

Genotype	w^{m4}	w^{m4}; *z2*/+	w^{m4}; *z2/z2*	w^{m4}; CTD	w^{m4}; DCTD
wt	P<0.001	P<0.001	P>0.4	P>0.5	P>0.8
w^{m4}	-	P>0.9	P<0.001	P<0.001	P<0.001
w^{m4}; *z2*/+	-	-	P<0.001	P<0.001	P<0.001
w^{m4}; *z2/z2*	-	-	-	P>0.8	P>0.5
w^{m4}; CTD	-	-	-	-	P>0.7

For each genotype the average relative enrichment from three sets of measurements were compared using a two-tailed Student's t-test.

Table 2 Statistical comparison of H3S10ph levels

Genotype	w^{m4}	w^{m4}; *z2*/+	w^{m4}; *z2/z2*	w^{m4}; CTD	w^{m4}; DCTD
wt	P<0.005	P<0.002	P<0.002	P<0.001	P<0.0001
w^{m4}	-	P>0.9	P>0.7	P>0.5	P<0.0001
w^{m4}; *z2*/+	-	-	P>0.8	P>0.6	P<0.0001
w^{m4}; *z2/z2*	-	-	-	P>0.7	P<0.0001
w^{m4}; CTD	-	-	-	-	P<0.0001

For each genotype the average relative enrichment from three sets of measurements were compared using a two-tailed Student's t-test.

CHAPTER 5. GENOME-WIDE ANALYSIS OF REGULATION OF GENE EXPRESSION AND H3K9me2 DISTRIBUTION BY JIL-1 KINASE MEDIATED HISTONE H3S10 PHOSPHORYLATION IN *DROSOPHILA*

A paper published in the *Nucleic Acid Research*

Weili Cai, Chao Wang, Yeran Li, Changfu Yao, Lu Shen, Sanzhen Liu, Xiaomin Bao, Patrick S. Schnable, Jack Girton, Jørgen Johansen and Kristen M. Johansen

Summary

In this study we have determined the genome-wide relationship of JIL-1 kinase mediated H3S10 phosphorylation with gene expression and the distribution of the epigenetic H3K9me2 mark. We show in wild-type salivary gland cells that the H3S10ph mark is predominantly enriched at active genes whereas the H3K9me2 mark largely is associated with inactive genes. Comparison of global transcription profiles in salivary glands from wild-type and *JIL-1* null mutant larvae revealed that the expression levels of 1539 genes changed at least two-fold in the mutant and that a substantial number (49%) of these genes were upregulated whereas 51% were downregulated. Furthermore, the results showed that downregulation of genes in the mutant was correlated with higher levels or acquisition of the H3K9me2 mark whereas upregulation of a gene was correlated with loss of or diminished H3K9 dimethylation. These results are compatible with a model where gene expression levels are modulated by the levels of the H3K9me2 mark independent of the state of the H3S10ph mark, which is not required for either transcription or gene activation to occur. Rather, H3S10 phosphorylation functions to indirectly maintain active transcription by counteracting H3K9 dimethylation and gene silencing.

Introduction

The JIL-1 kinase localizes specifically to euchromatic interband regions of polytene chromosomes and is the kinase responsible for histone H3S10 phosphorylation at interphase in *Drosophila* (1,2). Genetic interaction assays with *JIL-1* hypomorphic and null allelic combinations demonstrated that JIL-1 can counterbalance the gene-silencing effect of the three major heterochromatin markers H3K9me2, Su(var)3-7, and HP1a on position-effect variegation and that in the absence of histone H3S10 phosphorylation these epigenetic marks spread to ectopic locations on the arms of polytene chromosomes (3-7). These observations suggested a model for a dynamic balance between euchromatin and heterochromatin (3,5,6,8), where the level of gene expression is determined by antagonistic functions of the euchromatic H3S10ph mark on the heterochromatic H3K9me2 mark. In strong support of this model Wang et al. (6,9) recently provided evidence that H3K9me2 levels at reporter genes inversely correlate with their levels of expression and that H3K9me2 levels in turn are regulated by H3S10 phosphorylation. Thus, taken together these findings suggest that a major function of JIL-1 mediated histone H3S10 phosphorylation is to maintain an active state of chromatin by counteracting H3K9 dimethylation and gene silencing (3,6,9,10). In an alternative scenario Corces and co-workers have proposed that JIL-1 and histone H3S10 phosphorylation are required for active transcription by the RNA polymerase II machinery (11-13). However, the results of these studies have been controversial because it has been demonstrated that RNA polymerase II-mediated transcription occurs at robust levels in the absence of H3S10 phosphorylation in *Drosophila* (10,14,15).

In this study to explore the global interplay between the epigenetic H3S10ph and H3K9me2 chromatin modifications and gene expression, we conducted a genome-wide analysis of their enriched sites and combined it with an analysis of changes to the distribution of the H3K9me2 mark and of whole genome transcription level changes in the absence of H3S10 phosphorylation. In order to have the ability to specifically map and correlate the location of JIL-1 and H3K9me2 with the locations of the histone H3S10 phosphorylation mark, salivary gland cells from third instar larvae were analyzed. Salivary gland nuclei are all at interphase excluding contributions from mitotic histone H3S10 phosphorylation. We found that most of the identified JIL-1 binding peaks located at or near transcription start sites (TSS) whereas peaks for both H3S10ph and H3K9me2 enrichment were located around 600 bp downstream of the TSS. A comparison of the transcriptome profiles of salivary glands from wild type and *JIL-1* null mutants revealed that the expression levels of 1539 genes changed at least two-fold in the mutant. Interestingly, out of these genes the expression of 66% of normally active genes was repressed, whereas the expression of most normally inactive genes (77%) was activated. Furthermore, we show that in the absence of H3S10 phosphorylation the H3K9me2 mark redistributes and becomes upregulated on ectopic sites on the chromosome arms, especially on the X-chromosome, and that this H3K9me2 redistribution correlates with the activation of silent genes and the repression of active genes. Taken together these results provide direct support for the model that H3S10 phosphorylation mainly facilitates gene expression of active genes by maintaining an open chromatin structure at promoter regions by counteracting H3K9 dimethylation.

Materials and Methods

Drosophila melanogaster stocks

Fly stocks were maintained according to standard protocols (16). Canton S. was used for wild type preparations. The *JIL-1*^{z2} allele is described in Wang et al. (2) and in Zhang et al. (17).

ChIP-Sequencing and data analysis

For ChIP-sequencing, 50 pairs of salivary glands per sample were dissected from third instar larvae and fixed for 15 minutes at room temperature in 1 ml of fixative (50 mM HEPES at pH 7.6, 100 mM NaCl, 0.1 mM EDTA at pH 8, 0.5 mM EGTA at pH 8, 2% formaldehyde). Preparation of chromatin for immunoprecipitation was performed as previously described (18). Mouse anti-JIL-1 mAb 5C9 (19), mouse anti-H3K9me2 mAb 1220 (Abcam), or rabbit anti-H3S10ph pAb (Cell Signaling or Active Motif) were used for immunoprecipitation. For each sample, 10% of the chromatin lysate was used as control input DNA, and 90% was immunoprecipitated with the antibody. DNA from the immunoprecipitated chromatin fragments was purified using a Wizard SV DNA purification kit (Promega).

Before sequencing the purified ChIP-enriched DNA fragments were selected on an agarose gel for fragments 200 bp in size, linkers were added, and the library was amplified by PCR. Each library was sequenced at the Iowa State University DNA facility by a Genome Analyser II next-generation sequencing platform (Illumina). All samples were processed using the standard 36 bp single-end protocol (Illumina). All reads were mapped to version 3 of the *Drosophila melanogaster* genome using Bowtie V0.12.7 (20) with the

default settings and output to the SAM format. SAMtools V0.1.18 (21) and BEDtools V2.14.3 (22) were used to sort and transfer files. Enriched islands for JIL-1, H3S10ph and H3K9me2 (wild-type and *JIL-1*^{Z2}/ *JIL-1*^{Z2}) were identified using SICER V1.1 with 200 bp window size, 200 bp gap size, and an effective genome size of 72% of the *Drosophila* genome (23). Enriched islands with a false discovery rate (FDR) of 1% or less were considered to be valid. MACS V1.4 (24) was used to identify JIL-1 binding peaks with default settings and FDRs of 10% or less. Binding islands or the number of reads obtained in each genomic region scaled to the total number of reads were rendered in the integrated genome viewer (IGV 2.0). ChIP on chip profiles of Chromator were generated from data in Kc cells obtained by ModENCODE (25) and presented as average log2 signal ratio of IP over input. The ChIPpeakAnno bioconductor R package (26) was employed to annotate the binding sites to the nearest start of a gene and to map the distance to the nearest TSS. Density plots of the center of enriched binding islands relative to the distance from the TSS of nearby genes were made using SAS (SAS Institute Inc).

RNA-sequencing and data analysis

For RNA-sequencing total RNA from third instar salivary glands was isolated using the UltraClean Tissue and Cells RNA isolation Kit (Mo Bio). DNA was removed using the DNase I kit (Mo Bio). Two replicated samples of each Wild-type and *JIL-1*^{z2}/*JIL-1*^{z2} null mutant RNA were amplified and sequenced on an Illumina Hiseq2000 at the Iowa State University DNA facility using a paired-end protocol. Low quality nucleotides were removed from raw reads using Data2Bio's trimming script (27). GSNAP (Genomic Short-read Nucleotide Alignment Program, version 2013-10-12) (28), which allows for intron-spanning alignments, was used to map trimmed reads to the reference genome (BDGP 5.72/dm3 June 2013). Reads with one unique best match in the reference genome (BDGP 5.72/dm3

June 2013) with ≤2 mismatches every 75 bp were used for all subsequent analyses. The read depth of each gene was computed based on the coordinates of mapped reads and the annotated locations of genes in the reference genome (BDGP 5.72/dm3 June 2013). Reads per kilobase of exons per million uniquely mapped reads (RPKM) values were calculated as in Mortazavi et al. (29).

For identification of genes with different expression in the *JIL-1* mutant background the log-scale 75th percentile of library size normalization method was used to normalize wild-type and mutant RNA-Seq reads (30). The normalized reads were counted by HTseq(v0.5.4). The QuasiSeq (R package) was used to identify differentially expressed genes by negative binomial quasi-likelihood estimation (31). Genes were considered differentially expressed between wild-type and the mutant if they exhibited a greater than 2 fold change in expression and an FDR smaller than 0.05. Scatter plot representations of gene expression changes between wild-type and *JIL-1* null mutant salivary gland cells as well as regression analysis were performed using SAS (SAS Institute Inc). Gene Ontology (GO) term categories for genes identified as down- or up-regulated in *JIL-1* null mutant versus wild-type salivary glands were identified by DAVID (32) in Level 5 of biological process and molecular function. In addition, boxplots, bar charts, and pie charts were made used using the ggplot2 R package (33) and statistical analysis was performed with R (v3.0.1).

Chromatin immunoprecipitation and qPCR

ChIP experiments were performed as previously described (6,18). In short, for ChIP experiments, 50 pairs of salivary glands per sample were dissected from third instar larvae and fixed for 15 minutes at room temperature in 1 ml of fixative (50 mM HEPES at pH 7.6, 100 mM NaCl, 0.1 mM EDTA at pH 8, 0.5 mM EGTA at pH 8, 2% formaldehyde). Mouse

anti-JIL-1 mAb 5C9 (19), anti-H3K9me2 (Abcam), anti-GST mAb 8C7 (34), anti-H3S10ph (Cell Signaling, Active Motif) or purified rabbit IgG(Sigma) were used for immunoprecipitation. For each sample, the chromatin lysate was divided into equal amounts and immunoprecipitated with experimental and control antibody, respectively. DNA from the immunoprecipitated chromatin fragments (average length, 500 bp) was purified using a Wizard SV DNA purification kit (Promega).

Quantitative PCR was carried out using Brilliant® II SYBR Green QPCR Master Mix (STRATAGENE) in conjunction with an Mx4000 (STRATAGENE) PCR machine. The primers used for the various qPCR experiments are listed in Supplementary Table 1. Cycling parameters were 10 min at 95°C, followed by 40 cycles of 30 sec at 95°C, 30 sec at 55°C, and 30 sec at 72°C. Fluorescence intensities were plotted against the number of cycles using an algorithm provided by Stratagene. Template levels were quantified using a calibration curve based on dilution of concentrated DNA. For each experimental condition the relative enrichment was normalized to the corresponding control immunoprecipitation from the same chromatin lysate.

Immunohistochemistry

Polytene chromosome squash preparations were performed as in Cai et al. (35) using a 5 minute fixation protocol and double labeled with JIL-1 mAb 5C9 (19) and rabbit anti-histone H3K9me2 (Millipore). DNA was counterstained by Hoechst 33258 (Molecular Probes) in PBS. The appropriate species- and isotype- specific TRITC-, and FITC-conjugated secondary antibodies (Cappel/ICN, Southern Biotech) were used (1:200 dilution). The final preparations were mounted in 90% glycerol containing 0.5% n-propyl gallate. The preparations were examined using epifluorescence optics on a Zeiss Axioskop microscope and images were captured and digitized using a cooled Spot CCD camera.

Images were imported into Photoshop where they were pseudocolored, image processed, and merged. In some images non-linear adjustments were made to the channel with Hoechst labeling for optimal visualization of chromosomes.

Modeling of JIL-1

The structure of JIL-1 was modeled with the I-TASSER protein prediction server (36,37) and compared to the crystal structure of a nucleosome (PDB ID: 1AOI). I-TASSER generates models of proteins by excising continuous fragments from Local Meta-Threading-Server multiple-threading alignments and then reassembling them using replica-exchange Monte Carlo simulations (38). The comparison and visualization between the model of JIL-1 and the nucleosome was processed and rendered by PyMOL.

Data Access

The ChIP-Seq and RNA-Seq data of this study have been deposited in the NCBI Gene Expression Omnibus and is accessible for review purposes at: http://www.ncbi.nlm.nih.gov/geo/query/acc.cgi?token=jbkffaicascisfa&acc=GSE41047

Results

Mapping the genome-wide distribution of JIL-1, H3S10ph, and H3K9me2 in salivary gland cells

All DNA and RNA samples analyzed were from post-mitotic third instar larval salivary glands that included both sexes and issues of JIL-1's and H3S10 phosphorylation's role in

dosage compensation of the X-chromosome were not addressed in this study. For comparisons of gene transcription and H3K9me2 distribution in the absence of JIL-1 and H3S10 phosphorylation with wild-type we analyzed DNA and RNA from salivary glands of *JIL-1*^{z2}/*JIL-1*^{z2} homozygous larvae. *JIL-1*^{z2} is a true null allele generated by P-element mobilization (2). The global transcription profiles were generated by analysis of two independent RNA-Seq experiments. Based on the formula of Mortazavi et al. (29) we calculated that in salivary glands one read per kilobase of exons per million uniquely mapped reads (RPKM) corresponded to approximately one transcript per cell. Thus, genes with an RPKM of one or more were considered active, otherwise they were categorized as inactive. We further classified the active genes into three separate groups with low, moderate, or high expression levels reflected by RPKMs of from 1-5, >5-30, or >30, respectively. For ChIP-Seq analysis of JIL-1 genomic binding sites we used a previously characterized and highly specific mAb 5C9 (19) and conducted two independent experiments. Enriched chromatin binding sites were identified using the SICER algorithm (23) (Fig. 1A). The resulting two data sets were highly correlated (Supplemental Fig. S1) and we identified 2819 genes associated with binding sites enriched for JIL-1 present in both data sets that were used for the following analysis. For ChIP-Seq analysis of the genome-wide distribution of the H3S10ph mark we used two previously validated antibodies (6,9) from Cell Signaling (CS) and Active Motif (AM), respectively. As illustrated in Supplemental Fig. S1 the two data sets for these antibodies were strongly correlated and we identified 2948 genes enriched for H3S10ph present in both data sets that were used for the subsequent analysis. For analysis of the H3K9me2 mark we used the mAb 1220 (Abcam) verified for ChIP-analysis by ModENCODE (25) as well as by Wang et al. (6,9) and determined its global distribution in both wild-type and in the *JIL-1* null mutant background. Based on two independent ChIP-Seq experiments for each condition we

identified 833 genes enriched for H3K9me2 in both data sets for wild-type and 488 genes enriched for H3K9me2 in both data sets from the *JIL-1* null background (Supplemental Fig. S1). To further validate our RNA-Seq data we confirmed selected genes with qPCR assays (Supplemental Fig. S2).

Genome-wide DNA-enrichment profiles for JIL-1, H3S10ph, and H3K9me2

In order to determine the relative distribution of JIL-1 and the H3S10ph and H3K9me2 marks in salivary gland cells we generated high-resolution genome-wide DNA-enrichment profiles as exemplified in Fig. 1A and Supplemental Fig. S3. In addition, we compared these profiles to that of Chromator obtained by ChIP on chip analysis by ModENCODE in Kc cells (25). A caveat to this analysis is that the data are from different cells and tissues. Chromator is a chromodomain containing protein (34,39) that is a known binding partner of JIL-1 that co-localizes with JIL-1 at interband regions in immunolabeled polytene salivary gland squash preparations (40). To further characterize the enrichment in and around genes we plotted the distribution of the middle position of the enriched islands (clusters of enriched windows) determined by SICER (23) relative to transcription start sites (TSS) of genes (Fig. 1B). As illustrated in Fig. 1B genome-wide distance correlation revealed that the majority of the identified JIL-1 enriched islands were centered in close proximity to the TSS within ±500 bp and that the peak was aligned near 0 bp. Interestingly, the distribution of Chromator enriched islands with respect to the TSS was nearly identical to that of JIL-1 (Fig. 1B). Furthermore, analysis of discrete binding peaks of JIL-1 determined by the MACS peak-finding algorithm (24) revealed that they were highly correlated with Chromator binding peaks and located preferentially to the 5'-end of genes (Fig. 1C). These data suggest that JIL-1 and Chromator share the same specific binding sites although it has been demonstrated that neither depends on the other for its binding (40). Although the

majority of JIL-1 binding peaks map in the proximity of the TSS we also found the presence of many binding regions at the level of exons, introns, and the 3'-end of genes (Fig. 1A).

Although H3S10ph enrichment was highly correlated with that of JIL-1 (Fig. 1A and Supplemental Fig. S1), the profile of H3S10ph was markedly different from that of JIL-1 around the TSS (Fig. 1B). H3S10ph's distribution was much broader and the peak enrichment was shifted to about 600 bp downstream of the TSS. This suggests that JIL-1 may not phosphorylate histone H3 at the nucleosome to which it is bound. To explore this possibility we modeled the 3D-structure of JIL-1 using the I-TASSER structure prediction program (37) and compared it to the nucleosome crystal structure (41). As illustrated in Supplemental Fig. S4 considering that JIL-1 is known to bind the tail of H3 by the end of its carboxy-terminal domain (42) and that its folded structure is larger than a nucleosome, it is likely to have the capacity to phosphorylate histone H3 of one or more nucleosomes some distance away from its actual binding site depending on the state of higher order nucleosome packaging. Thus, as indicated by the present data the distribution of JIL-1 and H3S10 phosphorylation may not necessarily be coincident. Interestingly, the distribution of H3K9me2 binding around the TSS closely mirrored that of H3S10ph (Fig. 1B) indicating that these two epigenetic modifications may occur in similar genomic contexts.

H3S10 phosphorylation is enriched at active genes and correlated with enhanced gene expression

JIL-1 mediated H3S10 phosphorylation has been proposed to maintain an active state of chromatin (43). Consistent with this hypothesis we found that enrichment of JIL-1 and the H3S10ph mark predominantly were associated with active genes (79% and 67%, respectively) (Fig. 2A). In contrast, enrichment of the H3K9me2 mark had a more pronounced association with inactive genes (47%) (Fig. 2A). However, it should be noted

that JIL-1 and the H3S10ph mark were also enriched at many inactive genes (21% and 33%, respectively) whereas the enrichment of the H3K9me2 mark in many cases was associated with active genes (53%) (Fig. 2A). Thus, to further explore the correlation of gene expression's dependence on the presence of the H3S10ph and H3K9me2 marks we determined the average gene expression of genes enriched for the H3S10ph or H3K9me2 mark only and genes enriched for both marks. As illustrated in Fig. 2B the median gene expression for these groups of genes were significantly different from each other with the highest expression of genes enriched for the H3S10ph mark only and lowest expression of genes enriched with the H3K9me2 mark only, whereas gene expression for genes enriched for both marks were intermediate. We further compared the relative proportions of high expression, moderate expression, low expression, and inactive genes associated with enriched levels of the H3S10ph or H3K9me2 mark only and genes enriched for both marks (Fig. 2C). The results show that the proportion of both high, moderate, and low expression genes were greater when associated with enriched levels of the H3S10ph mark only and conversely that the proportion of inactive genes increased with enriched levels of the H3K9me2 mark only. The relative proportion of high, moderate, and low expressing genes was intermediate between genes with enrichment for both marks compared to the distribution of these classes of genes with single marks (Fig. 2C). Thus, taken together these results suggest that at a genome-wide level the enrichment for the H3S10ph mark is directly correlated with enhanced gene expression.

Loss of JIL-1 and H3S10 phosphorylation lead to both gene up- and downregulation

In order to determine the changes in gene transcription in the absence of H3S10 phosphorylation we compared global transcription profiles in salivary glands in two biological replicates from wild-type and *JIL-1*^{z2}*/JIL-1*^{z2} homozygous null larvae, respectively.

The replicate determinations were highly correlated with Pearson's coefficients (R^2) of 0.977 for the two wild-type samples and 0.998 for the two samples from *JIL-1* null larvae. The results showed that out of nearly 15,000 genes analyzed, the expression levels of 1539 genes changed at least two-fold and with an FDR smaller than 0.05. Interestingly, 51% of these genes were downregulated whereas 49% showed increased expression levels in the *JIL-1* null mutant background. This is illustrated in the scatterplot in Fig. 3A where each dot represents the changes in the expression level of each individual gene and in the box-plot in Fig. 3B. We further plotted the changes in gene expression levels of genes that were classified as active or inactive in wild-type salivary glands. As shown in the box-plot in Fig. 3C there was a significant difference in the expression changes between the two groups of genes. Most inactive genes had increased expression in the mutant background whereas active genes on average had a modest decrease. However, when active genes were further divided into groups with low, moderate, and high expression there was a clear trend that the higher the wild-type expression levels of a gene the more its expression levels were decreased in the mutant background (Fig. 3D). These data suggest in general that active genes become repressed but that many hitherto inactive genes become activated in the absence of H3S10 phosphorylation.

We next analyzed the up- and downregulated genes in terms of their GO categories (Fig. 3E). Strikingly, the results indicate that the downregulated set of genes in the mutant is enriched in categories related to salivary gland function and development whereas the upregulated list is enriched in DNA repair, cellular response to stress, and RNA processing and metabolism categories. That genes in salivary gland and tissue development specific pathways were particularly affected by downregulation in the mutant suggests that H3S10 phosphorylation may play a key role in keeping tissue and developmentally stage specific genes transcriptionally active.

H3K9me2 redistribution in the absence of H3S10 phosphorylation correlates with activation of silent genes and repression of active genes

One of the consequences of the absence of H3S10 phosphorylation is a redistribution of the H3K9me2 mark from pericentric heterochromatin to the euchromatic regions of the chromosome arms (3-7). This is illustrated by the H3K9me2 immunolabeling of polytene squash preparations from wild-type and *JIL-1* null mutant salivary glands in Fig. 4A with the redistribution especially prominent on the X-chromosome of both males and females (3). Thus, to further investigate this redistribution on a genome-wide level we generated maps of H3K9me2 binding by plotting normalized read numbers in 200 bp bins across the genome from wild-type and *JIL-1* null salivary glands. Fig. 4B shows an example of such maps comparing wild-type and *JIL-1* mutant X-chromosomes. The results show that in the *JIL-1* null mutant background the levels of H3K9me2 on the chromosome arms were markedly increased and that enriched levels occurred at sites previously not occupied by significant levels of the H3K9me2 mark. Interestingly, although the H3K9me2 mark was enriched on the X-chromosome compared to the autosomes, overall gene expression levels were not statistically different (Fig. 4C).

The study of Wang et al. (9) of gene expression of the *white* locus provided evidence that H3K9me2 levels at the *white* gene directly correlated with its level of expression and that the H3K9me2 levels in turn were regulated by H3S10 phosphorylation. Based on these findings we reasoned that in the absence of H3S10 phosphorylation gene repression should correlate with increased H3K9me2 binding to the gene, whereas gene activation should be correlated with a loss or decreased H3K9me2 binding. To explore this hypothesis we plotted the expression of all moderate and high expression genes in our data set without enriched levels of H3K9me2 that acquired the H3K9me2 mark in the *JIL-1*

mutant. As illustrated by the box plots in Fig. 5A, for 94 such genes there was a significant decrease in their average levels of expression. To further validate these findings we performed ChIP-assays as in Wang et al. (6,9) for five randomly selected genes among the genes analyzed above. Chromatin was immunoprecipitated (ip) from wild-type or *JIL-1* null mutant larval salivary glands using rabbit anti-H3S10ph antibody or purified rabbit IgG antibody (negative control) or mAbs to H3K9me2 or GST (negative control). Primers specific for each of the selected genes were used to amplify the precipitated material. Experiments were done in triplicate and relative enrichment of DNA from the H3S10ph and H3K9me2 ips were normalized to the corresponding control antibody ips performed in tandem for each experimental sample. As illustrated in Fig. 5B, at all five genes the relative enrichment of H3S10ph in the mutant was reduced to background levels whereas there was a significant increase of from 2 to 7 fold of the enrichment of the H3K9me2 mark. We next plotted the expression of all inactive and low expression genes in our data set that lost the H3K9me2 mark in the *JIL-1* mutant. The box plots in Fig. 6A show that for 69 such genes there was a significant increase in their average levels of expression. As above we validated these findings by performing ChIP-assays for five randomly selected genes among the genes analyzed. The results show that at all five genes there was a significant decrease of from 2 to 6 fold of the enrichment of the H3K9me2 mark (Fig. 6B). Furthermore, the results confirm that in this class of inactive genes there were very low wild-type levels of H3S10ph. Taken together these findings suggest that H3S10 phosphorylation modulates H3K9 dimethylation and that H3K9me2 redistribution in the absence of H3S10 phosphorylation correlates with activation of silent genes that lose the H3K9me2 mark and repression of active genes that acquire the H3K9me2 mark.

Discussion

In this study we have determined the relationship of JIL-1 kinase mediated H3S10 phosphorylation with gene expression and the distribution of the epigenetic H3K9me2 mark. We show in wild-type salivary gland cells that the H3S10ph mark is predominantly enriched at active genes whereas the H3K9me2 mark largely is associated with inactive genes. Furthermore, our data demonstrate that discrete binding peaks of JIL-1 are located preferentially to the 5'-end of genes near the TSS and that these peaks are coincident with binding peaks for the chromodomain protein, Chromator, a known binding partner for JIL-1 (40). This distribution of JIL-1 around the TSS is similar to that obtained by ChIP-Seq by Kellner et al. (13) in Kc cells but differs from that reported by Regnard et al. (10) using ChIP-chip analysis on custom tiling arrays in S2 cells. These latter workers found JIL-1 to be more or less equally distributed along the entire length of genes; however, this result may be a consequence of using lower affinity polyclonal antibodies combined with the lower resolution ChIP-chip approach. Interestingly, we found that although the enrichment profile of H3S10ph was highly correlated with that of JIL-1, the two profiles were not identical. The distribution of the H3S10ph mark was much broader and peak enriched regions were shifted about 600 bp downstream of the TSS. Modeling of the 3D-structure of JIL-1 relative to nucleosome structure suggested that a reason for this lack of overlap is that JIL-1 may have the capacity to phosphorylate the tail of H3 of one or more nucleosomes some distance away from its actual binding site depending on the state of higher order nucleosome packaging.

Comparison of global transcription profiles in salivary glands from wild-type and *JIL-1* null mutant larvae revealed that of the nearly 15,000 genes analyzed the expression levels

of 1539 genes changed at least two-fold in the mutant. Surprisingly, among these genes almost as many (49%) increased their expression as were downregulated (51%). This raised the question whether certain classes of genes were preferentially up- or downregulated and further analysis suggested that in general active genes became repressed, whereas hitherto inactive genes became activated in the absence of H3S10 phosphorylation. Furthermore, the results showed that downregulation of genes in the mutant was correlated with higher levels or acquisition of the H3K9me2 mark whereas upregulation of a gene was correlated with loss of or diminished H3K9 dimethylation. These findings directly demonstrate that H3S10 phosphorylation is not required for transcription or gene activation in *Drosophila* as proposed by Corces and colleagues (11-13). This conclusion is further supported by recent experiments by Wang et al. (9) analyzing *white* gene expression where levels of the H3S10ph mark can be manipulated and correlated with the resulting levels of the H3K9me2 mark using ChIP-assays. In wild-type there are moderate levels of the H3S10ph mark and low levels of the epigenetic H3K9me2 mark at the *white* gene resulting in its normal expression. However, in the w^{m4} allele heterochromatic factors can spread across the inversion breakpoint (5,6,43,44) leading to high levels of H3K9me2 at the *white* gene and silencing of gene expression. Interestingly, Wang et al. (9) demonstrated that this increase in H3K9me2 level can be prevented by ectopic H3S10 phosphorylation at the *white* gene restoring gene expression. In contrast, in the absence of H3S10 phosphorylation as it occurs in strong *JIL-1* hypomorphic mutant backgrounds there is a redistribution of heterochromatic factors to ectopic chromosome sites resulting in reduced levels of these factors at the pericentric heterochromatin (3). This leads to less heterochromatic spreading and lower levels of H3K9me2 at the *white* gene in the w^{m4} inversion, thus allowing for increased *white* gene expression (9). Thus, taken together these results are compatible with a model (Fig. 7) where gene expression levels

are directly correlated with the levels of the H3K9me2 mark independent of the state of the H3S10ph mark, which is not required for either transcription or gene activation to occur. However, H3S10 phosphorylation functions to indirectly regulate transcription by counteracting H3K9 dimethylation and gene silencing in a finely tuned balance (3,5,6,8).

That genes in GO categories for salivary gland specific pathways were particularly affected by downregulation in a *JIL-1* mutant background suggest that H3S10 phosphorylation may serve to keep genes transcriptionally active in a tissue and/or developmentally stage specific context. How JIL-1 and H3S10 phosphorylation get targeted to specific sets of genes is not known. However, it has been suggested as a general model that JIL-1 targeting to active chromatin may be facilitated by or dependent on the presence of the H3K36me2 and H4K16ac marks (10). Interestingly, the GO categories for genes becoming activated or upregulated in the absence of H3S10 phosphorylation were enriched in DNA repair, DNA and RNA metabolism, and cellular response to stress pathways. Upregulation of such genes would be consistent with a cellular attempt to compensate for the general downregulation of active genes and to the gross perturbation of chromatin structure occurring in *JIL-1* null mutant backgrounds (2,45). If this represents a specific response to alterations in the mutant it implies activation of unknown gene induction pathways independent of H3S10 phosphorylation. However, an alternative scenario is that when the H3S10ph mark, which normally serves to limit heterochromatic spreading, is lost in the *JIL-1* mutant, the H3K9me2 silencing mark can now disperse away from previously repressed locations, resulting in transcriptional activation of the now unmasked genes.

In summary, the findings of this study indicate that a major functional role of JIL-1 mediated H3S10 phosphorylation is to maintain active gene expression by serving as a protective epigenetic mark counteracting H3K9 dimethylation and gene silencing. This

suggests that different gene expression profiles are regulated by strategic deployment of silencing marks within the genome, and that H3S10 phosphorylation can be an effective means of counteracting silencing effects. This may also be relevant in other organisms where H3S10ph is implicated in the rapid yet transient induction of promoters in response to various inducers (46,47).

Acknowledgements

We thank Dr. D. Nettleton and members of the laboratory for discussion and advice. We also wish to acknowledge Mr. Atrez Norwood and Mr. Cheng-Ting Yeh for technical assistance.

References

1. Jin, Y., Wang, Y., Walker, D.L., Dong, H., Conley, C., Johansen, J. and Johansen, K.M. (1999) JIL-1: a novel chromosomal kinase implicated in transcriptional regulation in *Drosophila*. *Mol. Cell* **4,** 129-135.
2. Wang, Y., Zhang, W., Jin, Y., Johansen, J. and Johansen, K.M. (2001) The JIL-1 tandem kinase mediates histone H3 phosphorylation and is required for maintenance of chromatin structure in *Drosophila*. *Cell* **105,** 433-443.
3. Zhang, W., Deng, H., Bao, X., Lerach, S., Girton, J., Johansen, J. and Johansen, K.M. (2006) The JIL-1 histone H3S10 kinase regulates dimethyl H3K9 modifications and heterochromatic spreading in *Drosophila*. *Development* **133,** 229-235.
4. Deng, H., Bao, X., Zhang, W., Girton, J., Johansen, J. and Johansen, K.M. (2007) Reduced levels of Su(var)3-9 but not Su(var)2-5 (HP1) counteract the effects on chromatin structure and viability in loss-of-function mutants of the JIL-1 histone H3S10 kinase. *Genetics* **177,** 79-87.
5. Deng, H., Cai, W., Wang, C., Lerach, S., Delattre, M., Girton, J., Johansen, J. and Johansen, K.M. (2010) *JIL-1* and *Su(var)3-7* interact genetically and counterbalance each others' effect on position effect variegation in Drosophila. *Genetics* **185,** 1183-1192.

6. Wang, C., Cai, W., Li, Y., Deng, H., Bao, X., Girton, J., Johansen, J. and Johansen, K.M. (2011) The epigenetic H3S10 phosphorylation mark is required for counteracting heterochromatic spreading and gene silencing in *Drosophila melanogaster*. *J. Cell Sci.* **124,** 4309-4317.

7. Wang, C., Girton, J., Johansen, J., Johansen and K.M. (2011) A balance between euchromatic (JIL-1) and heterochromatic (SU(VAR)2-5 and SU(VAR)3-9) factors regulates position-effect variegation in Drosophila. *Genetics* **188,** 745-748.

8. Ebert, A., Schotta, G., Lein, S., Kubicek, S., Krauss, V., Jenuwein, T. and Reuter, G. (2004) *Su(var)* genes regulate the balance between euchromatin and heterochromatin in *Drosophila*. *Genes Dev.* **18,** 2973-2983.

9. Wang, C., Cai, W., L,i Y., Girton, J., Johansen, J. and Johansen, K.M. (2012) H3S10 phosphorylation by the JIL-1 kinase regulates H3K9 dimethylation and gene expression at the *white* locus in *Drosophila.* *Fly* **6,** 1-5.

10. Regnard, C., Straub, T., Mitterweger, A., Dahlsveen, I.K., Fabian, V. and Becker, P.B. (2011) Global analysis of the relationship between JIL-1 kinase and transcription. *PLoS Genetics* **7,** e1001327.

11. Ivaldi, M.S., Karam, C.S. and Corces, V.G. (2007) Phosphorylation of histone H3 at Ser10 facilitates RNA polymerase II release from promoter-proximal pausing in *Drosophila*. *Genes Dev.* **21,** 2818-2831.

12. Karam, C.S., Kellner, W.A., Takenada, N., Clemmons, A.W. and Corces, V.G. (2010) 14-3-3 mediates histone cross-talk during transcription elongation in *Drosophila. PLoS Genetics* **6,** e1000975.

13. Kellner, W.A., Ramos, E., Bortle, K.V., Takenada, N. and Corces, V.G. (2012) Genome-wide phosphoacetylation of histone H3 at *Drosophila* enhancers and promoters. *Genome Res.* **22,** 1081-1088.

14. Wang, C., Yao, C., Li, Y., Cai, W., Girton, J., Johansen, J. and Johansen, K.M. (2012) Evidence against a role for the JIL-1 kinase in H3S28 phosphorylation and 14-3-3 recruitment to active genes in *Drosophila. PLoS ONE* **8,** e62484.

15. Cai, W., Bao, X., Deng, H., Jin, Y., Girton, J., Johansen, J. and Johansen, K.M. (2008) RNA polymerase II-mediated transcription at active loci does not require histone H3S10 phosphorylation in *Drosophila*. *Development* **135,** 2917-2925.

16. Roberts, D.B. (1998) *Drosophila*: A Practical Approach, 2nd ed, IRL Press, Oxford, UK.

17. Zhang, W., Jin, Y., Ji, Y., Girton, J., Johansen, J. and Johansen, K.M. (2003) Genetic and phenotypic analysis of alleles of the Drosophila chromosomal JIL-1 kinase reveals a functional requirement at multiple developmental stages. *Genetics* **165,** 1341-1354.

18. Legube, G., McWeeney, S.K., Lercher, M.J. and Akhtar, A. (2006) X-chromosome-wide profiling of MSL-1 distribution and dosage compensation in *Drosophila*. *Genes Dev.* **20,** 871-883.

19. Jin, Y., Wang, Y., Johansen, J. and Johansen, K.M. (2000) JIL-1, a chromosomal kinase implicated in regulation of chromatin structure, associates with the MSL dosage compensation complex. *J. Cell Biol.* **149,** 1005-1010.

20. Langmead, B., Trapnell, C., Pop, M. and Salzberg, S.L. (2009) Ultrafast and memory-efficient alignment of short DNA sequences to the human genome. *Genome Biol.* **10,** R25.

21. Li, H., Handsaker, B., Wysoker, A., Fennell, T., Ruan, J., Homer, N., Marth, G., Abecasis, G. and Durbin, R. (2009) The Sequence Alignment/Map format and SAMtools. *Bioinformatics* **25,** 2078-2079.

22. Quinlan, A.R. and Hall, I.M. (2010) BEDTools: a flexible suite of utilities for comparing genomic features. *Bioinformatics* **1,** 841-842.

23. Zang, C., Schones, D.E., Zeng, C., Cui, K., Zhao, K. and Peng, W. (2009) A clustering approach for identification of enriched domains from histone modification ChIP-Seq data. *Bioinformatics* **25,** 1952-1958.

24. Zhang, Y., Liu, T., Meyer, C.A., Eeckhoute, J., Johnson, D.S., Bernstein, B.E., Nusbaum, C., Myers, R.M., Brown, M., Li, W. and Liu, X.S. (2008) Model-based analysis of ChIP-Seq(MACS). *Genome Biol.* **9,** R137.

25. Celniker, S.E., Dillon, L.A., Gerstein, M.B., Gunsalus, K.C., Henikoff, S., Karpen, G.H., Kellis, M., Lai, E.C., Lieb, J.D., MacAlpine, D.M., Micklem, G., Piano, F., Snyder, M., Stein, L., White, K.P., Waterston, R.H. and ModENCODE Consortium. (2009) Unlocking the secrets of the genome. *Nature* **459,** 927-930.

26. Zhu, L.J., Gazin, C., Lawson, N.D., Pagès, H., Lin, S.M., Lapointe, D.S. and Green, M.R. (2010) ChIPpeakAnno: a Bioconductor package to annotate ChIP-seq and ChIP-chip data. *BMC Bioinformatics* **11,** 237.

27. Liu, S., Yeh, C.T., Tang, H.M., Nettleton, D. and Schnable, P.S. (2012) Gene mapping via bulked segregant RNA-Seq (BSR-Seq). *PLoS ONE* **7,** e36406.

28. Wu, T. and Nacu, S. (2010) Fast and SNP-tolerant detection of complex variants and splicing in short reads. *Bioinformatics* **26,** 873-881.

29. Mortazavi, A., Williams, B.A., McCue, K., Schaeffer, L. and Wold, B. (2008) Mapping and quantifying mammalian transcriptomes by RNA-Seq. *Nat. Methods* **5,** 621-628.

30. Bullard, J.H., Purdom, E., Hansen, K.D. and Dudoit, S. (2010) Evaluation of statistical methods for normalization and differential expression in mRNA-Seq experiments. *BMC Bioinformatics* **11,** 94.

31. Lund, S.P., Nettleton, D., McCarthy, D.J. and Smyth, G.K. (2012) *Stat. Appl. Genet, Mol. Biol.* **11,** 1826.

32. Huang da, W., Sherman, B.T. and Lempicki, R.A. (2009) Systematic and integrative analysis of large gene lists using DAVID bioinformatics resources. *Nature Protocols* **4,** 44–57.

33. Wickham, H. (2009) *ggplot2: Elegant Graphics for Data Analysis.* Springer Press, Heidelberg, Germany.

34. Rath, U., Wang, D., Ding, Y., Xu, Y.-Z., Qi, H., Blacketer, M.J., Girton, J., Johansen, J. and Johansen, K.M. (2004) Chromator, a novel and essential chromodomain protein interacts directly with the putative spindle matrix protein Skeletor. *J. Cell. Biochem.* **93,** 1033-1047.

35. Cai, W., Jin, Y., Girton, J., Johansen, J. and Johansen, K.M. (2010) Preparation of polytene chromosome squashes for antibody labeling. *J Vis Exp* http://www.jove.com/index/Details.stp?ID=1748.

36. Zhang, Y. (2007) Template-based modeling and free modeling by I-TASSER in CASP7. *Proteins* **68,** 108-117

37. Roy, A., Kucukural, A. and Zhang, Y. (2010) I-TASSER: a unified platform for automated protein structure and function prediction. *Nature Protocols* **5,** 725-738

38. Zhang, Y. (2008) Progress and challenges in protein structure prediction. *Curr. Opin. Struct. Biol.* **18,** 342–348.

39. Yao, C., Ding, Y., Cai, W., Wang, C., Girton, J., Johansen, K.M. and Johansen, J. (2012) The chromodomain-containing NH_2-terminus of Chromator interacts with histone H1 and is required for correct targeting to chromatin. *Chromosoma* **121,** 209-220.

40. Rath, U., Ding, Y., Deng, H., Qi, H., Bao, X., Zhang, W., Girton, J., Johansen, J. and Johansen, K.M. (2006) The chromodomain protein, Chromator, interacts with JIL-1

kinase and regulates the structure of *Drosophila* polytene chromosomes. *J. Cell Sci.* **11,** 2332-2341.

41. Luger, K., Mader, A.W., Richmond, R.K., Sargent, D.F. and Richmond, T.J. (1997) Crystal structure of the nucleosome core particle at 2.8 Å resolution. *Nature* **389,** 251-260.
42. Bao, X., Cai, W., Deng, H., Zhang, W., Krencik, R., Girton, J., Johansen, J. and Johansen, K.M. (2008) The COOH-terminal domain of the JIL-1 histone H3S10 kinase interacts with histone H3 and is required for correct targeting to chromatin. *J. Biol. Chem.* **283,** 32741-32750.
43. Johansen, K.M. and Johansen, J. (2006) Regulation of chromatin structure by histone H3S10 phosphorylation. *Chromosome Res.* **14,** 393-404.
44. Lerach, S., Zhang, W., Bao, X., Deng, H., Girton, J., Johansen, J. and Johansen, K.M. (2006) Loss-of-function alleles of the JIL-1 kinase are strong suppressors of position effect variegation of the w^{m4} allele in *Drosophila*. *Genetics* **173,** 2403-2406.
45. Deng, H., Zhang, W., Bao, X., Martin, J.N., Girton, J., Johansen, J., Johansen, K.M. (2005) The JIL-1 kinase regulates the structure of *Drosophila* polytene chromosomes. *Chromosoma* **114,** 173-182.
46. Winter, S., Simboeck, E., Fischle, W., Zupkovitz, G., Dohnal, I. and Berger, S.L. (2008) 14-3-3 proteins recognize a histone code at histone H3 and are required for transcriptional activation. *EMBO J.* **27,** 88-99.
47. Zippo, A., Serafini, R., Rocchigiani, M., Pennacchini, A., Krepelova, A. and Oliviero, S. (2009) Histone crosstalk between H3S10ph and H4K16ac generates a histone code that mediates transcription elongation. *Cell* **138,** 1122-1136.

Figures

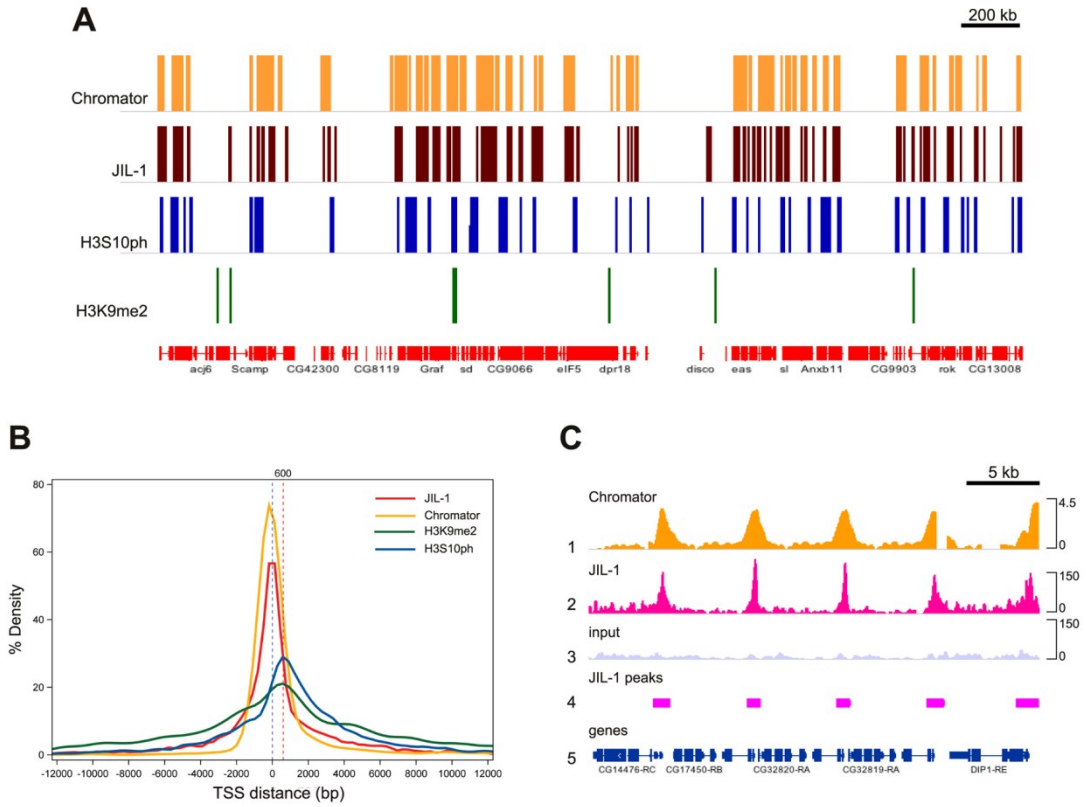

Figure 1. High resolution profiling of JIL-1, H3S10ph, and H3K9me2 enriched genomic regions in *Drosophila* salivary gland cells. (A) Comparison of enriched genomic islands for Chromator (data from ModENCODE), JIL-1 (data from JIL-1(2)), H3S10ph (data from H3S10ph(CS)), and H3K9me2 on a section of the X chromosome. The location of genes (in red) is indicated below. The enhanced genomic islands were identified using the SICER algorithm (23) with a 200 bp window and a 200 bp gap size. (B) Density of Chromator, JIL-1, H3S10ph, and H3K9me2 enriched islands as determined in (A) plotted relative to the distance from the TSS of nearby genes. Chromator and JIL-1 on average tend to localize to enriched islands with a peak centered near the TSS. H3S10ph and H3K9me2 on average tend to localize with a peak about 600 bp after the TSS. (C) JIL-1 enriched binding peaks strongly correlate with those of Chromator and are preferentially

located at the 5'-end of genes. Lane 1, ChIP on chip profile of Chromator (data from ModENCODE). The data is represented as average log2 signal ratio of IP over input. Lane 2, ChIP-Seq profile of JIL-1 (data from JIL-1(2)). The height of the peaks represents the number of reads obtained in each region scaled to the total number of reads. Lane 3, ChIP-Seq input profile. The height of the peaks represents the number of reads obtained in each region scaled to the total number of reads. Lane 4, Peak JIL-1 enriched binding regions determined by the MACS peak finding algorithm (24). Lane 5, The location of genes in the depicted section of the X chromosome.

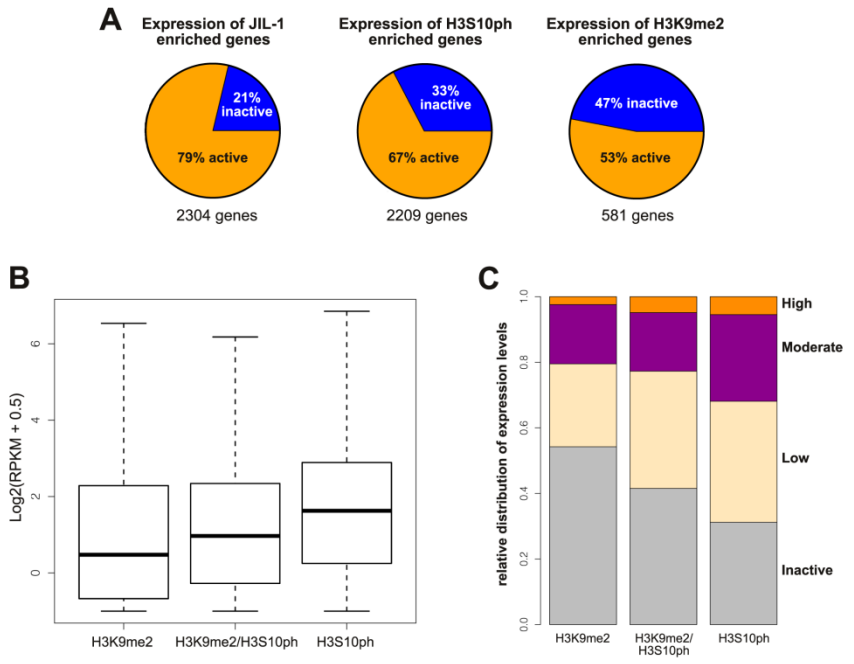

Figure 2. Expression levels of genes enriched for JIL-1, H3S10ph, and/or H3K9me2. (A) Pie charts of the relative proportion of inactive and active (RPKM≥1) genes enriched for JIL-1, H3S10ph, or H3K9me2, respectively. (B) Comparison of the expression of genes enriched for the H3K9me2 or H3S10ph mark only and genes enriched for both marks. Gene expression is represented as log2(RPKM + 0.5). The boxplot representation in this

and subsequent figures defines 25th to 75th percentiles (boxes), 50th percentile (lines in boxes), and ranges (whiskers, 1.5 times the interquartile range extended from both ends of the box or the maximal/minimal value). Outliers were removed from the analysis. The distribution of gene expression for all three categories was significantly different from each other (p-values<0.005; Pairwise Wilcoxon Rank Sum Tests). (C) Stack bar charts showing the distribution of expression of genes enriched for the H3K9me2 or H3S10ph mark only and genes enriched for both marks. Genes with an RPKM of less than one were categorized as inactive whereas active genes were separated into three groups with low, moderate, or high expression levels reflected by RPKMs of from 1-5, >5-30, or >30.

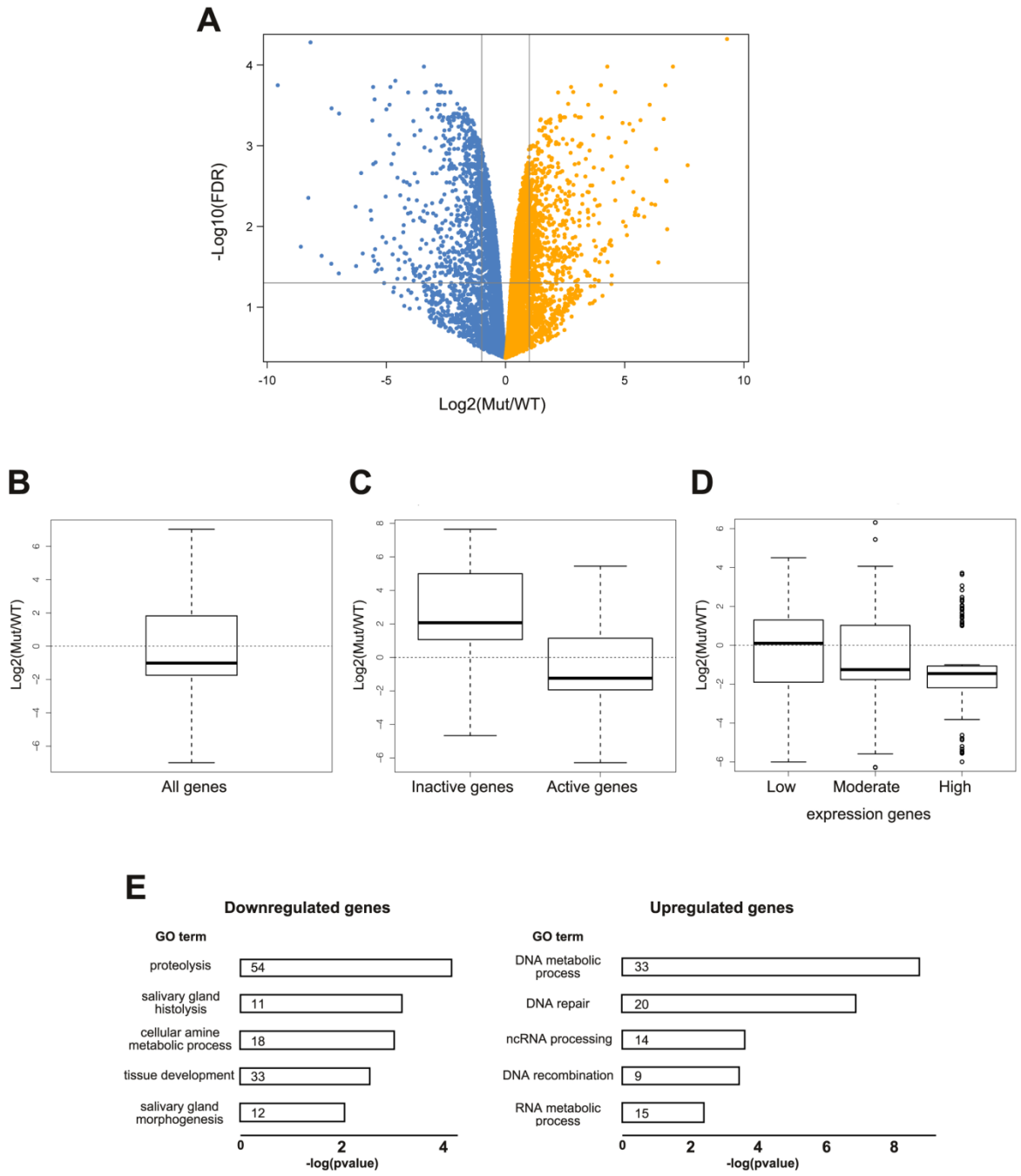

Figure 3. Gene expression can be either down- or upregulated in the absence of H3S10 phosphorylation. (A) Scatter plot of gene expression changes between wild-type and *JIL-1* null mutant salivary gland cells. Negative $\log_{10}$(p-values) from Fisher's exact test were plotted against the $\log_2$(mutant/wild-type) fold change for each gene. Each dot

represents a separate gene. Gray lines indicate the cut-offs for 2-fold changes with a FDR equal to 0.05. Downregulated genes in the *JIL-1* mutant are highlighted in light blue and upregulated genes in orange. (B) Box plot of gene expression changes between wild-type and *JIL-1* null mutant salivary gland cells of all genes changed at least 2-fold represented as log2(mutant/wild-type) fold change for each gene. The overall changes in gene expression between the mutant and wild-type were not statistically significant (p-value=0.3, Wilcoxon Signed Rank Test). (C) Box plot of gene expression changes between wild-type and *JIL-1* null mutant salivary gland cells of inactive versus active (RPKM≥1) genes that changed at least 2-fold represented as log2(mutant/wild-type) fold change for each gene. The distribution of gene expression for the two categories was significantly different from each other (p-value<0.0001; Wilcoxon Rank Sum Test). (D) Box plot of gene expression changes between wild-type and *JIL-1* null mutant salivary gland cells of active genes separated into three groups with low, moderate, or high expression levels (RPKMs of from 1-5, >5-30, or >30, respectively) that changed at least 2-fold represented as log2(mutant/wild-type) fold change for each gene. The distribution of gene expression for all three categories was significantly different from each other (low to moderate: p-value<0.01; moderate to high: p-value<0.05; low to high: p-value<0.0001; Pairwise Wilcoxon Rank Sum Tests). (E) Gene Ontology (GO) term of JIL-1 enriched genes identified as down-regulated (left) or up-regulated (right) in *JIL-1* null mutant versus wild-type salivary glands from third instar larvae. The number of genes in each category is shown within the bars. The GO term enrichment was identified by DAVID (32) in Level 5 of biological process, molecular function.

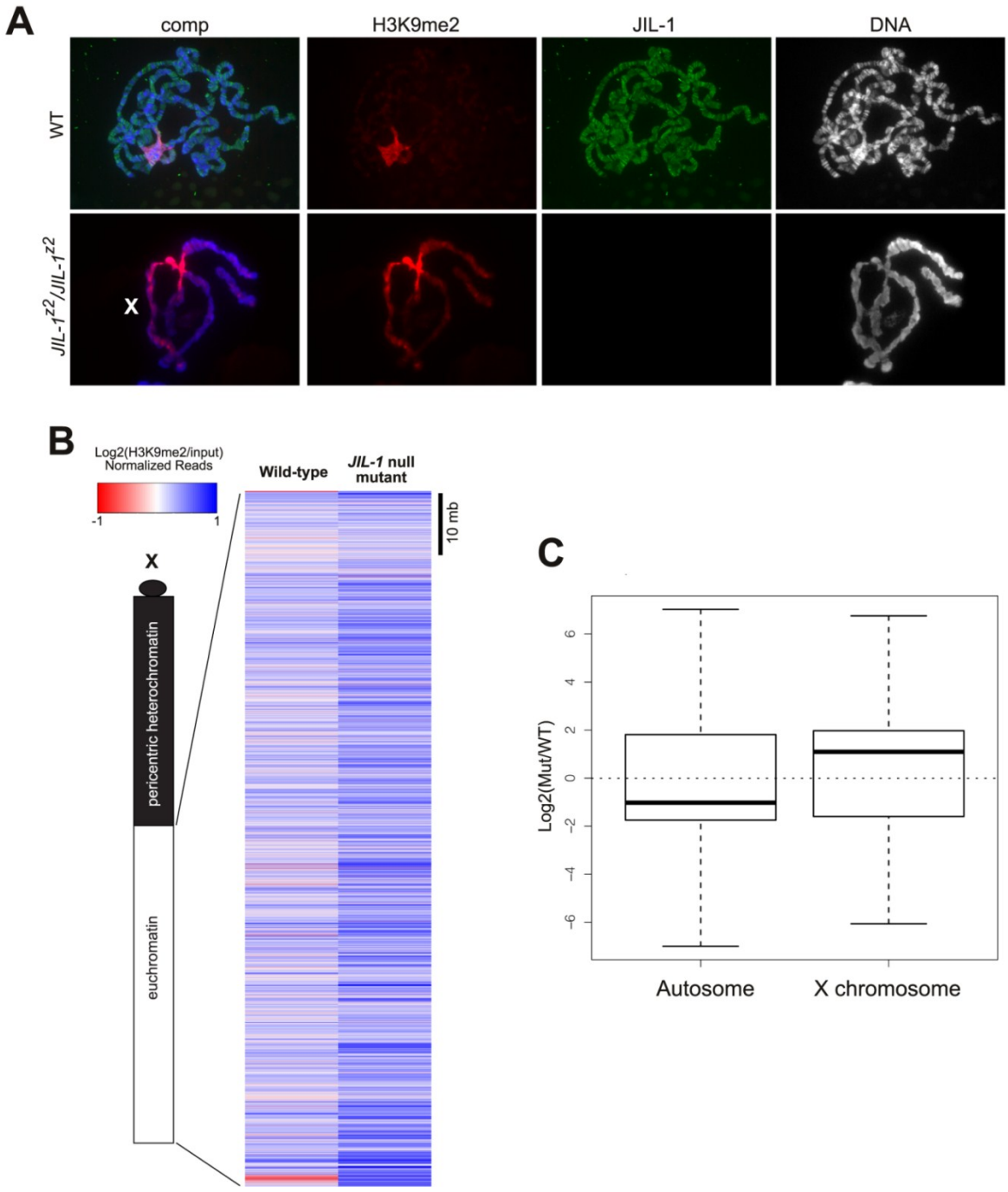

Figure 4. H3K9me2 is redistributed and upregulated on the X-chomosome in *JIL-1* null mutants. **(**A) Wild-type (WT) and *JIL-1* mutant (*JIL-1*^{z2}/*JIL-1*^{z2}) polytene squash preparations labeled with antibody to JIL-1 (in green), H3K9me2 (in red), and with Hoechst (DNA, in blue/gray). The X-chromosome in the *JIL-1* mutant is indicated with an X. (B)

Comparison of H3K9me2 distribution in wild-type and *JIL-1* null mutants. The maps show normalized (linear normalization by total library size) read numbers (log2(H3K9me2/input)) in 200 bp bins across the X-chromosome scaled from -1 (dark red) to +1 (dark blue). (C) Box plot of gene expression changes between wild-type and *JIL-1* null mutant salivary gland cells of autosomal versus X-chromosomal genes that changed at least 2-fold represented as log2(mutant/wild-type) fold change for each gene. The distribution of gene expression for the two categories was similar (p-value=0.4; Wilcoxon Rank Sum Test).

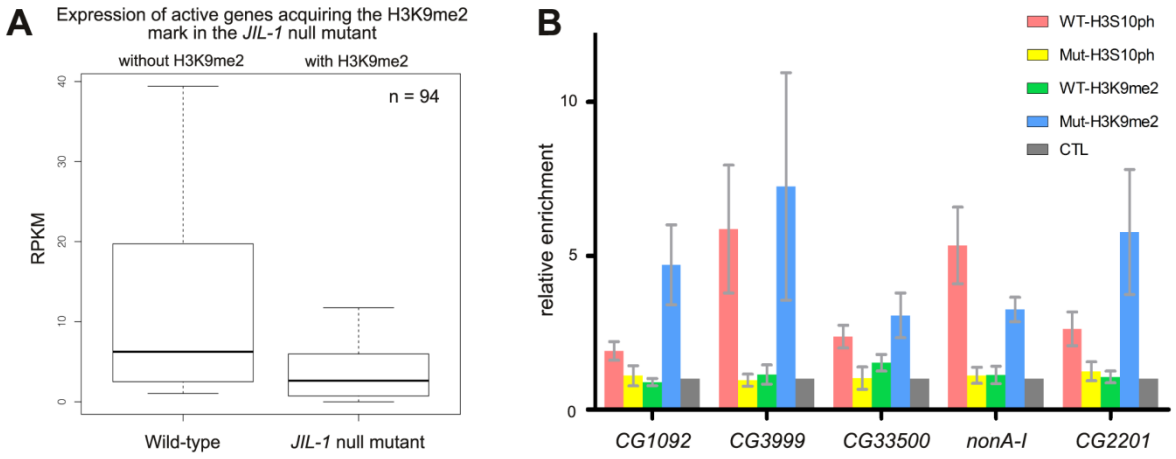

Figure 5. Downregulation of moderate and high expression genes acquiring the H3K9me2 mark in the *JIL-1* null mutant. (A) Box plots of RPKM of active genes (RPKM≥1) in wild-type that acquire the H3K9me2 mark in the *JIL-1* null mutant background. The distribution of gene expression between the two categories was significantly different (p-value<0.0001; Wilcoxon Rank Sum Test). (B) ChIP analysis of randomly selected active genes in wild-type that are downregulated in the *JIL-1* null mutant background. Histograms show the relative enrichment of chromatin immunoprecipitated by anti-H3K9me2 or anti-H3S10ph antibodies from third instar larval salivary glands from wild type (WT) and *JIL-1* null mutant larvae. For each experimental condition the average relative enrichment normalized to the corresponding control immunoprecipitation with anti-GST or anti-IgG

antibody from three independent experiments with SD is shown. The difference in H3K9me2 levels for all five genes between wild-type and *JIL-1* null salivary glands was statistically significant (p-values<0.05; two-tailed Student's t-tests).

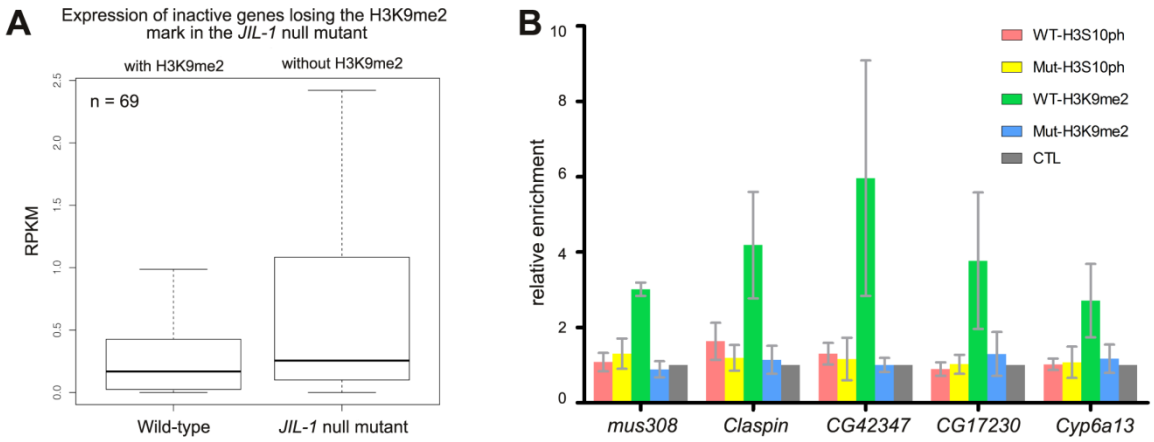

Figure 6. Upregulation of inactive genes losing the H3K9me2 mark in the *JIL-1* null mutant. (A) Box plots of RPKM of inactive genes (RPKM<1) genes in wild-type that lose the H3K9me2 mark in the *JIL-1* null mutant background. The distribution of gene expression between the two categories was significantly different (p-value<0.005; Wilcoxon Rank Sum Test). (B) ChIP analysis of randomly selected inactive genes in wild-type that are upregulated in the *JIL-1* null mutant background. Histograms show the relative enrichment of chromatin immunoprecipitated by anti-H3K9me2 or anti-H3S10ph antibodies from third instar larval salivary glands from wild type (WT) and *JIL-1* null mutant larvae. For each experimental condition the average relative enrichment normalized to the corresponding control immunoprecipitation with anti-GST or anti-IgG antibody from three independent experiments with SD is shown. The difference in H3K9me2 levels for all five genes between wild-type and *JIL-1* null salivary glands was statistically significant (p-values<0.05; two-tailed Student's t-tests).

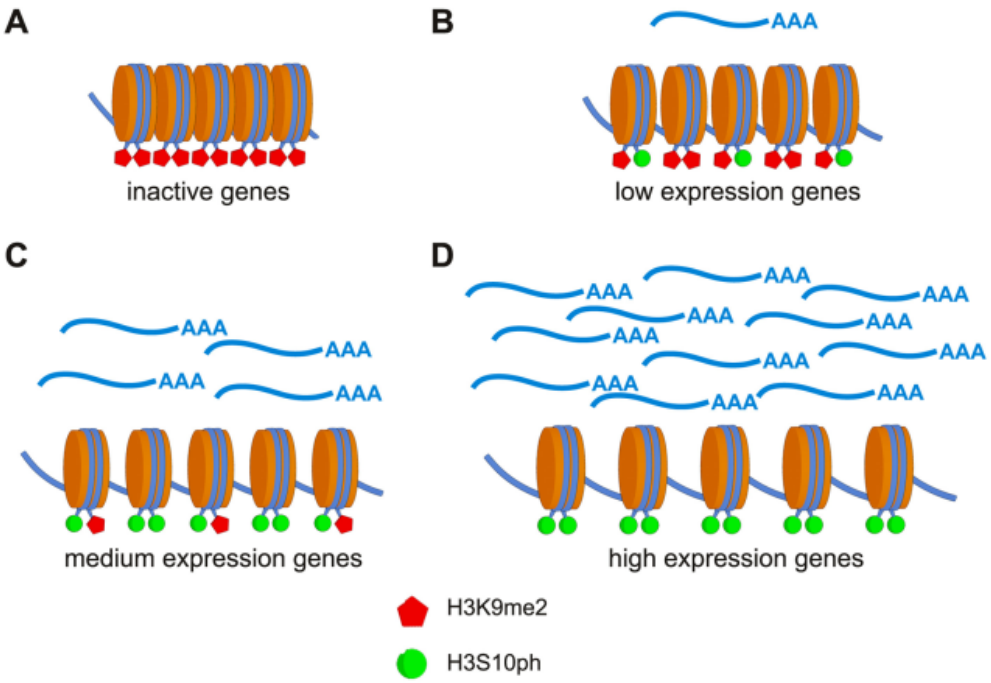

Figure 7. Model for indirect regulation of gene expression by H3S10 phosphorylation. (A) At inactive genes high levels of H3K9 dimethylation lead to a compact chromatin configuration and gene silencing. (B-D) At active genes H3S10 phosphorylation counteracts H3K9 dimethylation leading to a more open chromatin structure facilitating gene expression. In this model gene expression levels are directly correlated with the levels of the H3K9me2 mark independent of the state of the H3S10ph mark, which is not required for either transcription or gene activation to occur.

Supplemental Materials

Supplemental Figures

A

	JIL-1(5c9-1)	JIL-1(5c9-2)	H3S10ph (Active-Motif)	H3S10ph (Cell-Signaling)	H3K9me2 (WT-1)	H3K9me2 (WT-2)	H3K9me2 (*JIL-1Z2*-1)	H3K9me2 (*JIL-1Z2*-2)	Chromator (ModENcode)
JIL-1(5c9-1)	3387								
JIL-1(5c9-2)	2819	5417							
H3S10ph (Active-Motif)	1375	2142	3819						
H3S10ph (Cell-Signaling)	1813	2774	2948	6708					
H3K9me2 (WT-1)	422	709	725	1218	1583				
H3K9me2 (WT-2)	1180	1799	1299	2117	833	3422			
H3K9me2 (*JIL-1Z2*-1)	435	796	624	1047	471	764	1788		
H3K9me2 (*JIL-1Z2*-2)	344	639	432	716	312	694	488	1400	
Chromator (ModENcode)	1746	2229	1056	1335	246	786	359	245	3178

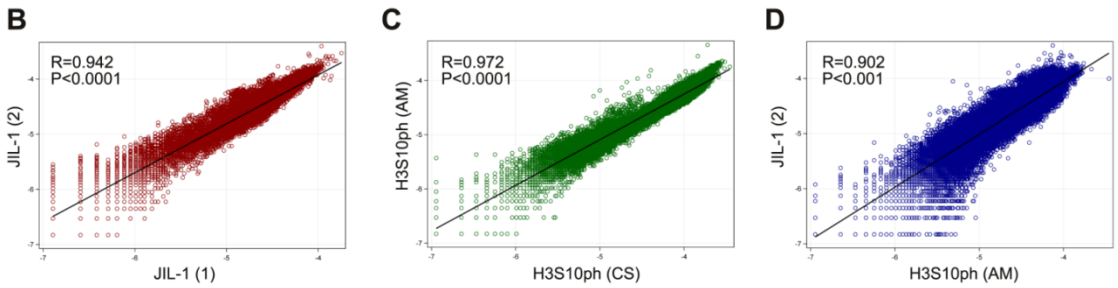

Figure S1. Overview and validation of ChIP-Seq experiments. (A) Table of the number of genes with enriched binding sites for the various modifications determined by ChIP-Seq and the overlap between them. JIL-1(1) and JIL-1(2) represent two independent replications of ChIP-Seq experiments with the JIL-1 mAb 5C9. H3S10ph(AM) and H3S10ph(CS) represent two independent ChIP-Seq experiments with antibodies to H3S10ph from Active Motif and Cell Signaling, respectively. Two sets of independent ChIP-Seq experiments for H3K9me2 were performed with DNA from wild-type (WT-1 and WT-2) and *JIL-1* null (*JIL-1Z2*-1 and *JIL-1Z2*-2) salivary glands using an anti-H3K9me2 mAb from AbCAM. The Chromator data was obtained by ChIP on chip analysis by ModENCODE in Kc cells (25). Enriched genomic islands were identified using SICER (23)

and genes with enriched binding or localization sites were annotated using the ChIPpeakAnno R package (26). The number of genes identified by replicated experiments or different antibodies are highlighted in yellow. (B-D) Pair-wise correlation of the JIL-1(1) versus JIL-1(2) (B), H3S10ph(AM) versus H3S10ph(CS) (C), and JIL-1(2) versus H3S10ph(AM) (D) data sets. The number of mapped reads from each data set were determined in 5 kb intervals across the entire genome and each interval was expressed as a proportion of total mapped reads. The data are plotted on a log10 scale and Pearson's coefficient and P-value are indicated on each plot. The data sets were highly correlated validating the results.

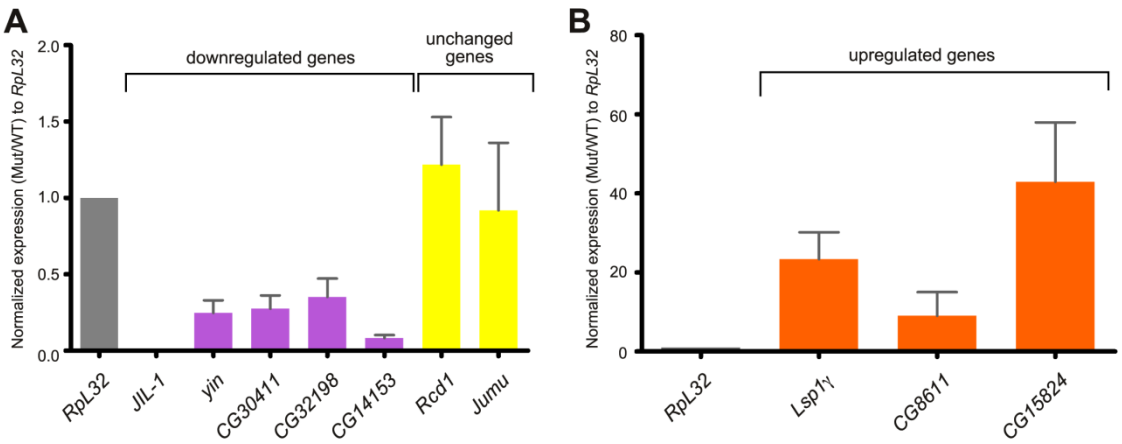

Figure S2. Validation of RNA-Seq experiments. In order to validate the RNA-Seq experiments comparing expression profiles in wild-type and in the *JIL-1* null mutant we performed quantitative PCR (qPCR) experiments on randomly selected genes that were either downregulated, unchanged, or upregulated in the *JIL-1* mutant in the RNA-Seq experiments. A gene's expression was considered down- or upregulated in the mutant if it changed at least two-fold compared to wild-type. In the histograms mutant/wild-type expression for each gene was normalized to the expression of *RpL32* which was unchanged in the *JIL-1* mutant background. For each gene the average normalized expression from three independent experiments with SD is shown. (A) The average

expression of all five genes selected based on their downregulation in the *JIL-1* mutant by RNA-Seq were also downregulated at least two-fold as determined by qPCR (in purple). The average expression of two genes selected based on their unchanged status in the *JIL-1* mutant by RNA-Seq were also unchanged as determined by qPCR (in yellow). (B) The average expression of three genes selected based on their upregulation in the *JIL-1* mutant by RNA-Seq were also upregulated at least two-fold as determined by qPCR (in orange).

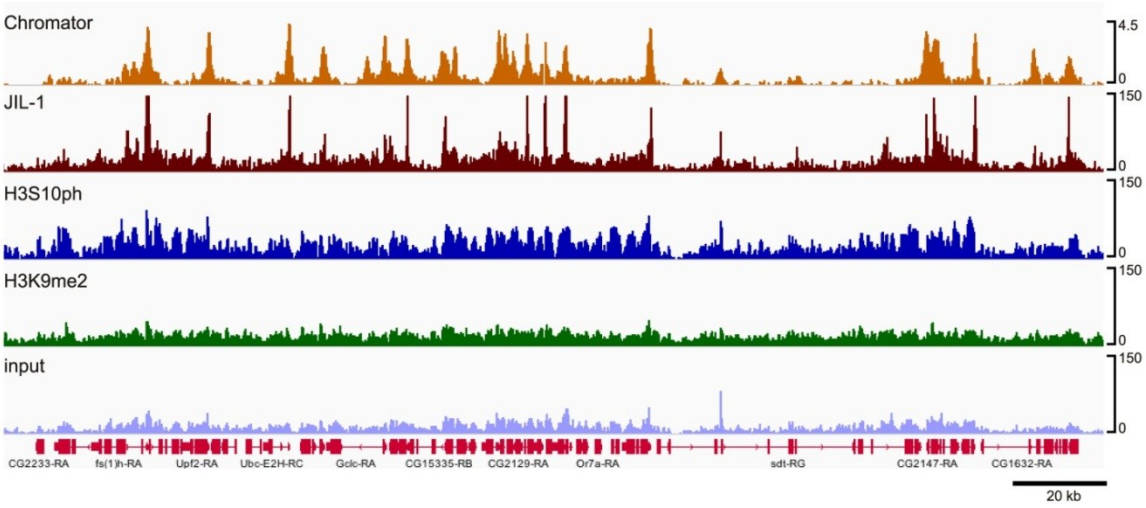

Figure S3. High resolution profiling of JIL-1, H3S10ph, and H3K9me2 genomic sites in *Drosophila* salivary gland cells. ChIP-Seq profiles of JIL-1 (data from JIL-1(2)), H3S10ph (data from H3S10ph(AM)), H3K9me2, and input. The height of the peaks represents the number of reads obtained in each region scaled to the total number of reads. The profile for Chromator shown for comparative purposes is based on ChIP on chip data generated by ModENCODE (25). The data is represented as average log2 signal ratio of IP over input. The location of genes in the depicted section of the X chromosome is shown in red.

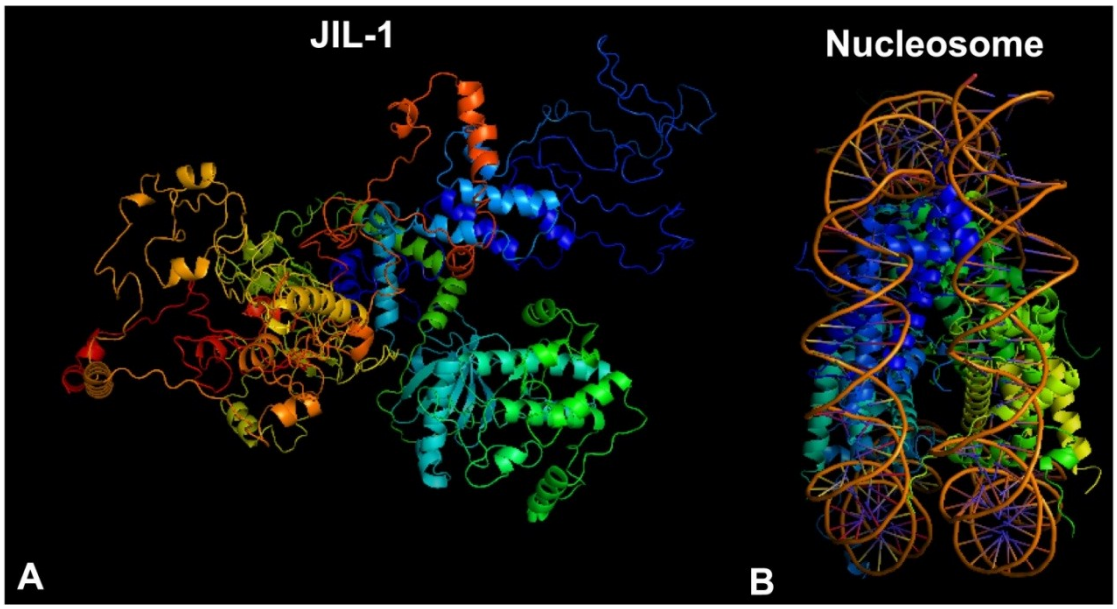

Figure S4. Comparison of the predicted structure of JIL-1 with that of a nucleosome. (A) JIL-1's structure was modeled using the I-TASSER structure prediction platform (37). The amino-terminal domain is rendered in blue, the first kinase domain in green, the second kinase domain in yellow, and the carboxy-terminal domain in red. (B) The crystal structure of a nucleosome (PDB ID: 1AOI). The structures were rendered in PyMOL.

Supplemental Table 1. Primers used for qPCR.

Gene	5'-primer	3'-primer
Mus308	CTGCGTGACTTGCGAAATCT	CCAATCAGGACTCTGAGGAT
nonA-l	TCGACCAATAAGAACCTGGGCA	TCGATTGCGATTTCTGGAA
Cyp6a13	GCCTCGAGTGTAATAGTCTC	TGTAGTCCAATGTCTGGCGT
CG2201	TTTGCAGGTTGGTGGCCAT	TGAAACCGTTAACGGAGACT
CG17230	GTCTAGCTTCATGGAGGCA	CTCAAGATCCTGCGTAGCA
Claspin	TCTTCGACGAGGAAGACGA	TGATCCTCCTGGTTGACCT
CG33500	GTGGCTTCCGTCATTATGTG	CAGAGTCTTTCGGAGAACCT
CG42347	ATGCTGCAGCAACAGCCGCTT	TCGCAGAGCTTAGCAATCTA
CG1092	AGACTGCTATCGTGAGACCT	TTCTGTGCTGCTCCAGATTG
CG3999	GAATATTAGGTGATGGAGTG	GTCCGAGTACGAGACTATAT
RpL32	ATGACCATCCGCCCAGCATACAGG	AACGTTTACAAATGTGTATTC CGACC
JIL-1	CCGAATTCATGAGTCGCTTGCAAAAG	ATGGTACCGTCATTCAGACTA ACGGC
Lsp1g	GCTCAACGACAAGATGACGT	ACGTCATCTTGTCGTTGAGC
CG32198	TTGCTCTTGATGATCCCACA	GCTCACGGATCACGACTTCA
yin	ATGCTGTAGAGTCTACCTTC	TTCACTCCAGATGACCGAGT
CG14153	CACCTCAACTTCAGCCATAT	ATTGCTAATGGCTCTTGAGG
Jumu	ATGTTCGAACTAGAGGATTATTCG	GAGGAATTACGCCGTTGAAGC
Rcd1	AGCAGCTATCGACGATGATG	GAGCTACCTCCAGATGATCA
CG8611	TTTCGCTGTGAGTGGCAAACG	GACATAGCCACTAACCTGTTG
CG15824	GAACCGAAGTGTTGCCACCCT	CATTCCTTGGCGACGCAGCAT
CG30411	AATGGTTGCCAGCGATGTTC	CCTAGATCTTCGACATGCAC

CHAPTER 6. GENERAL CONCLUSION

H3S10 phosphorylation mark is required to counteract heterochromatic spreading and gene silencing

The CTD domain of the JIL-1 kinase has been demonstrated to be necessary and sufficient for proper localization to chromatin (Bao et al., 2008). The JIL-1 gain-of-function *Su(var)3-1* allele, which has a truncation of the C-terminal domain of JIL-1, has a strong suppressor effect of PEV for the w^{m4} allele (Bao et al., 2007, Ebert et al., 2004).

When the CTD-domain of JIL-1 kinase was expressed in a wild-type background, it had a dominant negative effect and essentially phenocopied the effect of hypomorphic JIL-1 alleles on PEV. These effects on PEV correlated with the spreading of the heterochromatic mark H3K9me2 to the chromosome arms and a decrease in H3S10 phosphorylation levels.

Furthermore, expression of the CTD-domain in a *JIL-1* null mutant background enhanced PEV of the *118E-10* allele. Interestingly, although spreading of the heterochromatic H3K9me2 mark was not counteracted by expression of the CTD in the absence of H3S10 phosphorylation, the grossly perturbed polytene chromosomes of the *JIL-1* null mutant were restored to wild-type morphology. And the 'kinase dead' version of JIL-1 did not prevent the heterochromatic spreading.

These findings suggest that: (1) the enhancer phenotype in PEV resulting in gene silencing from JIL-1 loss of function mutants is independent of the gross perturbation of polytene chromosome morphology. (2) The epigenetic H3S10 phosphorylation mark is required for preventing the observed heterochromatic spreading.

In previous studies, assays testing for viability and rescue of polytene chromosome

morphology assay did not detect a genetic interaction between *JIL-1* and *Su(var)2-5* (Deng et al. 2007). However, results of PEV assays with *JIL-1* and *Su(var)2-5* or *Su(var)3-9* double mutants demonstrated that the haplo-enhancer effect of JIL-1 has the ability to counterbalance the haplo-suppressor effect of both *Su(var)3-9* and *Su(var)2-5* on the PEV of two different alleles.

The present experiments, taken together with those of Deng et al. (2010) using a *JIL-1* null allele, provide strong evidence that a finely tuned balance between the levels of JIL-1 and all of the major heterochromatin components Su(var)3-9, HP1, and Su(var)3-7 contributes to the regulation of PEV and gene expression.

For future study, one interesting direction would be to identify the interaction partners of JIL-1 kinase by Mass Spectrometry. Identifying partners such as chromatin remodelers, transcription regulators and histone modification enzymes may help us elucidate the mechanism underlying JIL-1 mediated H3S10ph regulation of heterochromatin spreading and gene expression.

Genome-wide analysis of JIL-1, H3S10ph, and H3K9me2 localization and regulation of gene expression.

The PEV and genetic interaction assays indicated H3S10ph can counteract heterochromatin spreading and regulate gene expression (Bao et al., 2007; Deng et al., 2008; Deng et al., 2010). To further examine the exact level of H3K9me2 and H3S10ph at a reporter *white* gene locus that is responsible for position effect variegation, we performed the ChIP-qPCR experiment. The result suggests that H3K9me2 levels at the *white* gene

directly correlate with its level of expression and that H3K9me2 levels in turn are regulated by H3S10 phosphorylation levels.

To further assess whether there is a global counterbalancing of H3S10ph and H3K9me2, we performed a genome-wide analysis of JIL-1 targeting sites and H3S10ph, H3K9me2 distribution by ChIP-seq. In order to assess whether changes in H3K9me2 and H3S10ph distribution influenced gene expression profiles, we performed RNA-seq analysis in the absence of JIL-1 and interphase H3S10 phosphorylation. We show in wild-type salivary gland cells that the H3S10ph mark is predominantly enriched at active genes whereas the H3K9me2 mark is largely associated with inactive genes. Furthermore, our data demonstrates that discrete binding peaks of JIL-1 are located preferentially to the 5'-end of genes near the TSS. This result supports the result from Kellner et al. (2012), although Regnard et al. (2011) reported 3'-end localization of JIL-1. Interestingly, we found that the enrichment profile of H3S10ph was highly correlated with that of JIL-1, but not identical. The distribution of the H3S10ph mark was much broader and peak enriched regions were shifted about 600 bp downstream of the TSS. A 3-D structure model of JIL-1 relative to nucleosome structure by prediction software suggested that a possible explanation for this lack of overlap is that JIL-1 may have the capacity to phosphorylate the tail of H3 of one or more nucleosomes some distance away from its actual binding site depending on the state of higher order nucleosome packaging. Furthermore, the results show that down-regulation of genes in the mutant is correlated with higher levels or acquisition of the H3K9me2 mark whereas up-regulation of a gene is correlated with loss of or diminished H3K9me2.

In summary, our results suggest a model where the function of JIL-1 mediated epigenetic H3S10ph is to maintain active gene expression by serving as a protective epigenetic mark counteracting H3K9me2 and gene silencing.

In future studies, we will try to find the binding motif of JIL-1 kinase. The gene ontology study on JIL-1, H3S10ph and H3K9me2 target genes can help us further understand the mechanism of JIL-1 mediated H3S10ph regulating heterochromatin status and gene expression.

References

Bao X, Deng H, Johansen J, Girton J, Johansen KM. (2007) Loss-of-function alleles of the JIL-1 histone H3S10 kinase enhance position-effect variegation at pericentric sites in *Drosophila* heterochromatin. *Genetics*. 176(2):1355-8.

Bao X, Cai W, Deng H, Zhang W, Krencik R, Girton J, Johansen J and Johansen KM. (2008) The COOH-terminal domain of the JIL-1 histone H3S10 kinase interacts with histone H3 and is required for correct targeting to chromatin. *J Biol Chem*. 283:32741-32750.

Deng H, Bao X, Zhang W, Girton J, Johansen J and Johansen KM. (2007) Reduced levels of SU(VAR)3-9 but not SU(VAR)2-5 (HP1) counteract the effects on chromatin structure and viability in loss-of-function mutants of the JIL-1 histone H3S10 kinase. *Genetics.* 177:79-87.

Deng H, Bao X, Cai W, Blacketer MJ, Belmont AS, Girton J, Johansen J and Johansen KM (2008) Ectopic histone H3S10 phosphorylation causes chromatin structure remodeling in *Drosophila*. *Development* 135: 699-705.

Deng, H, Cai W, Wang C, Lerach S, Delattre M, Girton, J, Johansen J and Johansen KM. (2010) JIL-1 and SU(VAR)3-7 interact genetically and counterbalance each others' effect on position effect variegation in *Drosophila*. *Genetics.* 185:1183-1192.

Ebert A, Schotta G, Lein S, Kubicek S, Krauss V, Jenuwein T, Reuter G.(2004) Su(var) genes regulate the balance between euchromatin and heterochromatin in Drosophila. *Genes Dev.*18(23):2973-83.

Kellner, W.A., Ramos, E., Bortle, K.V., Takenada, N. and Corces, V.G. (2012) Genome-wide phosphoacetylation of histone H3 at *Drosophila* enhancers and promoters. *Genome Res.* 22**,** 1081-1088.

Regnard, C., Straub, T., Mitterweger, A., Dahlsveen, I.K., Fabian, V. and Becker, P.B. (2011) Global analysis of the relationship between JIL-1 kinase and transcription. *PLoS Genetics* 7, e1001327.

ACKNOWLEDGEMENTS

First, I would give my special thanks to Dr. Kristen Johansen and Dr. Jørgen Johansen for their enthusiastic guidance, supervision, encouragement and support on all my researches. In these years of my Ph.D study, they help me develop experimental and critical thinking skills as well as the scientific attitude.

I thank Dr. Jack Girton for helping me on many hard genetic problems and suggestions on experimental designs. I would like to thank Dr. Yanhai Yin and Dr. Michael Shogren-Knaak, for serving in my POS committee, and for their kind suggestions on my research and dissertation. I wish to thank Dr. Chong Wang, Dr. Peng Liu and Dr. Dan Nettleton for helping me on statistical analysis and inference.

I thank all the people that have been involved in the JIL-1 project. I especially thank Dr. Weili Cai for mentoring at the initiation of my research life. I also thank Yeran Li for her collaboration and discussion on all of my research projects. I wish to thank all the present and past members in this laboratory, including Dr. Changfu Yao, Saheli Sengupta, and Mr. Laurence Woodruff for their generous help, suggestions and friendship.

Finally, I wish to give my deep thanks to my family, particularly my wife Xiaomeng Zhang, for her support and understanding in these years!